國立交通大學

機械工程研究所

博 士 論 文

渦卷式壓縮機族群設計最佳化之研究

Family design of scroll compressors with optimization

研 究 生：張鈺炯

指導教授：洪景華 教授、曾錦煥 教授

中 華 民 國 九十六 年 一 月

渦卷式壓縮機族群設計最佳化之研究

Family design of scroll compressors with optimization

研 究 生：張鈺炯　　　　　Student : Yu-Choung Chang

指導教授：洪景華教授　　　Advisors : Dr. Chinghua Hung
　　　　　曾錦煥教授　　　　　　　　Dr. Ching-Huan Tseng

國 立 交 通 大 學

機 械 工 程 學 系

博 士 論 文

A Dissertation
Submitted to Department of Mechanical Engineering
College of Engineering
National Chiao Tung University
in partial Fulfillment of the Requirements
for the Degree of
Doctor
In

Mechanical Engineering

January 2007

Hsinchu, Taiwan, Republic of China

中華民國九十六年一月

國立交通大學

論文口試委員會審定書

本校___機 械 工 程___學系博士班___張鈺炯___君

所提論文(中文)___渦卷式壓縮機族群設計最佳化之研究___

_____

(英文) Family design of scroll compressors with optimization

_____

合於博士資格水準、業經本委員會評審認可。

口試委員：

指導教授：

系主任：_____ 教授

中華民國　96　年　元　月　22　日

渦卷式壓縮機族群設計最佳化之研究

研究生： 張鈺炯　　　　　　　　　指導教授：洪景華教授、曾錦煥教授

國立交通大學機械工程研究所 博士班

摘　　　要

　　本論文為提出一套結合工程經驗之最佳化方案的系統設計流程，特色為應用互動判定法來解決工程實務上常面臨的離散式參數與非線性數學模型的目標函數。運用此系統設計流程，本研究實際應用於要求低成本與高性能化的渦卷式壓縮機之商品族群設計案例，所完成之設計成果，不但零件共用率達 80% 以上，其性能也優於國際頂級商品，證明本論文之研究，頗具實用性。

　　本項系統設計流程包含：(1)渦卷式壓縮機設計架構創意；(2)建構設計參數化模型與模擬分析軟體，並完成相關測試驗證；(3)開發渦卷式壓縮機族群設計最佳化方案；(4)實作雛型壓縮機，並完成相關測試驗證。

　　所發展的族群設計最佳化方案包含：具離散式參數與非線性模型之目標函數的定義、關鍵設計參數的選擇、相關製造與組裝限制之拘束設定、以及植入工程經驗之互動判定法則的計算迴圈研究等。

　　本族群設計最佳化方案，以完成兩種用途的渦卷式壓縮機之族群設計為研究案例，並且皆完成雛型實作與性能測試驗證，所開發之雛型壓縮機的性能，皆能滿足國際商品目標的需求。第一案例之族群設計，為應用於定轉速的渦卷式壓縮機，第二案例則以第一案例所完成的族群設計目標及要求零件共用化為基礎，開發結合可變轉速之高效率馬達的渦卷式壓縮機，於相同運轉條件下，所開發之可變轉速的渦卷式雛型壓縮機，其能源效率比第一案例之定轉速渦卷式壓縮機，提高 12%以上。

　　此外，為了匹配可變轉速之渦卷式壓縮機的開發，本研究也同步運用專利分

析及功效矩陣比較法，匹配有限元電磁場計算模擬分析而進行永磁同步無刷馬達的實務創作，所完成之創意構想，已獲得台灣、中國大陸及美國等三地區的專利權。

　　本論文不僅完成系統設計最佳化方案的模擬演算，並且實際建構設計流程來進行工程實務開發，經由渦卷式壓縮機族群設計開發的實作及雛型樣品之性能測試驗證，證明所推導的方法與流程，皆具完整性與實用性。

Family design of scroll compressors with optimization

Student：Yu-Choung Chang　　Advisors：Dr. Chinghua Hung
　　　　　　　　　　　　　　　　　　　　　　Dr. Ching-Huan Tseng

Institute of Mechanical Engineering

National Chiao Tung University

ABSTRACT

This dissertation proposes a systematic optimum design procedure for the scroll type compressor (STC) family development.　Based on engineering practices, an optimization algorithm combined with interactive session and discrete variable design has been carried out.　The major result is that over 80% of the common components can be shared in the developed STC family.　The STC prototype's performance will be able to compete with other world-level commercial products.

The major procedures of the proposed systematic design include: (1) to propose an innovative STC design structure, (2) based on the innovated STC structure, to build-up and validate the performance simulation tools, (3) to implement a practical STC family design process that combines with the optimization algorithm, (4) to evaluate the prototype's performance of the developed STC family.
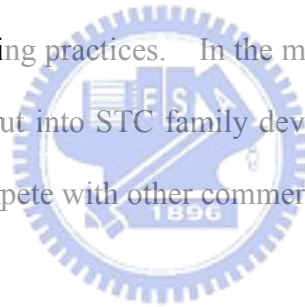
The developed optimization algorithm comprises the non-linear objective function definition and critical design parameters selection to identify the constraints that relate to manufacturing and assembly limitations.　An iterative process approach was carried out with interactive session using the given set of discrete variables which were decided by engineering experience.

Two case studies of STC family design with optimization have been put into practice and prototyped.　The first case of STC family design is used for constant

speed application, and based on the design specifications and the requirement of sharing common as many components as possible. An equivalent STC operated at variable speed and controlled by an inverter-fed motor, has been investigated in this study also, and the efficiency is 12% higher than that of the first case of the STC family.

In addition, an interior permanent magnet synchronous motor (IPMSM) has been innovated to be used in the variable-speed STC. This IPMSM innovation development is incorporated with function matrix, computer-aided engineering simulation and patent around skills. Meanwhile, the newly developed IPMSM has issued patents in Taiwan, mainland China and United States of America.

This study has built-up an effective systematic optimum design algorithm and methodology in engineering practices. In the meantime, the innovated design process has been validated and put into STC family development. The results show that the developed STCs can compete with other commercial products in the world.

ACKNOWLEDGEMENT

TABLE OF CONTENTS

LIST OF TABLES

LIST OF FIGURES

LIST OF FIGURES (Continued)

NOMENCLATURES

A clearance area (mm)

C flow coefficient

COP_{el} coefficient of performance based on electrical power input (W/W)

D diameter (mm)

F_b backpressure force (N)

F_m inertial force (N)

F_t thrust force (N)

F_θ tangential force (N)

$F_{1,2}$ the forces acting on Oldham coupling surface (N)

f_m motor operating frequency (Hz)

G_c rigidity of cutting tool

G_c rigidity of cutting tool

G_c rigidity of cutting tool

G_w rigidity of scroll wrap

h enthalpy (kJ/kg)

h_e height (mm)

k thermal conductivity (W/m·°C)

L　　　length (m)

M　　　force moment (N·m)

M_b　　backpressure moment (N-m)

$\dot{m}$　　　mass flow rate (kg/h)

N　　　turn number of scrolls

n　　　polytropic index

P_c　　　total power consumption to compress the working fluid (kW)

P_{motor}　overall power consumption (kW)

P_r　　　Prandtl number

P_s　　　power consumption of isentropic compressing work (kW)

P_{shaft}　total power consumption to drive the STC (kW)

p　　　pressure (kgf/cm^2)

p_t　　　pitch (mm)

Q_c　　　cooling capacity (W)

R_e　　　Reynolds number

r　　　radius (mm)

T　　　Torque (N·m)

t　　　thickness (mm)

$\dot{V}$　　　volume rate (m^3/h)

V_d displacement volume (m^3/rev)

v$_r$ volumetric ratio

x,y coordinates

δ_a assembly tolerance (mm)

δ_e end side clearance between the tip and bottom of the scroll wraps (cm)

η_c compression efficiency

η_m mechanical efficiency

η_v volumetric efficiency

θ rotation angle

κ specific heat ratio

μ frictional coefficient

v_k kinematic viscosity (mm^2/sec)

ρ density (kg/m^3)

ϕ_r roll angle of scrolls

ω_c rotating speed of crankshaft (rev/min)

Subscripts

B bearing

Bd driving bush

Bm main journal bearing

Bl	lower journal bearing
b	base circle
d	discharge, downstream
dw	downstream
e	end surface
f	flank surface
i	inside
in	inlet
l	leakage
max	maximum value
min	minimum value
motor	motor
o	outside
ob	orbiting scroll
or	orbiting radius
out	outlet
p	flat plate
r	refrigerant
s	suction

s,h   superheat

shaft   crankshaft

tu   tube

u   upstream

w   scroll wrap

INTRODUCTION

1.1 Family Design

The design of families for commercial product has received considerable attention from industry and academia in recent years. While designing a new family, the goal is to standardize as many components as possible for those functions that are common to the entire family. The use of commonality components typically helps in lowering the complexity, cost and lead-time of product development. Kota et al. (2000) has introduced the use of commonality components in product families and given a good guideline to develop commercial products with family design.

As the compressor industry is a huge volume market, the family design of commercial products has evolved into something more powerful than just a cost-reduction method. It has become a strategic weapon in market competition (McDermott and Stock, 1994). Very few papers have presented the related research for compressor design with families up to now. Therefore, this work implemented the family design approach combined with optimization and practical engineering skills to develop a series of scroll-type compressor (STC) products for commercialization.

1.2 Optimum Design in Practice

It is a challenge for engineers to design efficiently and cost-effectively. The computer-aided design and optimization processes can help in this regard. Figure 1.1 shows the basic optimum design process (Arora, 2004). This process forces the designer to identify explicitly a set of design variables, an objective function to be

optimized, and the constraint functions for the system. Meanwhile, the optimization process can substantially benefit from the designers experience and intuition in formulating the problem and identifying the critical constraints. Thus the best approach would be an optimum design process that is aided by the designer's interaction and the use of graphical display of various data and information to facilitate the interactive decision-making process (Arora and Tseng, 1988).

Interactive design optimization algorithms are based on utilizing the designer's input during iterative process. They are in some sense open-ended algorithms in which the designer can specify what needs to be done depending on the current design conditions. The basic interactive optimum design process is shown in Fig. 1.2.

In many practical applications of optimization, the design variables for a problem must be selected from a given set of values. For example, compressor components must be chosen from those that are commercially available. This is related to discrete variable optimization, which is essential to economize on fabrication costs for the design.

Therefore, not only the general optimization design algorithm includes multi-variables, direct search, and inequality constraints, should be approached, but also the interactive session with graphical display and discrete variable design optimization skills to meet design requirement and manufacturing constraint, also have been employed in this research to develop the STC family optimum design.

1.3 Scroll-type Compressor (STC)

Simplicity, higher efficiency, quiet operation and good reliability are the special features of the scroll-type compressor (STC), which is one type of positive displacement compressors and has been widely employed in residential and

commercial air-conditioning, refrigeration and heat-pump applications, as well as automotive air-conditioning. It is said that the STC is the ideal candidate to completely replace the reciprocating compressor. Thus the STC is selected as the research target in this study.

The basic scroll concept has existed since 1886, when an Italian patent was issued (Beseler, 1987), and the first American patent was granted in 1905 to Léon Creux, a citizen of the Republic of France, who disclosed the practical device including two interactive members each having an end plate and an involute spiral element or so-called "scroll" (Léon Creux, 1905). The fixed scroll, is held stationary, while the other, the orbiting scroll is made to orbit but not rotate, around a fixed point on the stationary scroll. These two scroll members are typically a geometrically matched pair and assembled with a 180° phase difference, in the meantime, they are maintained angularly and radially offset so that both spiral elements interfit to make a plurality of moving contacts, which create a series of contact pairs with symmetric, crescent-shaped pockets, and then carry the gas to be handled. There are two types of contacts, which define these pockets formed between scroll members: line contacts between spiral cylindrical surfaces and area contacts between plane surfaces. The relative orbital motion of the two scroll members shifts the line contact along the spiral cylindrical surfaces, therefore, the gas pockets change in volume. The volume of the gas pockets increases or decreases depend on the direction of the orbital motion. Therefore, the scroll-type apparatus is applicable to compress, expand or pump gases.

Figure 1.3 shows the operation principle of the STC and depicts the generation principle of involute spiral elements, gas flow procession and moving contact status. The suction gas enters the scroll unit at the periphery and is compressed progressively into an increasingly smaller pocket as it moves from the periphery toward the center discharge port of the stationary scroll from where it is discharged from the compressor.

There are no suction or discharge valves so that during compression, gas flow through the compressor is continuous and all of the gas pockets are filled with gas in various stages of compression. The resulting smooth flow of gas through the compressor reduces gas pulsations and flow losses to a very low level. Therefore, no valve disturbance and with perfectly force balance, results in a STC operated at low torque pulsation, low noise and vibration levels, starting and restarting become easier. In advance, due to the continuous flow of gas through the compressor and no valve losses during suction and discharge operation, the volumetric efficiency and the operating reliability of the STC are relatively high (Uchikawa *et al.*, 1987).

Moreover, for a typical STC, the key parts consist of a fixed scroll, an orbiting scroll, an Oldham coupling, an eccentric shaft, motor, and one set of compliant mechanism only, such as shown in Fig. 1.4. This simplified structure presents inherent high durability of an additional advantage of STC with a minimal number of movable parts.

Although the concept of a scroll machine has been known for many years and has been recognized as having several advantages for industrial applications, the scroll apparatus was not commercialized successfully before the 1970's, primarily because of the requirement of high precision fabrication and assembly technology with low cost for their key components—including fixed scroll, orbiting scroll, Oldham ring, mainframe and crankshaft. The other critical issue is the STC requires special sealing mechanism for refrigerant leak prevention and to get better efficiency in real operation requirements.

In the 1970's, Arthur D. Little, Inc. (ADL), best known for its research and management consulting activities in U.S.A., which had resulted in the attractive usage of scroll compressors in the world firstly and breathed new life into the old principle. During this period, John E. McCullough, et al., the members of Scroll program of ADL,

disclosed nine U.S. patents (Young *et al.*, 1975; McCullough *et al.* 1976; Hidden *et al.*, 1979) and presented two papers about the scroll machine development during this decade (Moore, 1976; McCullough, 1979), which guide the technological growth and put scroll machines into practice.

Based on the rapid advance in numerically controlled fabrication skills and machines, the STC used for residential and commercial air-conditioning market has been commercialized since the 1980's. Sanden Corp. was the first company to claim the commercialization of STC. Its open-shaft compressors for automotive air-conditioning applications entered the market in 1981 (Terauchi *et al.*, 1984). Thereafter, Hitachi Ltd. was the first company to enter the commercial air-conditioner market using hermetic STC in 1983's (Tojo *et al.*, 1982). Trane Co. was the first company going to production STC for using in unitary commercial air-conditioning equipment before the end of 1987 (Beseler, 1987). From 1988 up to now, the Copeland Corp. has turned STC theory into practical reality with mass production over million units per year and has become the leader in hermetic STC applications in the world. Copeland Scroll® compressors employ many special design concepts to get better performance and are easily brought to fabrication and assembly with low cost (Caillat *et al.*, 1988). At present, the overall production capacity of Copeland Scroll® compressors exceeds 7 million units per year, shares more than 50% of total STC market in the world, and has been overwhelmingly dominating the STC market.

Over 1700 US patents have been disclosed in STC products area during the years 1900~2006. Figure 1.5 presents the US patents growing trend during these years and lists the major applicants companies. From the STC patent and market share analysis, it shows that Copeland Corp. is the biggest competitor in STC's world.

To develop the new STC product, the first objective is to do the patent around and create a reliable sealing and moving mechanism structure. Thereafter, the designer

must build-up the know-how to get the balance between performance and cost for STC commercialization.

The major contributions of this study on STC development include: (1) to propose an innovative STC design structure that can be implemented, (2) based on the innovated STC structure, to build-up the performance simulation tools and validate it, (3) to create a practical family design procedure that combines with the optimization method and the STC simulation package for using in STC commercial product development and to further address this problem of balancing cost and manufacturing effectiveness, (4) to implement the prototype's performance of the developed STC family can compete with that of Copeland Scroll® compressors.

1.4 Variable speed STC

A constant speed compressor used with single-phase or multi-phase alternating-current (AC) induction motor, is a cheap and simple method. It is operated at one specified rotating speed and supplies a definite cooling capacity. A family of constant speed STC is formed by a series of STC units shared with many common components, and supplies multiple cooling capacities for a series of air-conditioners.

Traditionally, the air-conditioner with constant-speed STC is usually designed with its rated working conditions or its maximum thermal loads. It means that this kind of air-conditioner has a good performance only at one design point. In fact, the working condition at which an air-conditioner operates is dependent on its real thermal load. But the thermal load usually varies with the variety of environment temperature while an air-conditioner works. In order to match the cooling capacity with the variety of thermal load, the STC must be turned on and off according to the temperature in the adjusted room and reflect that the STC is not operated at the usually

required condition point. Therefore, the energy consumption of STC with on/off control is wasted too much. On the other hand, with the switching on and off, the STC will be accompanied with loud noise and also induce large amplitude vibration to the pipes and panels surrounding the compressor (Ishii, 1984). To improve the defect, the most important way is to set up the air-conditioner ability to match the variety of thermal load. Up to now, the best solution is using a compressor with variable-speed to supply variable cooling capacity for the air-conditioner (Li *et al.*, 2002).

A variable-speed compressor is the use of a variable speed motor and driven by inverter-fed controller, to supply multiple cooling capacities to match the variety of thermal load. It means one air-conditioning system driven by a variable speed compressor, can replace a series of traditional compressors with constant speed. It also depicts that one family of constant speed STCs can be replaced by one set of variable speed STC while the air-conditioner is inverter-fed controlled.

In other words, to consider a compressor for variable speed operation, there is always a question to what type of compressor mechanism is most suitable. If the vibration problem is the major consideration item, the STC with low-level vibration characteristics will be the most suitable candidate used for the variable speed air-conditioning system (Ishii *et al.*, 1988). The STC has many compression chambers, which are simultaneously compressed at any speed and loading condition such as Fig. 1.3b shows. Therefore, the dynamic behavior in terms of minimal fluctuation in speed and low levels of mechanical vibration are far below those of other types of compressor.

Therefore, developing the variable speed STC also is one kind of family design for STC products. The key technologies comprise to develop the compromise scroll wrap, reliable mechanism, specified variable speed motor and inverter-fed driver, to match with multiple cooling capacity requirements with higher efficiency. Based on

the developed STC family with constant speed, this study has implemented an equivalent STC with variable speed to match with the series of required performance. Meanwhile, the performance comparisons between constant speed and variable speed of the developed STCs, also have been investigated.

1.5 Motor types and drivers used for variable speed STC

For improving the efficiency of a variable speed compressor, the efficiency of the driving motor must be upgraded firstly. Traditionally, an AC induction motor with three-phase (which has a squirrel cage rotor type and requires conductors) used in the variable speed compressor, has many advantages which include simple structure, low cost, and easy implementation in a wide range of required capacity HVAC systems. But their operating efficiency is lower than the synchronous motor with a rotor that is mounted with permanent magnets (PMSM).

The magnetic field of three-phase induction motor created by the stator windings and the conductors in the rotor, a voltage is induced in the rotor and the current produced by this induced voltage interacts with the magnetic field to produce torque. However, in order to have the induced voltage and develop torque, the rotor must rotate at a speed below that of magnetic field in stator. This relative difference between synchronous speed and actual speed of rotor in operation is called "slip" (Engelmann *et al.*, 1995). The effect of the slip of the AC induction motor in operation is power loss and reduced torque. It is the major limit of the three-phase induction motor to get more operating efficiency.

PMSMs are free from induced losses, the stator structure is similar to that of a three-phase AC induction motor and the rotor is mounted with multiple permanent magnets. Based on the information supplied by the rotor position sensors, the

electronic controller decides which stator phases should be energized at any instant and drive the rotor to rotate synchronously (Engelmann *et al.*, 1995).

It is said the interior permanent magnet synchronous motor (IPMSM) can be derived to larger torque and higher efficiency than AC induction motor and surface permanent magnet (SPM) brushless motor (which is one type of PMSM) at same size (Igata *et al.*, 1998). Figure 1.6 has shown the embodiment of each configuration of these three types of motor.

For the IPMSMs, there are already many patents in the world that relate to rotor configuration and driving method. In this study, patent survey and innovative skill have been used to develop a new configuration of the IPMSM, and the applied patent has been granted in three areas as Taiwan, mainland China and United States of America, respectively. In the meantime, the innovation of IPMSM has been implemented in this study.

To drive the IPMSM used for variable speed STC, a position-sensorless controller combined with power electronic converter, inverter, A/D converter and process control microprocessor, is needed to develop in robustly (Mohan *et al.*, 1995). The control block diagram has shown as Fig. 1.7. In this study, the controller is supported by Energy and Environment Research Laboratory (EEL) of Industrial Technology Research Institute (ITRI) in Taiwan, and compatible with the developed STC to achieve the required performance.

1.6 Dissertation Structure

A brief description of this dissertation content is given as follows. Chapter 1 is the introductions about family design, optimum design, STC's motivation, variable speed STC with compatible motor and inverter-fed control. Chapter 2 depicts the STC design model from patents and literatures review, and then proposes a new STC design structure and a design model. Based on the research results, a computer simulation package for STC development has been built-up also by this study. In Chapter 3, a validation model for STC simulation package is described. Thereafter, the experimental validation combined with the simulation results have been carried out and discussed. Based on the developed STC mechanism structure and validated design model, Chapter 4 presents the investigation of STC family design used with optimization algorithm that is created by this study. The refrigerant is HCFC22 (R22) and the STC family is operated at constant-speed. Following on the identical optimum design algorithm that Chapter 4 approached, three types of variable speed STC with AC induction motor, SPM motor and IPMSM have been investigated in Chapter 5. Meanwhile, the performance comparisons between constant-speed STC family and variable-speed STC have been investigated also. At last, some conclusions of this dissertation are made in Chapter 6.

In addition, the Appendix 1 introduces the detailed calculation inputs and outputs of the developed STC simulation package. About the innovative processes and the patent descriptions of the new IPMSM developed by this study, have also been disclosed and summarized in the Appendix 2 of this dissertation.
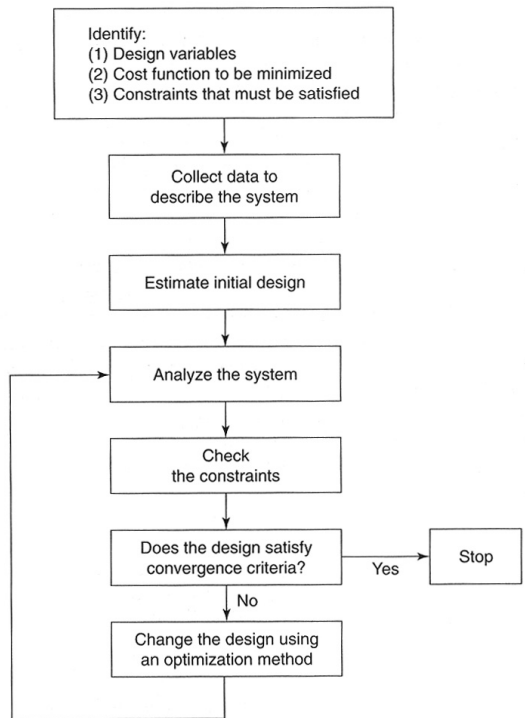
Fig. 1.1 Basic optimum design process (Arora, 2004)
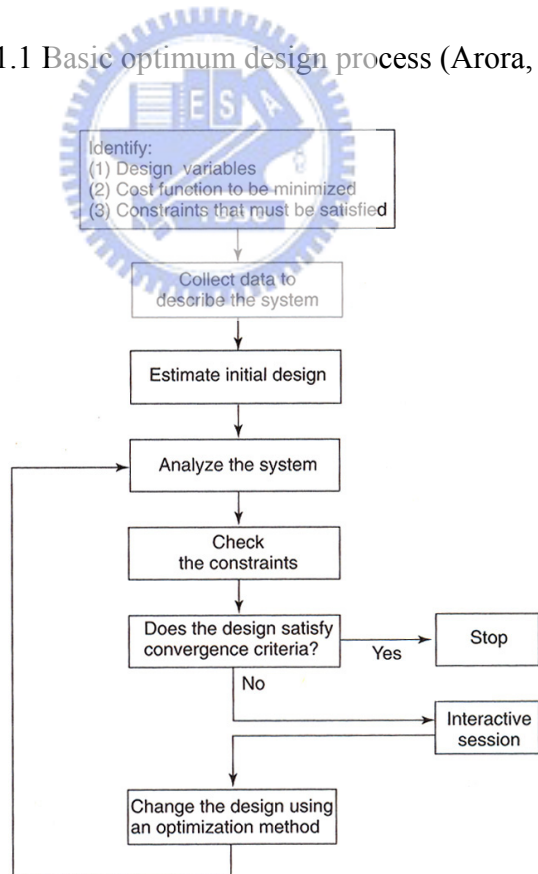
Fig. 1.2 Basic interactive optimum design process (Arora, 2004)
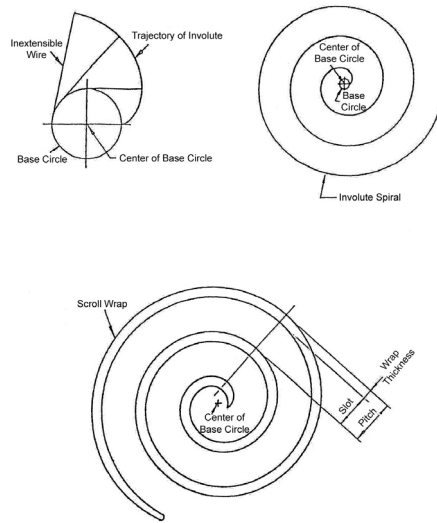
(a) Generation principle of involute spiral element
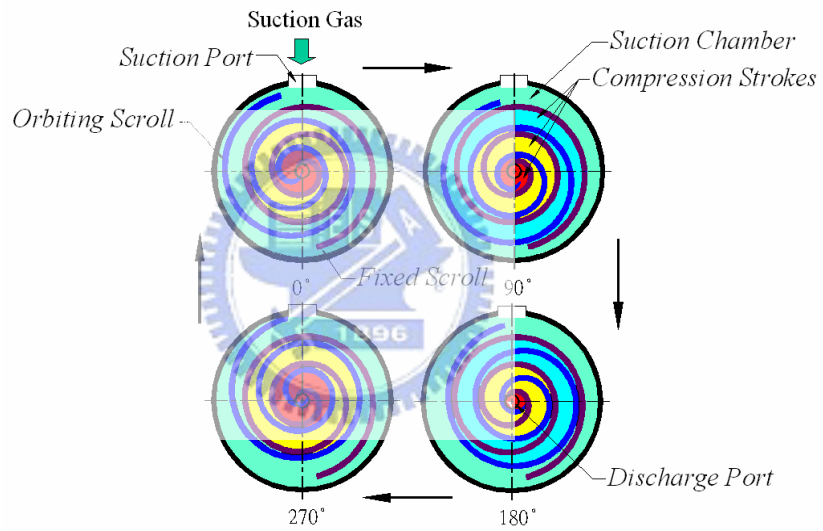
(b) Gas flow during compression process of STC
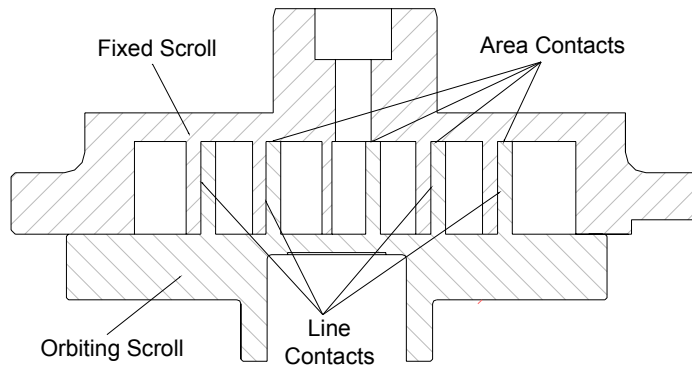
(c) Moving contact status of STC

Fig. 1.3 Operation principle of scroll-type compressor

Fixed scroll

Orbiting scroll

Anti-rotation coupling
(Oldham ring)

Eccentric shaft

Balancer &
Compliant mechanism

Main Frame

Motor
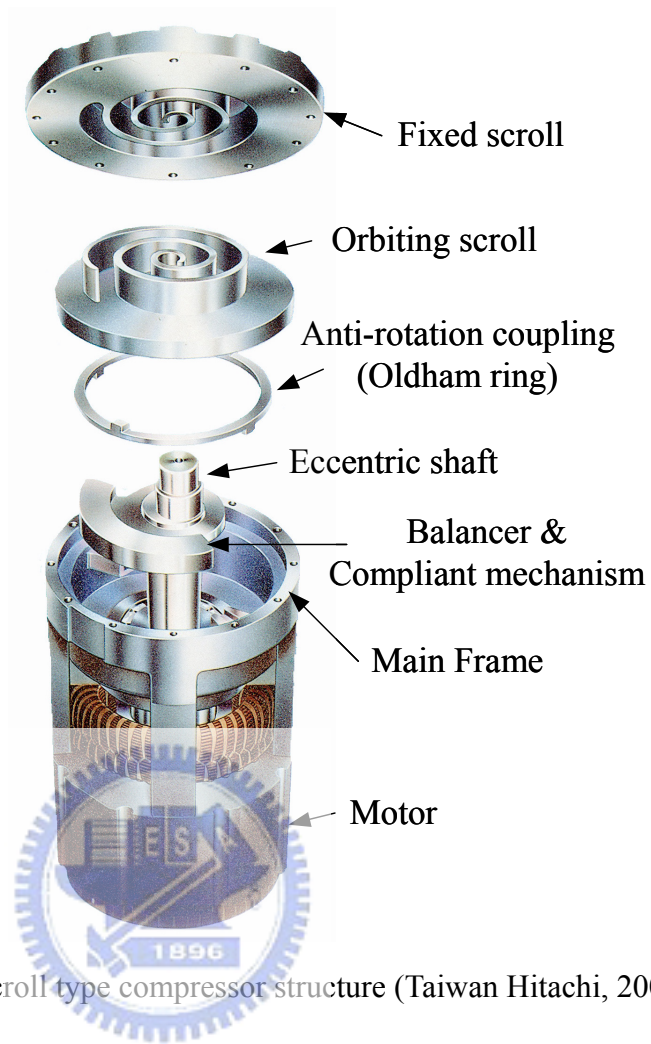
Fig. 1.4 Basic Scroll type compressor structure (Taiwan Hitachi, 2000)
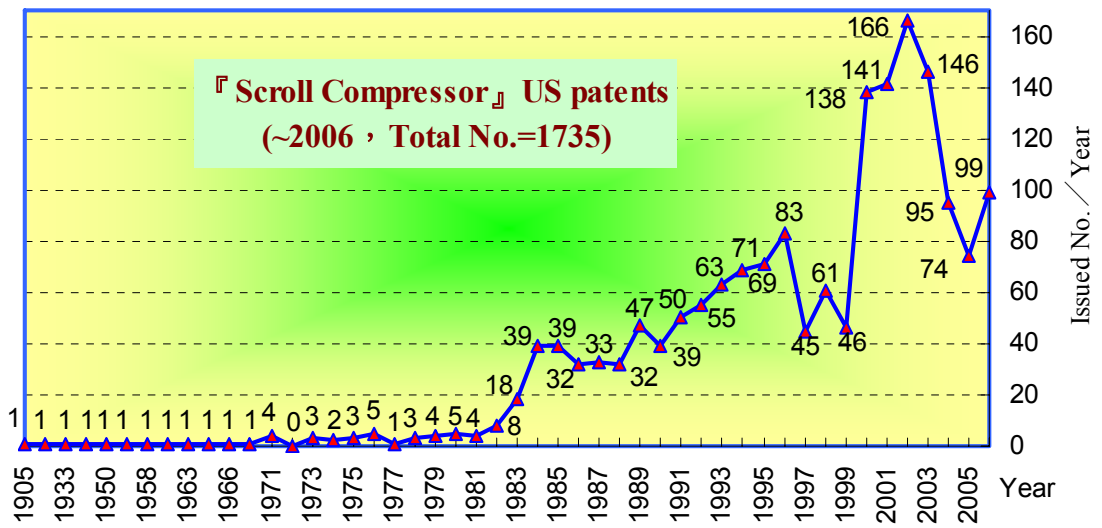
(a) US patents growing trend of STC
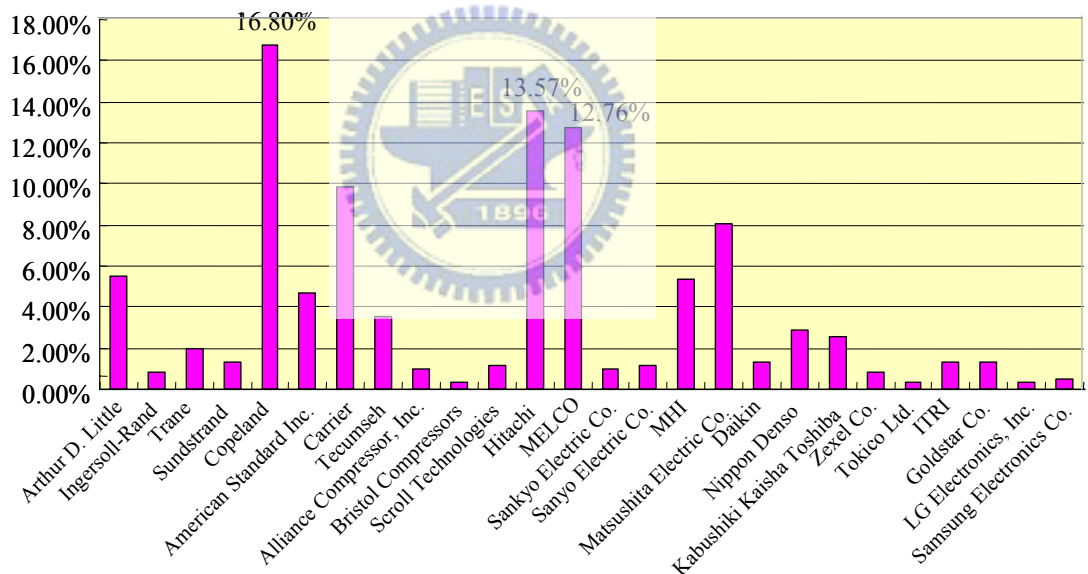
Major competitors : Copeland、Carrier、 Hitachi、MHI、Melco、Matsushita
The biggest competitor: Emerson Copeland Corp. (50% market share)

(b)Major competitor comparison of STC manufacturers from US patent analysis

Fig. 1.5 US patents statistical maps of STC
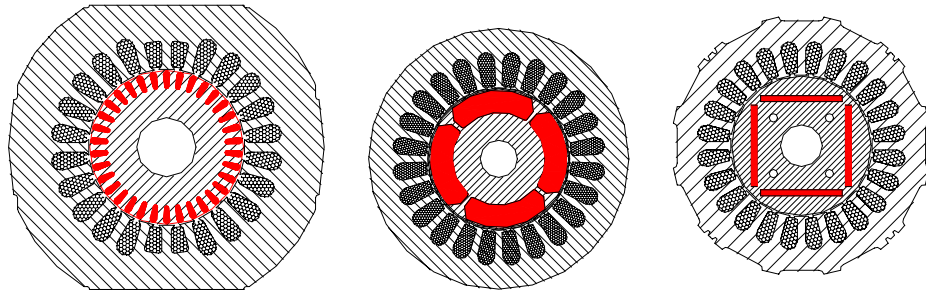
(a)AC Induction Motor   (b)SPM brushless DC motor   (c)IPMSM

Fig. 1.6 Three types of motor used in compressor with variable speed control
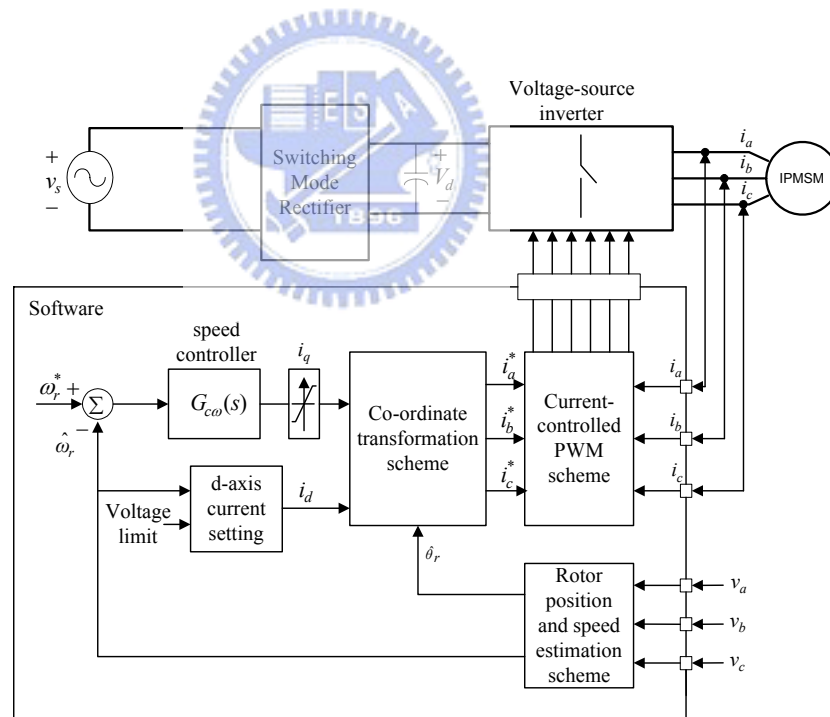
Fig. 1.7 The IPMSM driver configuration used in this study

CHPATER 2

STC DESIGN MODEL

Starting to develop the scroll-type compressor (STC), a preferred design approach should be understood ahead. The design configurations, sealing mechanism, mathematical model of a hermetic STC, all will be introduced in this section. Meanwhile, this study proposes a new available design structure and design model as the research base, the computer simulation package for STC design has been created also.

2.1 Design Configurations of STC

Two major configurations with different types of gas distribution housing are used in scroll compressors: low side shell and high side shell.

Low side shell means the motor and the scroll set are located in suction pressure side. The suction gas passes through the housing and into the chamber around the compressor's mechanism and motor. Conversely, the housing is filled with discharge pressure in high side shell and the inlet is connected to the suction cavity of the scroll set directly. Figure 2.1 has shown the schematics of these two types of STC.

The selection of shell configuration is a key determinant in STC design. Different design configuration, the forces generated by the scroll set during the compression process, leakage models, sealing mechanism, oil lubricating flow design, temperature distribution, noise controlling strategy etc., will all be different. In 1992, Richardson and Gatecliff presented the design requirements of the high side and the low side structures of STC in detail and depicted the high side shell configuration has

many advantages which include minimal suction gas heating and discharge pressure pulses, simple axial and radial compliance mechanism, simple lubricant flow path design and so on.   But the motor is easily overheated under high compression ratio, lower operating efficiency of STC due to working in high discharge temperature and high oil circulation, which are not mentioned in the paper presented by Richardson and Gatecliff.   From the commercial products disclosed, almost STCs that get higher efficiency were developed in low side shell.

Therefore, this study adopted the developed STC is operated at low side shell configuration as Chang *et al.* (2003) presented.

2.2 Sealing mechanisms of STC
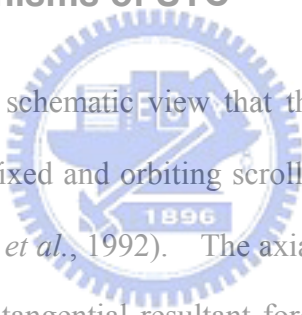
Figure 2.2 shows a schematic view that the scroll piece is acted on by major forces at the time when fixed and orbiting scroll members are in compression motion (Nieter *et al.*, 1992; Bush *et al.*, 1992).   The axial resultant thrust forces F_t to separate the scrolls axially.   The tangential resultant force F_θ and the inertial resultant force F_m will generate an overturn moment to make scroll members with unstable operation. It is therefore conceivable that these three resultant forces must be effectively overcome to prevent the compressed working fluid leakage severely from two scroll members, and to operate the STC operation silently.   Figure 2.3 shows the available leakage path of pressurized gas during STC is in operation.   Leakage can occur at the gaps on the flanks of the scroll (line contacts leakage) and between the tips of the scroll and the opposing base plates (area contacts leakage).   Youn *et al.* and Cho *et al.*, have analyzed the leakage characteristics of STC in the proceedings of the 2000 international compressor conference at Purdue.

In order to ensure higher efficiency, the internal leakage must be effectively

controlled in STC design.   To minimize the tip and flank leakages of scroll wrap, the characteristics of these leakages and the corresponding sealing compliant mechanisms in STC, have to be analyzed.   Compliant mechanisms not only enable the STC to minimize the leakage clearance between scroll wraps, they also provide tolerance to release solid contaminants and liquid slugs when STC is in compression.   Nieter and Barito have conducted the dynamics model of radial and axial compliant sealing mechanisms used in STC in 1996.   Compliance in radial direction can insure the radial clearances at the flanks of the mating scroll wraps to minimize, and the axial compliance is as approach to insure the axial clearances at the tips of the mating scroll wraps to eliminate.

2.2.1 Radial compliant sealing mechanisms

Flank leakage can be controlled to a minimal through the use of very accurately machined skill or by a radial compliant sealing mechanism that holds the scroll wrap of the orbiting scroll compliantly against the scroll wrap of the fixed scroll through radial force while the compressor is in operation.   This not only tends to keep the flanks of scroll wrap constantly in contact, but also the radial compliance has the added benefit to increase the resistance while the compression chambers have slugs or contaminants, since the orbiting scroll can "unload" to some extent as it encounters obstacles or non-uniform hydraulic pressures (Bush and Elson, 1988), in the meantime, this mechanism can improve the function of lubrication (Caillat and Seibel, 1990).

Table 2.1 shows the patent list of U.S.A. about radial compliant sealing mechanisms of the scroll machines.   This study categorizes it to four types of radial sealing mechanisms as: (1) Eccentric links, (2) Swing links, (3) Slider block, (4) Driving bushing.   The major embodiments of these radial compliant mechanisms

have shown as Fig. 2.4 respectively (Muir *et al.*, 1986; Butterworth, 1983; Fraser *et al.*, 1991; Caillat *et al.*, 1990).

As Fig. 2.4 shows, the driving bushing is the simplest sealing mechanism to do as the radial compliance. A prior art of driving bushing is selected as the radial compliant sealing mechanism and built in the developed STC of this study, which patent has passed the expiration date (Ekelöf, 1933) and the mechanism is simplicity such as Fig. 2.5 shows. The basic principle is a bushing with two parallel flat surfaces and located on the crank pin of eccentric shaft so as to permit to move a little in radial direction and push two scrolls to go in contact under influence of the centrifugal force while the STC is in operation.   Meanwhile, the orbiting scroll can be unloaded to release the slugs or contaminants as the compression chambers encounter non-uniform pressures.

2.2.2 Axial compliant sealing mechanisms

Tip leakage can be minimized either by seal means at the tips of the spiral or by a pressure balance of axially compliant mechanism which forces the scrolls together axially.   Many advantages claimed for the latter type, such that the compliant feature gives the compressor a superior tolerance for handling liquid or foreign material, the pressure is released when the unit is shut down, allowing the STC to start unloaded thereby improving durability and eliminating the friction loss.

Over hundred US patents disclosed the axial compliant sealing mechanisms of the scroll machines, such as Table 2.2 shows.   This study also has categorized four types of axial sealing mechanisms as: (1) Located sealing means on the tips of scroll wrap, (2) Inducing pressurized gas to the back of orbiting scroll, (3) Inducing pressurized gas to the back of fixed scroll, (4) Located pressing members in the back of fixed scroll or

orbiting scroll.   The major embodiments of four types of axial compliant mechanisms
have shown as Fig. 2.6 respectively (McCullough *et al.*, 1976; Tojo *et al.*, 1982;
Anderson *et al.*, 1992; Richardson *et al.*, 1995) and all have commercial products of
STC in the market.

Simple mechanical structure is the merit of the four types axial sealing
mechanism of mentioned above.   But located sealing means on the tips of scroll wrap
always have leakage path on the sides of sealing means, inducing pressurized gas to
the back of fixed scroll or orbiting scroll should generate greater force to overcome the
overturn moment such as Fig. 2.7 shows, using pressing members in the back of fixed
scroll or orbiting scroll have reliability problem.   These axial sealing mechanisms all
should be modified better.

The author, Chang *et al.* (1994, 2002, 2003) proposed a new and better axial
sealing mechanism with solid force as backpressure on the back of fixed scroll.   It is
similar with the type of inducing pressurized gas to the back of fixed scroll, but the
backpressure applied to the fixed scroll is solid force to achieve tip-sealing behavior
during STC operation.   Figure 2.8 shows the innovated structure and available
mechanisms.

2.2.3 Axial Sealing Mechanism with solid force

Figure 2.9 shows the developed STC with new axial sealing mechanism that is
disposed in the back of the fixed scroll member and composed of an isolating member
and a predetermined number of pressing members.   The pressurized gas is induced to
the back of the pressing members in the isolating member for pushing the pressing
members.   The fixed scroll is urged by the solid force from the pressing members to
move axially to remain in a close contact with the orbiting scroll so as to overcome the

leak that takes place in the end surface between the two scroll members. The pressing members may be one solid ring or multi-pins and located on the circumferential planar surface of the back of the fixed scroll.

As Fig. 2.8 shows in detailed, the contact position of the pressing member can be located at the outermost circumferential area, the anti-overturn arm of backpressure force F_b on the fixed scroll member is therefore lengthened. The anti-overturn moment of force F_b so produced can become more flexible because of the solid force and the anti-overturn arm length can all be tuned easily. As the result, the friction loss of the operating scroll members can be minimized, meanwhile, the developed STC operated more stably and at a lower noise. The author, Chang *et al.* (2003) has introduced two STC practical embodiments with this new axial sealing mechanism developed by this study, one is for constant speed, and the other is used for variable speed drive, all presents very good performance.

Based on this new axial sealing design structure, this dissertation is to develop the STC families in advance.

2.3 Literatures review of STC Mathematical models

Many theoretical and experimental studies about STC mathematic models have been introduced and verified in detail. The mathematic models can be categorized into geometrical model, dynamics model and global analytical models.

2.3.1 Geometrical modeling of scroll wrap

Scroll wrap is an appropriate curve for an involute such as Fig. 1.3(a) shows. If one unwraps a string from a circle, keeping the string taut, the end of the string will trace out an involute spiral. To generate the orbiting and fixed scrolls, both with inner

and outer spiral curves respectively, must be specified.

In 1984, Morishita and Sugihara, two engineering members of Mitsubishi Electric Corporation in Japan, derived the geometrical model of scroll-type compressor in detail. Their paper takes into account the geometric derivation of the scrolls which comprises the curve generation of orbiting and fixed scroll wraps, the shape of the discharge portion determined by cutter forming, the calculating volumes and areas associated with the different compressing chambers and volume variation of compressing chamber with respect to orbiting angle. In addition, the displacement volume and built-in volume ratio are also given. The basic geometric derivations of scroll wrap can all be obtained from their investigations.

2.3.2 Dynamics modeling

Due to the compression of pressurized gas, several forces are exerted on the orbiting scroll and fixed scroll, as shown in Fig. 2.10. Ikegawa *et al.* (1984), the STC design group of Hitachi in Japan, have studied the dynamic characteristics with the defined backpressure model. Meanwhile, an experiment to investigate the proper range of backpressure also has been carried out. From the studied results, it shows the proper range of measured backpressure is about 105~110% of the calculated backpressure, where the efficiency is near the maximum and stable operation can be maintained. This force model has a controlled thrust force mechanism by self-adjusting backpressure automatically on the plate of the orbiting scroll, which has been claimed to U.S. patent by Tojo *et al.* in 1982.

Morishita *et al.* (1986) and Ishii *et al.* (1986, 1988), have described the dynamic behavior of the STC with fixed radius crank and variable radius crank mechanisms in more detail. The equations of motion are established for the crankshaft, the scroll set

and the Oldham coupling. The thrust bearing load, the friction, the torque and the power to drive the STC, have all been investigated. The gas forces, overturning forces, reaction forces, thrust forces and the moments, which act on the orbiting scroll, Oldham ring and thrust bearing, are also clarified.

Additionally, the fundamental equation for the journal bearing which is applied to the crank bearing, the forces acting on each lubricated element and the losses occurring in each lubricated element have been investigated by Hayano *et al.* (1988) of Toshiba Corp. in Japan.

Nevertheless the axial compliant sealing mechanism of the above studies were focused on the mechanism of inducing pressurized gas to the back of orbiting scroll as self-adjusting backpressure, the dynamics model also can be transferred easily to the new axial sealing mechanism which is proposed by this study.

2.3.3 Analytical modeling

Bush *et al.* (1986) and Caillat *et al.* (1988), the research group of Copeland Co. in U.S.A., introduced the developing global model of STC firstly, which includes thermofluid model, dynamics analysis, energy balance and overall efficiency predictions. Recently, Schein and Radermacher (2001), Chen *et al.* (2002), the research groups of mechanical engineering of Maryland and Purdue universities of U.S.A. respectively, have developed a more comprehensive model to simulate the performance and operation of STC. The other STC developing group of Korea, Lee and Kim (2001), has presented the overall structure of a computer program and the calculation equations for STC performance estimation that they developed, which includes simultaneous consideration of the compression process, dynamic behavior of the moving parts, and heat transfer between the main compressor components. Ooi *et*

al. (2004), the professor of Nanyang Technological University of Singapore, who developed the fluid flow and heat transfer used with two-dimensional numerical model in the working chamber of the STC.   These literatures filled up the insufficiencies of the overall mathematical models of STC.

Summarizing these literature studies mentioned above, combined with the geometric modeling, dynamics modeling and the global analytical modeling of STC, the overall computer simulation for STC design can be built.   Chang *et al.* (2004) have constructed a STC design model and implemented a computer simulation package for STC development that is used in the current study.

2.4 The STC design model

While developing a STC design model, the first step is to identify the specifications of design requirements that will come from the operation conditions and required performance of the air-conditioning system.   Fig. 2.11 shows the simplified vapor-compression refrigeration cycle that is most widely used for defining a real air-conditioning system and operating at steady conditions.   It consists of four processes:

   1-2   Polytropic compression in a compressor (for example: in a STC).

   2-3   Approximate constant pressure heat rejection process in a condenser

   3-4   Throttling in an expansion device or capillary tube

   4-1   Approximate constant pressure heat absorption process in an evaporator

In a simple vapor-compression refrigeration cycle, the refrigerant enters the compressor (STC) at state 1 as slightly superheated vapor and is compressed polytropically to condenser pressure.   While this polytropic compression is processing, the temperature of the refrigerant increases to well above the temperature of the surrounding medium.   The refrigerant then enters the condenser as superheated

vapor at state 2 and leaves as subcooled liquid at state 3 as a result of heat rejection to the surroundings.   The temperature of the refrigerant at this state is still above the temperature of the surroundings.   The subcooled liquid refrigerant at state 3 is throttled to the evaporator pressure by passing it through an expansion valve or capillary tube and the temperature of the refrigerant drops below the temperature of the refrigerated.   The refrigerant enters the evaporator at state 4 as a low-quality saturated mixture, and it completely evaporates by absorbing heat from the refrigerated space. The refrigerant leaves the evaporator as superheated vapor and reenters the compressor (STC), completing the cycle.   Based on the definite cycle, the design model can be derived in detail.

2.4.1 Cooling capacity and displacement evaluations

When the required cooling capacity, $\dot{Q}_c$, the operating conditions and the properties of refrigerant are defined, the mass flow rate of the suction vapor inlet to the STC, $\dot{m}_s$, and the suction volume rate, $\dot{V}_s$, can be calculated as:

$$\dot{m}_s = \frac{\dot{Q}_c}{(h_{in} - h_{out})} \tag{2-1}$$

$$\dot{V}_s = \frac{\dot{m}_s}{\rho_s} \tag{2-2}$$

where h_{in} and h_{out} are the enthalpies of refrigerant at evaporator inlet and outlet respectively, and ρ_s is the refrigerant density in the suction port of the STC.   To obtain the properties of the refrigerant, this study uses REFPROP 6.01 (1998).

At a specified operation speed ω_c and volumetric efficiency η_v, the displacement volume of the STC, V_d, can be estimated as follows:

$$V_d = \frac{\dot{V}_s}{\eta_v \cdot \omega_c} = \frac{\dot{m}_s}{\eta_v \cdot \omega_c \cdot \rho_s} \qquad (2\text{-}3)$$

where volumetric efficiency, η_v, is defined as:

$$\eta_v = \frac{m_{s,h}}{m_s} \cdot \left(1 - \frac{\dot{m}_l}{\dot{m}_{s,h}}\right) = \frac{\dot{m}_{s,h} - \dot{m}_l}{\dot{m}_s} \qquad (2\text{-}4)$$

The (heated) flow $\dot{m}_{s,h}$ from the suction gas inlet into the suction chamber of the scroll pump is heated by the suction import pipe and suction baffle, a process simulated in this investigation using two successive stages of turbulent flow-heated models.

In the first stage, external refrigerant flows into the compressor through a circular tube and the heat transfer coefficient conforms to the Dittus-Boelter equation (Ozisik, 1977):

$$h_{tu} = 0.023 \cdot \left(\frac{k_r}{D_i}\right) \cdot R_e^{0.8} \cdot P_r^{0.4} \qquad (2\text{-}5)$$

In the second simulated stage, the internal refrigerant flows over a flat plate into the suction chamber for compression, and the local heat transfer coefficient conforms to the Johnson-Rubesin equation (Ozisik, 1977):

$$h_p = 0.0296 \cdot \left(\frac{k_r}{L}\right) \cdot R_e^{0.8} \cdot P_r^{\frac{1}{3}} \qquad (2\text{-}6)$$

Then, the heated suction flow rate $\dot{m}_{s,h}$ can be evaluated.

As regards to the leakage flow rate, $\dot{m}_l$, two types of leakage flow models have been proposed. The end side leakage is caused by a clearance area between the tip and bottom of the scroll wraps and has been given a useful model by Yanagisawa and Shimizu (1985):

$$\dot{m}_{l,e} = \frac{\pi \delta_e^3 (p_i - p_o)}{6 \nu_k \ln(r_o / r_i)} \qquad (2\text{-}7)$$

The flank surface leakage is caused by differential pressure between the compression chambers that causes leakage to flow through a clearance area between

two adjacent walls of the scroll wraps.   This type of leakage flow rate can be depicted using Chu et al.'s formulation (1978):

$$\dot{m}_{l,f} = C \cdot A_f \cdot \sqrt{p_u \cdot \rho_u \cdot \frac{2n}{n-1}\left[\left(\frac{p_u}{p_{dw}}\right)^{\frac{2}{n}} - \left(\frac{p_u}{p_{dw}}\right)^{\frac{n+1}{n}}\right]} \qquad (2\text{-}8)$$

The leakage flow rate is obtained by

$$\dot{m}_l = \dot{m}_{l,e} + \dot{m}_{l,f} \qquad (2\text{-}9)$$

Summarizing Eqs. (2-1) to Eqs. (2-9), the cooling capacity can be expressed as

$$\dot{Q}_c = \eta_v \cdot \omega_c \cdot (h_{in} - h_{out}) \cdot \rho_s \cdot V_d \qquad (2\text{-}10)$$

Using Morishita et al.'s (1984) derivation for the STC analytical model, the displacement volume V_d is obtained as follows:

$$V_d = (2N-1) \cdot \pi \cdot p_t \cdot (p_t - 2t) \cdot h_e \qquad (2\text{-}11)$$

where N is the turn number of the scrolls and can be determined by scroll wrap roll angle:

$$\phi_r = 360° \cdot (N + \frac{1}{4}) \qquad (2\text{-}12)$$

Therefore, the cooling capacity becomes

$$\dot{Q}_c = \left\{\eta_v \cdot \omega_c \cdot (h_{in} - h_{out}) \cdot \rho_s\right\} \cdot \left\{[2 \cdot (\frac{\phi_r}{360} - \frac{1}{4}) - 1] \cdot \pi \cdot p_t \cdot (p_t - 2t) \cdot h_e\right\} \quad (2\text{-}13)$$

As the refrigerant properties, operation conditions and the suction paths all can be specified, the cooling capacity can be evaluated.   While the refrigerant properties, operation conditions and suction paths are assumed as the same, the cooling capacity can be evaluated from four major design variables: ϕ_r, p_t, t and h_e. Fig. 2.12 shows the geometrical definitions of these four relevant design variables, which are used to define the basic dimension of the scroll set.   It also illustrates how a series of cooling capacities is obtained from tuning these four design variables under the same

outside diameter limitation and within certain practical constraints.

2.4.2 Power consumptions estimations

The overall power consumptions is defined as:

$$P_{motor} = \frac{P_{shaft}}{\eta_{motor}} = \frac{T_{shaft} \cdot \omega_c}{\eta_{motor}} \tag{2-14}$$

The motor efficiency can be obtained by the performance test with dynamometer. The torque T_{shaft} to drive the STC is the sum of the torque that counters the tangential bearing load and the friction moment of the bearing, which was derived in detail by Morishita *et al.* (1986):

$$
\begin{aligned}
T_{shaft} &= F_{B\theta} \cdot r_{or} + \sum M_B \\
&= \left\{ F_\theta + F_m + \mu_t F_t + (\mu_1 F_1 + \mu_2 F_2)\sin\theta_{or} + (-F_1 + F_2)\cos\theta_{or} \right\} \cdot r_{or} \\
&\quad + \mu_{Bd} F_{Bd} r_{Bd} + \mu_{Bm} F_{Bm} r_{Bm} + \mu_{Bl} F_{Bl} r_{Bl}
\end{aligned}
\tag{2-15}
$$

where $r_{or} = \dfrac{p_t}{2} - t$, is the orbiting radius. The first term in { } of Eq. (2-15) represents the gas compression force, the second term is the inertia force of acceleration (when angular velocity is constant, $F_m = 0$), and the third term is the thrust-bearing friction on the main frame. The fourth and fifth terms depict the frictional and inertia forces of the Oldham ring. The last three terms indicate the friction moments of the driving bush inside the orbiting scroll boss, main journal bearing and lower journal bearing, respectively. In Eq. (2-15), the frictional coefficient of each journal bearing and the Oldham coupling can all be collected by friction and wear tests (Bailey and Cutts, 1996).

Assuming the journal bearings and the Oldham coupling used in the developed STCs are the same, it should be noted that this model makes it possible to obtain the

motor efficiency and compressor speed, the several work losses and the torque T_{shaft},

and the overall power consumption P_{motor}, can be evaluated while the design variables

of p_t and t are defined. Meanwhile, the total power consumption to compress the

working fluid, the mechanical power consumption and the mechanical efficiency of the

STC can be given as:

$$P_c = F_\theta \cdot r_{or} \cdot \omega_c \tag{2-16}$$

$$P_{shaft} = T_{shaft} \cdot \omega_c \tag{2-17}$$

$$\eta_m = \frac{P_c}{P_{shaft}} \tag{2-18}$$

From the second law of thermodynamics leads to the determination of isentropic

compressor work as: (Cengel and Boles, 1998)

$$P_s = \eta_v \left\{ \left(\frac{\kappa}{\kappa - 1} \right) \cdot p_s \cdot V_s \cdot \left[\left(\frac{p_d}{p_s} \right)^{(\kappa-1)/\kappa} - 1 \right] \cdot \omega_c \right\} \tag{2-19}$$

And the compression efficiency defined as:

$$\eta_c = \frac{P_s}{P_c} \tag{2-20}$$

Note that the cooling capacity, compressor speed, the torque to drive the STC, the

efficiencies and the overall power consumption are offered, the coefficient of

performance based on electrical power input (*COP_el*) of the developing STC can be

obtained as:

$$COP_{el} = \frac{\dot{Q}_c}{P_{motor}} \tag{2-21}$$

To summarize the above derivations, the STC computer simulation package has

been accomplished by the author and the colleagues of ITRI (Chang *et al.,* 2004).

The design structure and the calculation flowchart developed by this study are shown

as Fig. 2.13 and Fig. 2.14, respectively. About the detailed calculation inputs and outputs of this developed STC simulation package have been introduced in Appendix 1.

2.5 Conclusions

The study results of this section are summarized as below:

(1) A new STC configuration used with solid force as sealing compliant mechanism has been innovated.

(2) The global analytical model of STC, which includes geometrical definition, thermofluid simulation, dynamics analysis, energy balance and overall efficiency predictions, has all been reviewed and systematized from prior literatures.

(3) A STC design model with parametric algorithm has been constructed. Meanwhile, a practical computer simulation package for STC design has also been built-up which can evaluate overall performance of STC in detail.

(4) According to the market requirement, the COP_{el} has been selected as the basis of STC performance description. Meanwhile, the COP_{el} is defined as the objective function in this study for optimization approach.

Table 2.1 Patents list of radial sealing mechanisms of STC in U.S.A

Types / Assignees	Eccentric Link	Swing Link	Slider Block	Driving Bushing
Individual Persons	US 3,011,694 US 3,560,119 US 3,600,114		US 3,567,348	US 1,906,142
Arthur D. Little	US 3,874,827 US 3,884,599	US 3,924,977 US 3,986,799 US 3,994,633 US 3,994,635 US 3,994,636 US 4,065,279 US 4,082,484 US 4,892,469	US 4,160,629	
Trane Co.		US 4,413,959		
Sanden Corp.	US 4,575,319	US 4,435,136 US 4,580,956 US 4,808,094		
Sanyo		US 4,838,773		
American. Standard		US 4,934,910		
Mitsubishi Denki Kabushiki Kaisha			US 5,328,342 US 5,433,589	US 4,585,402 US 4,585,403 US 4,715,796 US 5,312,229
Copeland	US 4,609,334			US 4,836,758 US 4,954,057 US 5,197,868 US 5,295,813 US 5,378,129 US 5,545,019 US 5,588,819 US 5,772,416 US 5,931,649 US 6,264,445
Matsushita Co.			US 4,764,096 US 5,536,152	US 5,562,436
Carrier Corp.			US 5,017,107 US 5,076,772	US 5,011,384 US 5,174,738 US 5,439,360 US 5,496,157 US 5,496,158
Hitachi, Ltd.			US 5,040,958	
MHI			US 5,165,879 US 5,199,862 US 5,582,513	
Goldstar Co.				US 5,174,739 US 5,520,527
Toyoda			US 5,452,995	
Nippondenso Co.			US 5,575,635	
Scroll Technologies				US 6,053,714 US 6,179,592 US 6,352,417 US 6,361,297

Table 2.2 Patents list of axial sealing mechanisms of STC in U.S.A.

Types / Assignees	Sealing Means	Pressurized gas to the back of Orbiting Scroll	Pressurized gas to the back of Fixed Scroll	Pressing member
Individual Persons		US 5,833,442	US 3,874,827	
Arthur D. Little	US 3,986,799 US 3,994,633 US 3,994,635 US 3,994,636 US 4,199,308 US 4,395,205	US 3,884,599 US 3,994,633		
Hitachi, Ltd.	US 4,487,560	US 4,216,661 US 4,350,479 US 4,357,132 US 4,365,941 US 4,557,675 US 4,596,520 US 4,861,245	US 5,829,959 US 6,174,150 US 6,589,035	
Leybold-Heraeus GmbH				
Trane Co.	US 4,415,317 US 4,416,597 US 4,462,771			
Sanden Corp.	US 4,437,820 US 4,453,899 US 4,460,321 US 4,627,799 US 4,701,115 US 4,722,676 US 4,753,583 US 4,890,987 US 4,968,232 US 5,122,041 US 5,702,241 US 6,126,421	US 5,082,432		
American Standard Inc.	US 6,126,422 US 6,270,713	US 4,522,575		
Mitsubishi Denki Kabushiki Kaisha	US 4,564,343 US 4,732,550 US 4,740,143 US 4,824,343		US 5,743,720 US 5,800,142 US 5,846,065 US 5,853,288	US 4,846,639
Toshiba		US 4,696,630		
Copeland			US 4,767,293 US 4,877,382 US 5,102,316 US 5,156,539 US 5,482,450 US RE35216 US 5,580,230	
Iwata Air Compressor Co. (Anest Iwata Corp.)	US 4,869,658 US 6,179,590			
Tecumseh		US 4,884,955 US 5,088,906 US 5,131,828 US 6,139,294 US 6,168,404		US 5,383,772
Carrier Corp.	US 5,037,281	US 4,938,669 US 4,992,032 US 4,993,928 US 5,040,956 US 5,085,565 US 5,090,878 US 5,145,345 US 5,256,044 US 5,762,483 US 5,873,711 US 6,149,413 US 6,517,332		
Toyoda	US 5,076,771 US 5,364,247 US 5,545,020 US 5,547,353			
MHI	US 6,585,501		US 5,186,616 US 5,257,920 US 5,447,418	
General Motor Corp.	US 5,226,233 US 6,074,185			
Sanyo Electric Co.			US 5,242,284	
ITRI		US 5,252,046		US 5,277,563 US 5,474,433 US 5,527,166 US 6,048,184 US 6,368,088
Goldstar Co.				US 5,487,653 US 5,540,572
Matsuahita Co.	US 5,562,434	US 5,848,883 US 5,630,712		US 5,520,526 US 5,951,272
LG Electronics, Inc.			US 5,562,435 US 5,823,757 US 6,299,417	
Nippondenso Co.	US 5,580,228 US 6,074,141			
Bristol Compressors, Inc.		US 5,588,820 US 5,593,295	US 6,030,192	
Air Squared, Inc.	US 5,632,612 US 6,511,308			
Scroll Technologies		US 5,989,000 US 6,077,057 US 6,171,008 US 6,224,059 US 6,290,478 US 6,527,528 US 6,554,592	US 6,309,197 US 6,416,301	
Varian, Inc.	US 6,068,459			
Mind Tech Corp.	US 6,071,101			
Rechi. Precision Co., Ltd.			US 6,537,044	US 6,257,852
Fujitsu General,.Ltd.		US 6,389,837 US 6,561,776		
Daikin Industries, Ltd.		US 6,533,561	US 6,514,060	
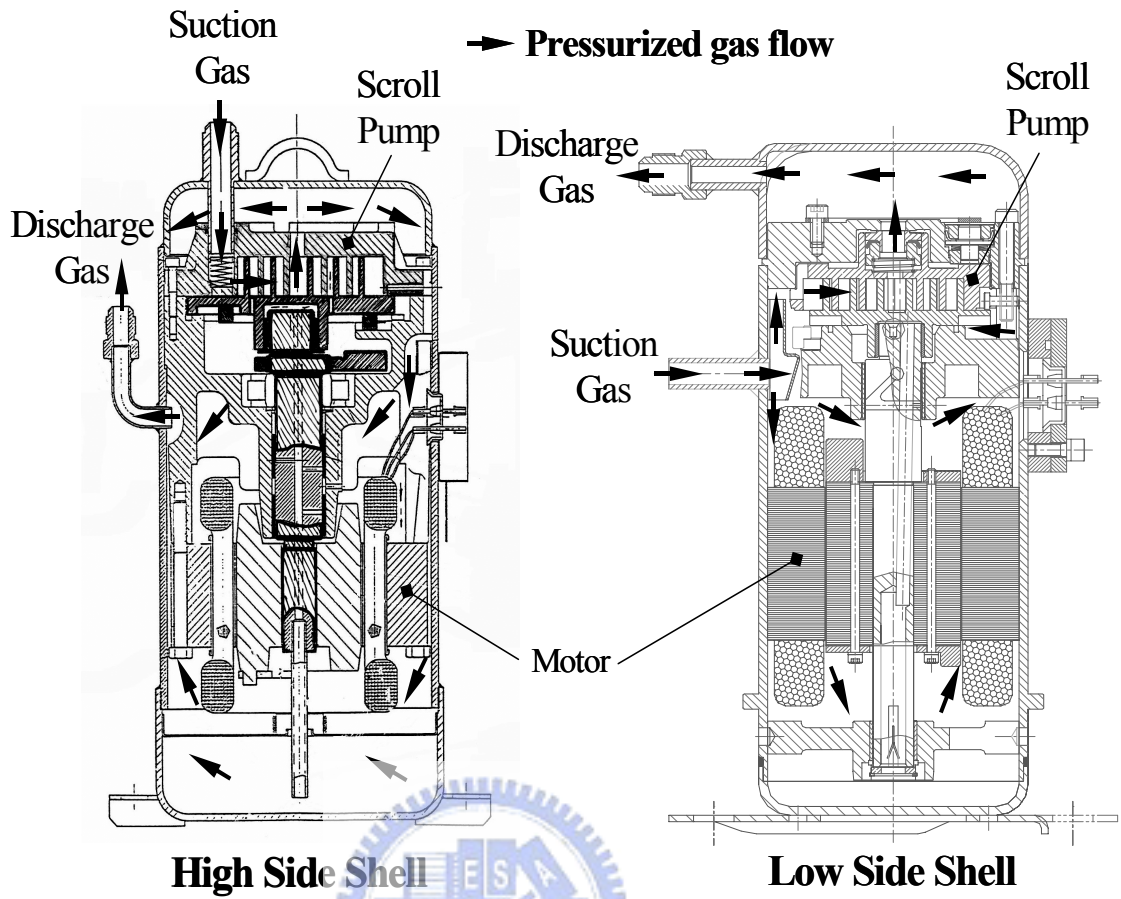
Fig. 2.1 High side and low side configuration of STC

Fixed scroll

F_θ & F_m

Orbiting scroll

F_t
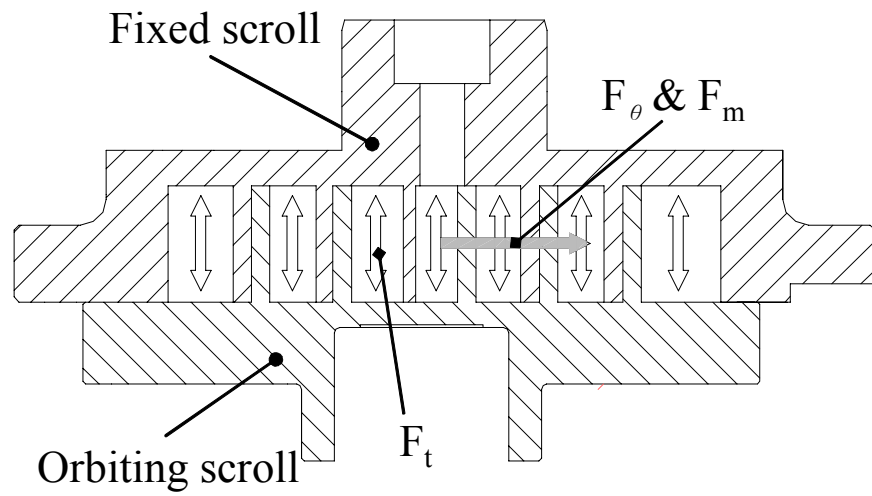
Fig. 2.2 Major forces acting on the scroll set during compression operation

Area contacts leakage
(Tips leakage)

Low pressure chamber

High pressure chamber

Gas leakage flow

Line contacts leakage
(Flanks leakage)

High pressure chamber

Gas leakage flow

Low pressure chamber
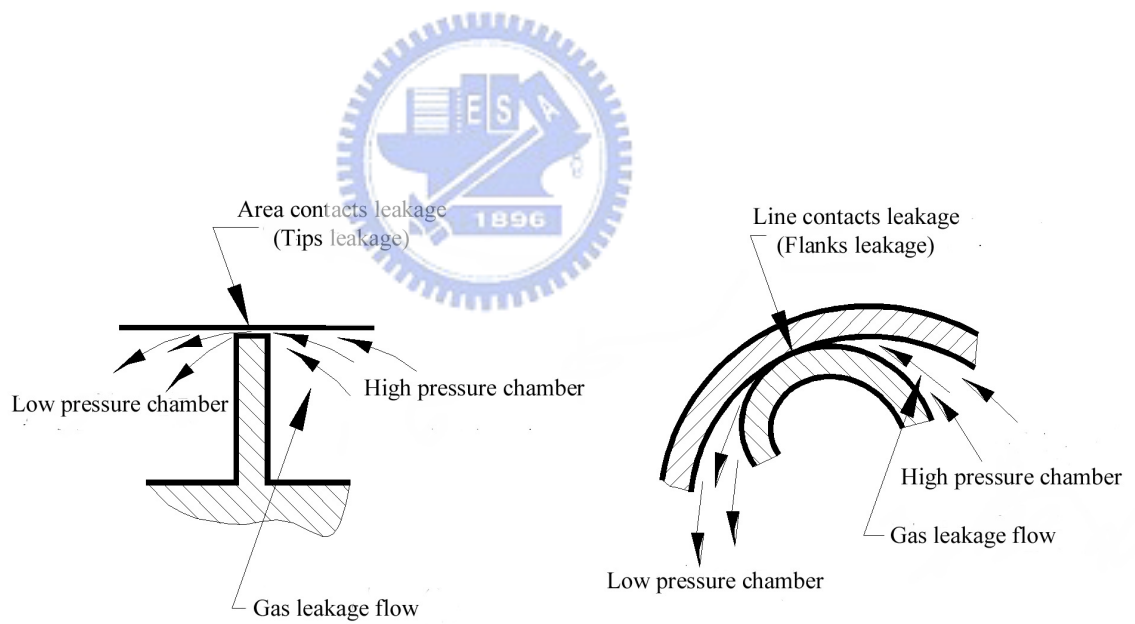
Fig. 2.3 Internal leakage patterns of STC
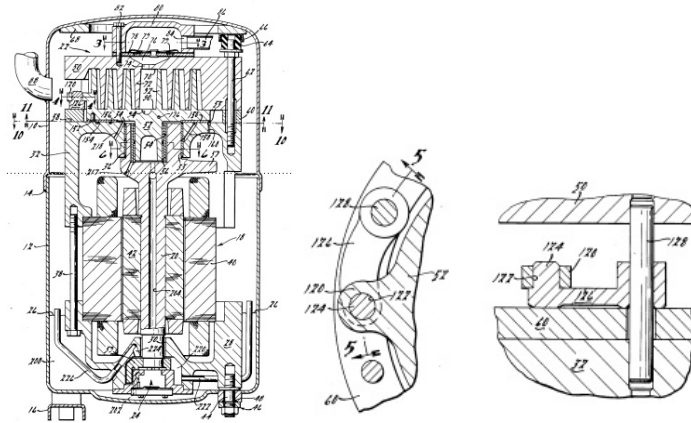
(a) Eccentric links (Issued by Copeland Co. in US 4,609,334 at Sep.02, 1986)
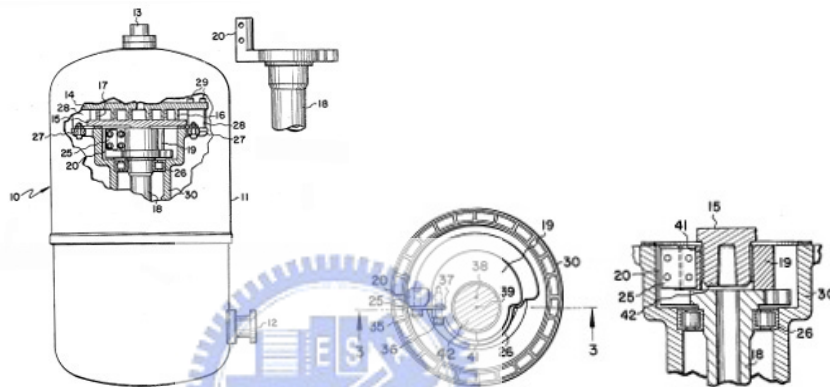
(b) Swing links (Issued by Trane Co. in US 4,413,959 at Nov. 08, 1983)
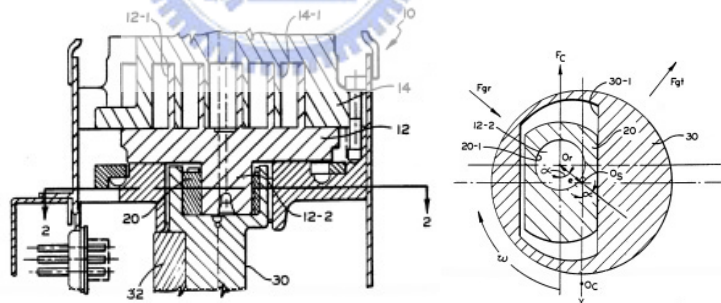
(c) Slider block (Issued by Carrier Co. in US 5,017,107 at May 21, 1991)
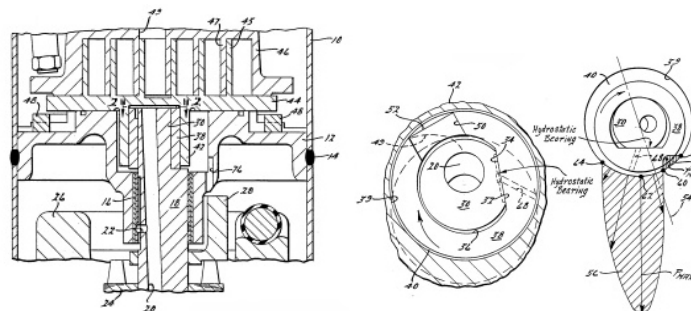
(d) Driving bushing (Issued by Copeland Co. in US 4,954,057 at Sep. 04, 1990)

Fig. 2.4 Major embodiments of radial compliant sealing mechanism of STC

Prior art of
Driving Bushing
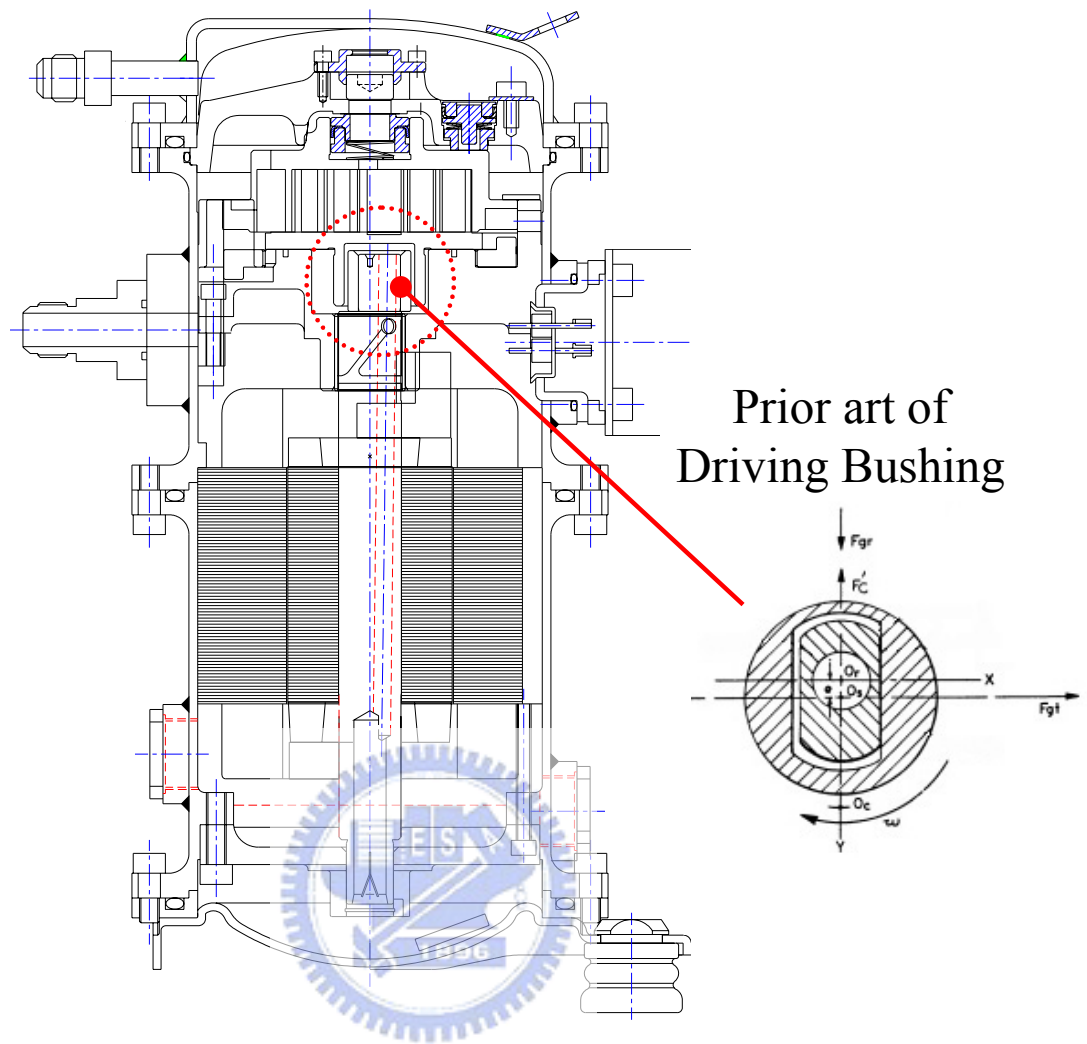
Fig. 2.5 Prior art of driving bushing used in the developed STC of this study
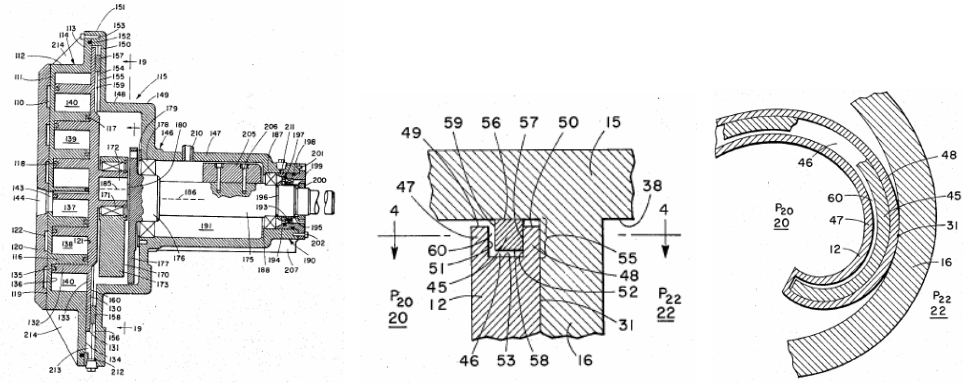
(a) Sealing means
(Issued by Arthur D. Little, Inc. in US 3,994,636 at Nov. 30, 1976)
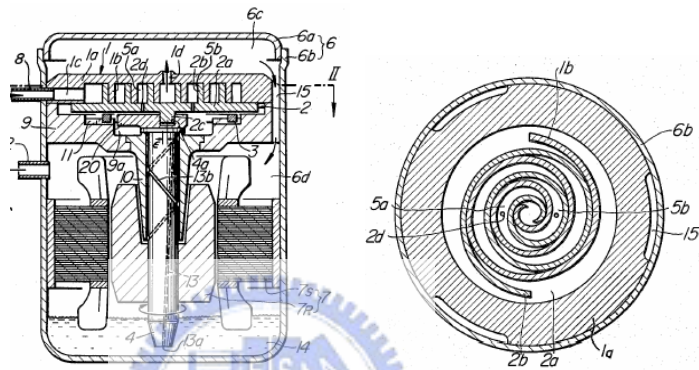
(b) Pressurized gas to the back of orbiting scroll
(Issued by Hitachi, Ltd. in US 4,365,941 at Dec. 28, 1982)
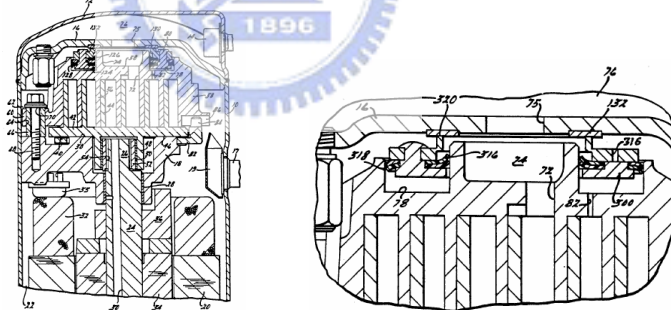
(c) Pressurized gas to the back of fixed scroll
(Issued by Copeland Corp. in US 5,156,539 at Oct. 20, 1992)
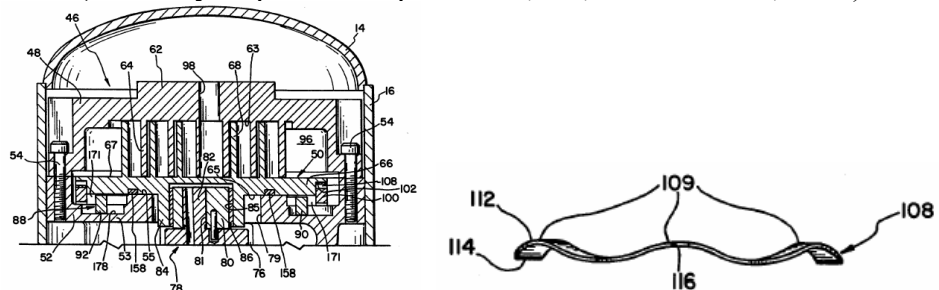
(d) Pressing member
(Issued by Tecumseh Co. in US 5,383,772 at Jan. 24, 1995)

Fig. 2.6 Major embodiments of axial compliant sealing mechanism of STC

37
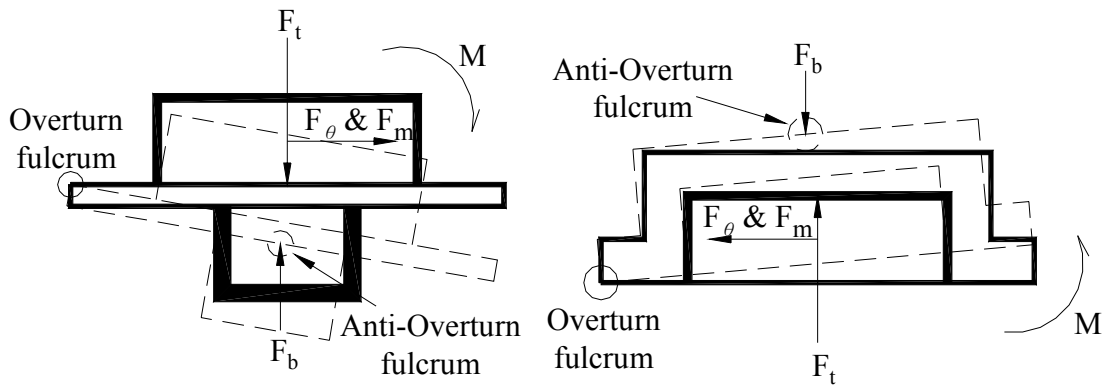
Fig. 2.7 Prior art of guiding pressured fluid as backpressure on scroll member
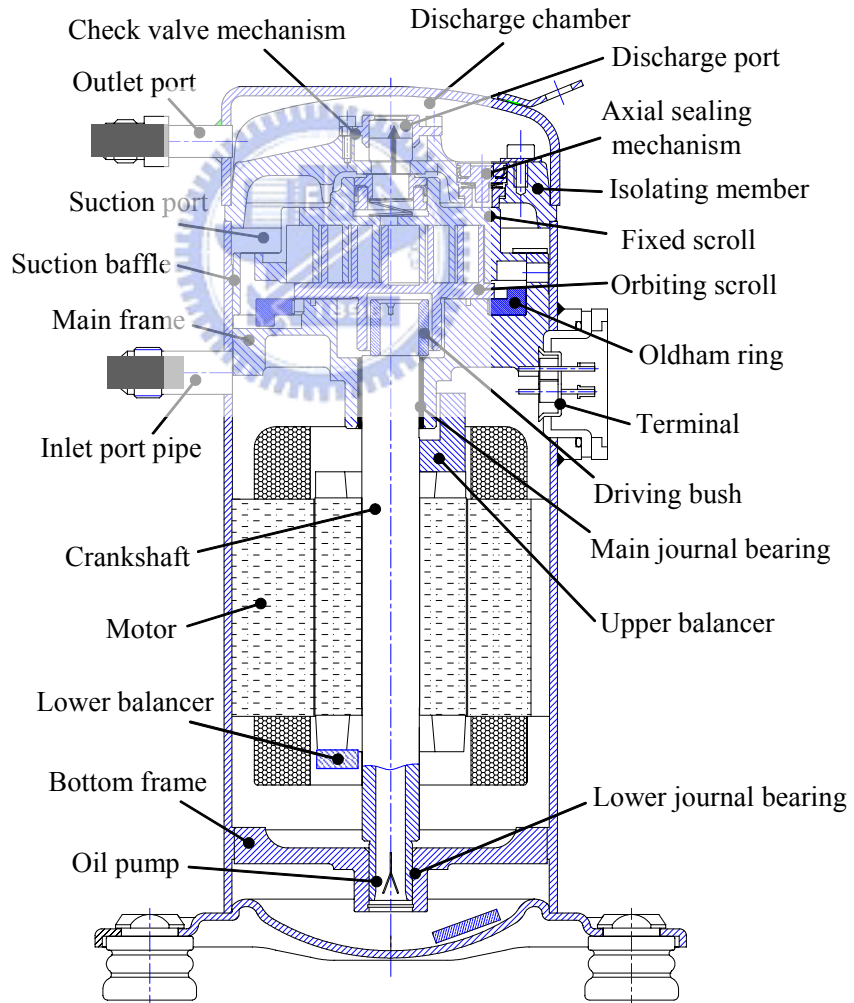
Fig. 2.8 The new STC schematic of this study proposed
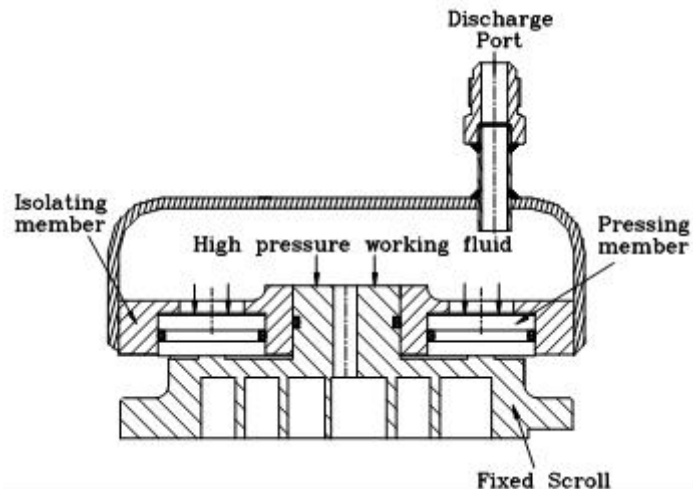
(a) Solid force sealing compliant mechanism structure
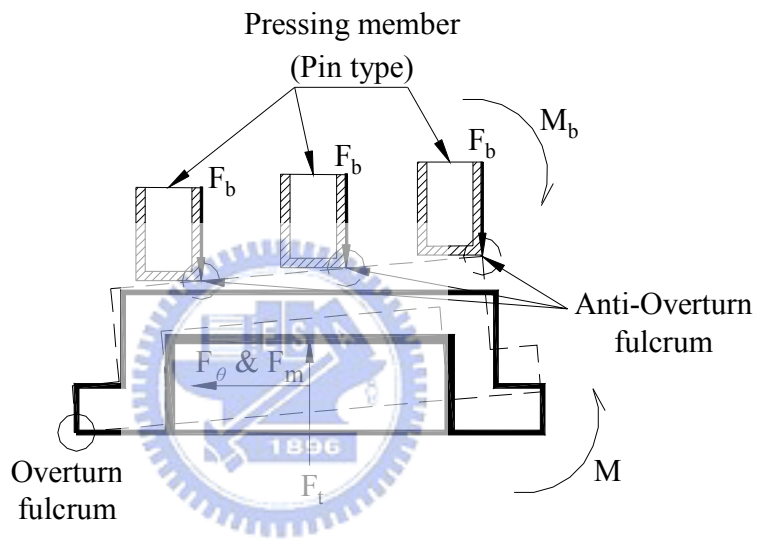
(b) Solid force sealing compliant mechanism with pin-type
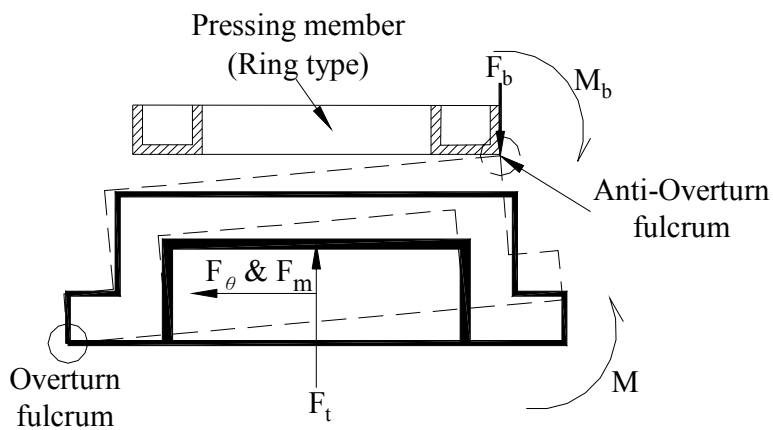
(c) Solid force sealing compliant mechanism with ring-type

Fig. 2.9 STC Solid axial compliant sealing mechanism innovated by this study
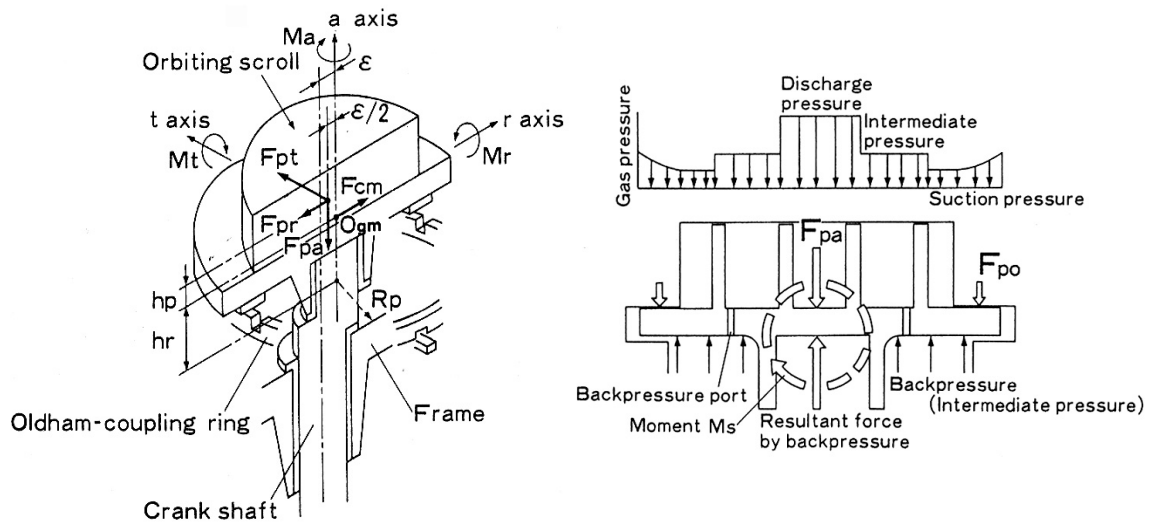
F_{pa} : axial gas force
F_{pr} : radial gas force
F_{pt} : tangential gas force
F_{po} : gas force of the integration of pressure distribution
       in suction pressure area
F_{cm} : centrifugal force
O_{gm} : center of mass of orbiting scroll
R_{p} : reaction force
M_{a} : moment of force about tangential gas
M_{r} : moment of force about radial gas
M_{t} : moment of force about axial gas
h_{p} : distance between the action line of F_{pt} and O_{gm}
h_{r} : distance between the action line of R_{p} and O_{gm}
ε : orbit radius

Fig. 2.10 Detailed forces exerted on the orbiting scroll (Ikegawa *et al.*, 1984)
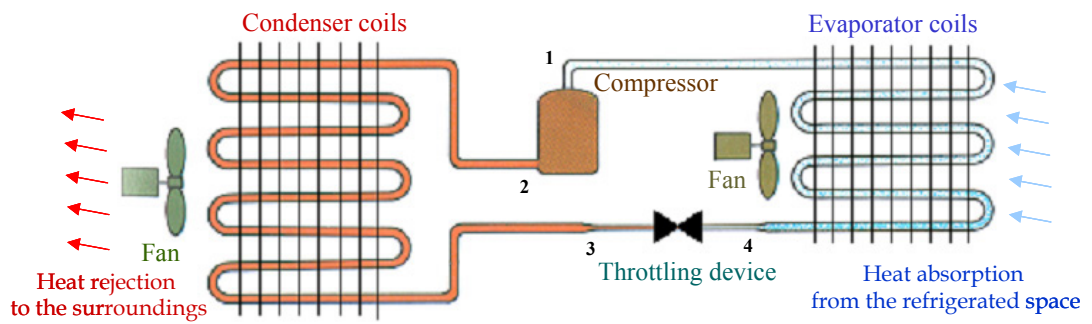
(a) Schematic of vapor compression refrigeration cycle

1-2 polytropic compression process
(in compressor)
2-3 Approximate constant pressure heat rejection process
(in condenser unit)
3-4 Throttling process
(in expansion valve or capillary tube)
4-1 Approximate constant pressure heat absorption process
(in evaporator unit)
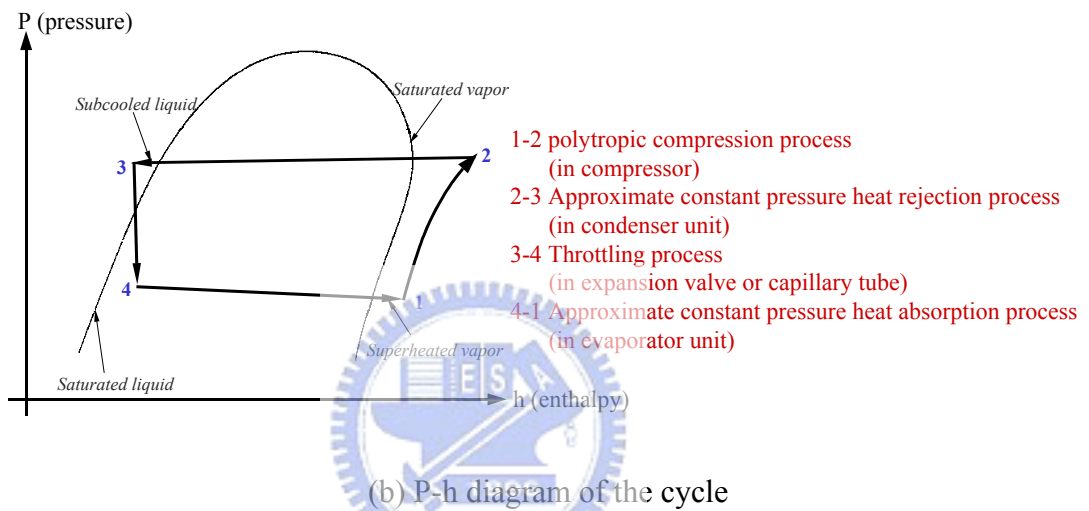
(b) P-h diagram of the cycle

Fig. 2.11 The simplified refrigeration cycle for defining a real air-conditioner
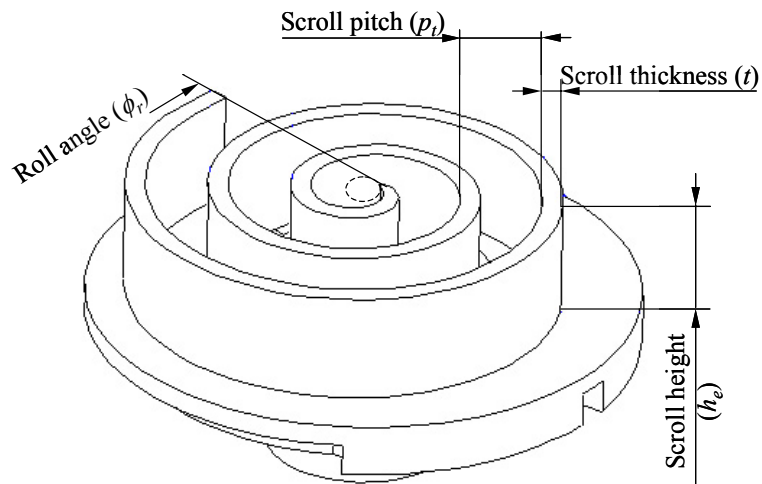
Fig. 2.12 Four major design variables of scroll wrap
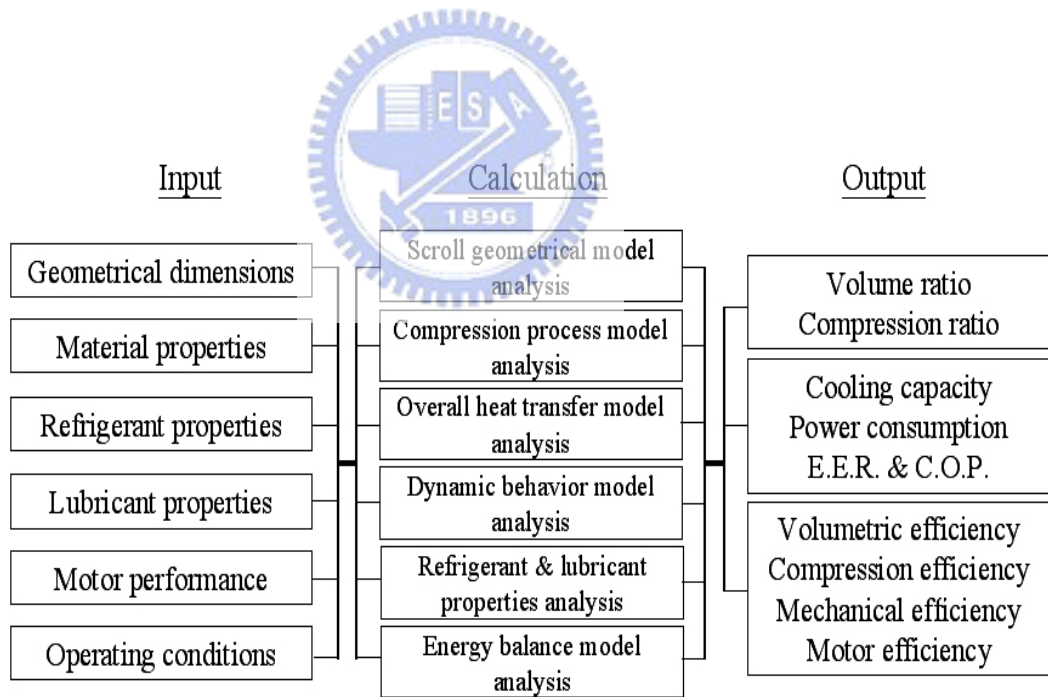
Fig. 2.13 The design structure of STC simulation tool
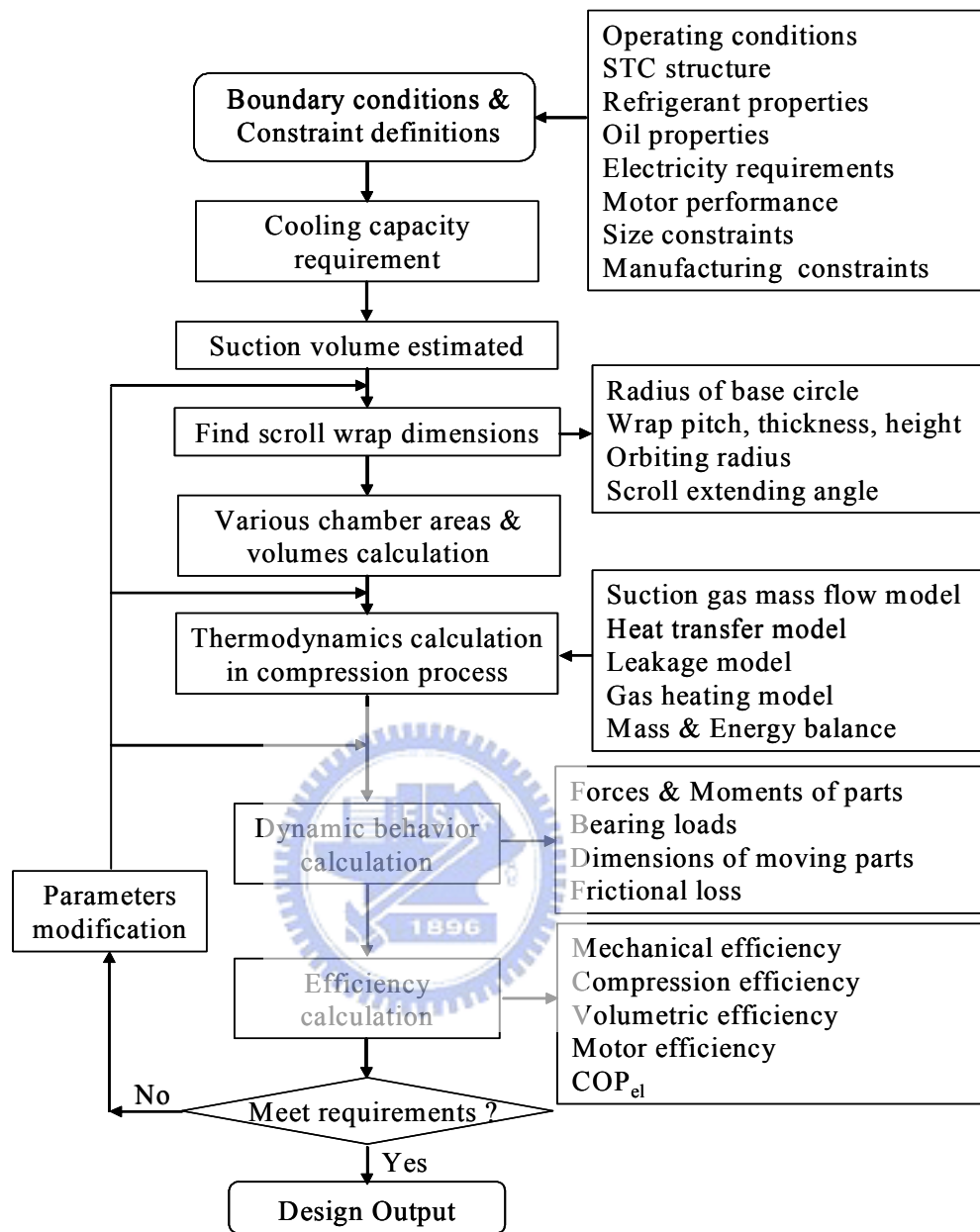
Fig. 2.14 The flowchart for STC performance simulation in this study

CHAPTER 3

THE STC DESIGN MODEL VALIDATION

To bring new STC products to market, the critical issue is to be able to create a practical and validated computer simulation package. In this section, based on the computer simulation package for estimating STC performance that this study developed in Chapter 2, the experimental analysis with R22 refrigerant to validate the results data of which the simulation tool calculated has been carried out. The deviation between predicted and measured data of the verified STC is under 4%. As a result, the validated STC simulation package can be used to guide the STC to practical development.

3.1 Literatures Review

To validate the simulated results with accurate experiments is a very important procedure to put in practice for STC commercial products development. DeBlois and Stoeffler (1988) have taught the detailed techniques used for measuring pressure-crank angle, pressure-volume and suction-compression-discharge processes of scroll compressor. The techniques feature the measurement of shaft speed and instantaneous pressure within the scroll compressor chambers in conjunction with the use of pressure and temperature measuring instrumentations, digital oscilloscope and data acquisition system. Marchese (1992) exhibited an experimental effort to measure the instantaneous pressure acting on an axially compliant orbiting scroll in detail. Therefore, following on the experimental techniques described, a valuable evaluating system to validate the STC simulation tool has been implemented in this

investigation.

3.2 Experimental system description

Figure 3.1 shows the schematic of the laboratory prototype that is semi-hermetic STC with low-side shell structure and applied with R22 refrigerant. Table 3.1 shows the detailed items and functions of each measuring component used in this study that are strategically located in the STC to measure and monitor the temperatures and instantaneous pressures. The developed experimental system include 6 dynamic pressure transducers, 18 K-type thermocouples, one set of proximity probe systems, two pieces of high-pressure feed-through, one set of PC-based monitor systems combined with a digital oscilloscope, power amplifier, and data acquisition system with high-speed.

Figure 3.2 describes the specified 18 temperatures and 6 pressures measuring points that will be observed during experimental validations. The 18 temperatures are used to monitor the thermal status inside of the STC, to ensure the STC in operation is stable and controllable. Table 3.2 lists the detail measuring positions of the 18 located thermocouples.

In particular, the measurement of instantaneous shaft speed and pressure within the scroll elements are useful in understanding the details of the scroll compression process. Six pressure measuring points are located to track continuously from suction to discharge while the STC is in operation. The locations of these pressure transducers should be tuned to precise position with no pressure leakage so as to make sure the detected pressure data is stable and correct. Meanwhile, a magnetic position sensor is used in conjunction with a shaft-mounted single-tooth gear to provide an angular reference position and to trigger the oscilloscope and a second sensor is used is

used in conjunction with a multi-tooth gear to provide instantaneous angular position information.　Figure 3.3 depicts the schematic of this pressure acquisition system and Fig. 3.4 shows the photos of this laboratory STC embedded with several sensors and located on the compressor calorimeter to do the validation test.　Table 3.3 has described the specifications of compressor calorimeter used in this experimental study.

3.3 Experimental Procedure

1. While setting up the experimental system, every measuring instrument must be calibrated, in the meantime, the laboratory STC prototype for testing ought to be assembled and checked to be running properly.　The STC has 18 located thermocouples for measuring temperatures at specified positions, 6 pressure transducers to measure operating pressure inside the compression chambers.

2. The second procedure is to check whether the high-pressure feed through has leakage or not.　In this study, a pressurized refrigerant gas with $10kgf/cm^2$ is given to do this check.　Thereafter, readout information from data acquisition system and digital scope, to verify the measuring data from 18 temperatures, 6 pressures and power consumption is reliable and accurate.

3. Install the laboratory STC for testing in the calorimeter.　Specified 6 operating conditions as Table 3.4 listed have been carried out as the first stage calibration.

4. While the STC is in operation, the HP3852 data acquisition system acquired the detecting data of temperature and pressure versus crankshaft angle position based on 100kHz catch speed, and the measuring data have been collected into the personal computer, in the meantime, the waveforms of pressure versus crankshaft angle also have been plotted.

5. Analyze these measuring data and check the deviations between real detected and

the calculated results.

6. Revise the experimental system and the developing STC simulation package, to validate experiments continuously until the deviation of results between prediction and measurement can be accepted in practice.

3.4 Experimental Results

3.4.1 First stage calibration

1. At first stage calibration, the STC are working on lower pressure conditions as conditions 1 and 2. Figure 3.5(a) shows the STC has over-compression phenomenon while it is operating at 40Hz. The discharge pressure is raised to 20kgf/cm^2 as conditions 3 and 4, and operated at 60Hz. Note that the same results of over-compression status have been shown as Fig. 3.5(b) and also presented that the higher suction pressure of STC will produce higher over-compression pressure.

2. To make sure the over-compression problems, the STC is operated at conditions 5 and 6 with 50Hz and 60Hz, respectively. The over-compression appears as usual even though the STC is driven at different crankshaft speeds. Figure 3.5(c) shows the tested results.

3. Above experimental results depict the discharge port dimension of fixed scroll has some problems because the over-compression is always present in spite of the STC operating at lower pressure ratio or at higher pressure ratio conditions.

4. Furthermore, the results of above experiments also show that the captured pressure from piezoelectric pressure transducers have the interlaced phenomenon during intermediary pressured gas (P2, P3 locations) progress to higher pressure chambers (P4, P5 locations) in the compression process. This phenomenon expresses that the locations of piezoelectric pressure transducers should be tuned so as to prevent

the interference of pressure detection while the pressured gas is progressing.

3.4.2 Second stage validation

1. After modifying the discharge port dimension and tuning the locations of P2~P5 of the piezoelectric pressure transducers, the over-compression and interlaced phenomenon are minimized such as Fig. 3.6 shows.

2. Based on above calibrations, Fig. 3.6 also depicts the comparison of pressure versus crankshaft rotation angle between predicted results and measured results of which the STC is operated at ARI conditions, that condition No. 1 of Table 3.5 shows.   The acceptable deviation of results between computer simulation and testing measurement is shown as Table 3.5.

3. From Fig. 3.6 shows, the deviation of pressure versus crankshaft rotation angle between predicted results and measured results is very small.   Meanwhile, Fig. 3.7 also shows the 18 temperature measurements data at six different operation conditions, which indicates the laboratory STC prototype has stable thermal distribution within the compressor housing.   This measurement data is extremely valuable when used in predicting STC performance with the developed STC simulation package.

4. As Table 3.5 shows the results, the maximum deviations of cooling capacity, power consumption and COP_{el} between calculated results and real measured results are 1.31%, 2.89% and 3.89%, respectively.

3.5 Conclusions

The study results in this section are summarized below:

(1) A practical computer estimation package of STC has been constructed to evaluate

overall performance of STC in detail.

(2) Using an on-line data acquisition system combined with experimental measurement techniques, the pressures and temperatures during the compression process can be captured to understand the details as the scrolls operate during the compression process. Meanwhile, from the detecting data at first stage, the experimental system has been calibrated accurately.

(3) After the calibration of temperature and pressure measurements, the validation between calculated results and real measured data has been carried out. Finally, the deviation of the verified STC's performance between predicted results and experimental measured results, are under 4%. It means the validated STC simulation package that this study developed, can be used in the STC practical design works.

(4) Based on the research results and technical facilities, the other validations about the temperature distribution on scrolls and the distribution of the thermal deformation on scrolls have been approached continuously by Lin *et al.* (2005) and given a practical reference for the developed STC simulation tool.

Table 3.1 The items and functions of measuring components and instruments.
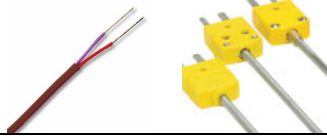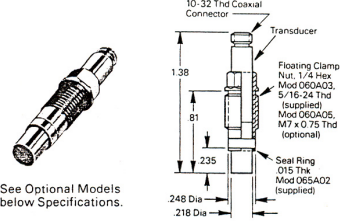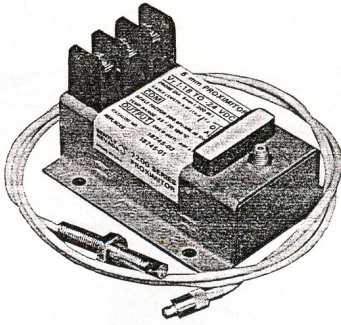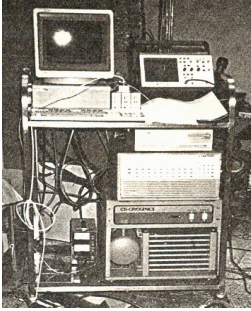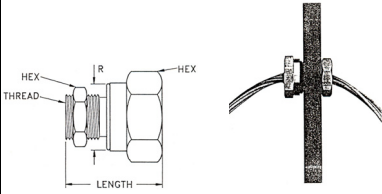
Items & Functions	Photos

1. T-type thermocouples and connectors:
 	
    Max. pressure rating is 400psi,
 	
    Operating temp. is – 45 ~ 150ºC	

2. PCB 111A20 Dynamic pressure transducers: Pressure measuring range: (1) PCB 111A21: ~125psi, (2) PCB 111A26: ~500psi	

3. Bently Nevada 7200 proximity transducer system:
 	
  (1) High-pressure feed through:
 	
    Max. pressure rating is 400psi,
 	
    Operating temp. is – 45 ~ 121ºC
 	
  (2) Proximity probe:
 	
    Power: -17.5 ~ -26VDC,
 	
    calibration range: 2mm (80Mils),
 	
    Scale factor: 200MV/Mil,
 	
    Operating temperature: -34~177ºC
 	
  (3) Proximitor:
 	
    Operating temperature: -51~100ºC,
 	
    Power: -17.5~-26VDC,
 	
    Scale factor: 200MV/Mil	

4. PC based monitor system: Personal computer with 200Hz CPU, PCB 482A10 Amplifying power unit, HP 54602B digital scope operated at 150MHz, HP 3852A Data acquisition system with 20channels. HP 82341D HP-IB interface card.	
5.Others: OMEGA Feed through: Max. pressure is 2000psi	

Table 3.2 The measuring points of temperatures

Symbols	Measuring points	Notes
T1	Discharge port of scroll set	To measure the accurate discharge temperature after compression operation
T2	Discharge port at isolating member	
T3	Pressing members of axial sealing mechanism	
T4	Back plate of fixed scroll	To monitor the fixed scroll temperature variations
T5	Orbiting scroll plate	To monitor the orbiting scroll temperature variations
T6	Inside hole of motor stator	To monitor the motor temperature variations
T7	Upper side of motor stator coils	
T8	Middle side of motor stator coils	
T9	Lower side of motor stator coils	
T10	Lower journal bearing	To measure the accurate suction temperature before inlet to suction port of scroll set
T11	Upper side of isolating member	
T12	Moddle side of isolating member	
T13	Lower side of isolating member	
T14	Suction inlet of scroll set	
T15	Driving bushing	To measure each bearing temperature variations and to monitor the oil supply status
T16	Main journal bearing	
T17	Upper side of motor stator	
T18	Oil sump	

Table 3.3 The specifications of calorimeter used for measuring STC performance.

Items	Specifications	
General description of system	According to ISO 917, this equipment is designed for fully automatic measurements	
Compressor loop refrigerant	R22	
Capacity measuring range	1500W~12000W	
Measuring method and required accuracy	(1) The equipment is employed for the secondary refrigerant system and liquid flow meter system. (2) The value of the estimated error for the cooling capacity from the secondary refrigerant system calculated should be lower than liquid flow meter system. (3) The deviation of cooling capacity and COP_{el} measuring results between the secondary refrigerant and liquid flow meter system should be within ± 4%. (4) The accuracy of refrigerant flow-measuring instruments should be within ±1% (5) The accuracy of speed-measuring instruments should be within ±0.75% (6) Repeatability ≤ 1%	
The background noise of compressor chamber	≤ 40dBA when Fan is closed	
Control items	Range	Stability
Compressor discharge pressure	10~30 kg/cm^2	± 0.1 kg/cm^2
Compressor suction pressure	1.67~9.28 kg/cm^2	± 0.15 kg/cm^2
Compressor suction temperature	-25~50℃	±0.5℃

Table 3.4 The operating conditions used for the first stage calibration.

Condition No.	Discharge pressure (kgf/cm^2)	Suction pressure (kgf/cm^2)	Motor operating frequency (Hz)
1	10	2	40
2	10	2	60
3	20	4	60
4	20	5	60
5	20.86	5.36	50
6	20.86	5.36	60

Table 3.5 The comparisons between simulations and experimental measurements.

Operating Conditions			Cooling Capacity (W)			Power Consumption (W)			COP_{el} (W/W)		
No.	Evap. Temp.	Cond. Temp.	Comput.	Real	Error (%)	Comput.	Real	Error (%)	Comput.	Real	Error (%)
1	7.2℃	54.4℃	9244.22	9247.59	-0.04	3347.1	3329.4	0.53	2.76	2.78	-0.84
2	5.0℃	40.0℃	9890.50	9938.53	-0.48	2493.7	2567.8	-2.89	3.98	3.87	2.70
3	5.0℃	50.0℃	9010.92	9007.90	0.03	3008.3	3038.4	-0.99	3.00	2.97	1.18
4	5.0℃	60.0℃	7948.99	7846.18	1.31	3659.0	3751.1	-0.02	2.17	2.09	3.89
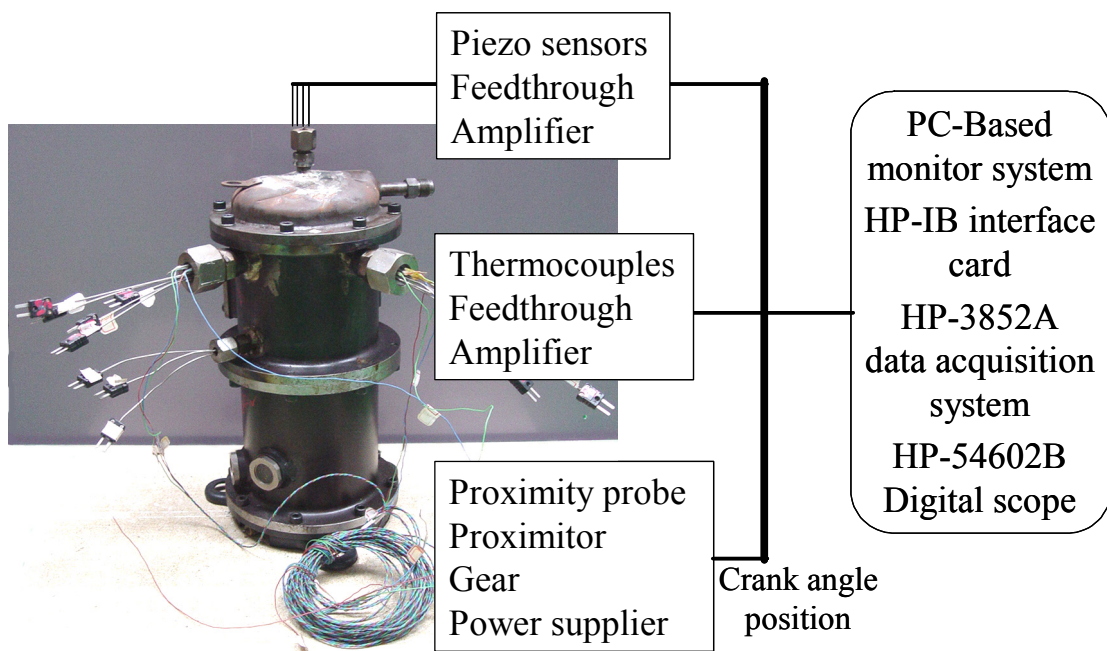
Fig. 3.1 Experimental apparatus for STC model validation in this study

(a) 18 thermocouple locations for
temperature measurements

(b) 6 piezo sensor locations for pressure
measurements
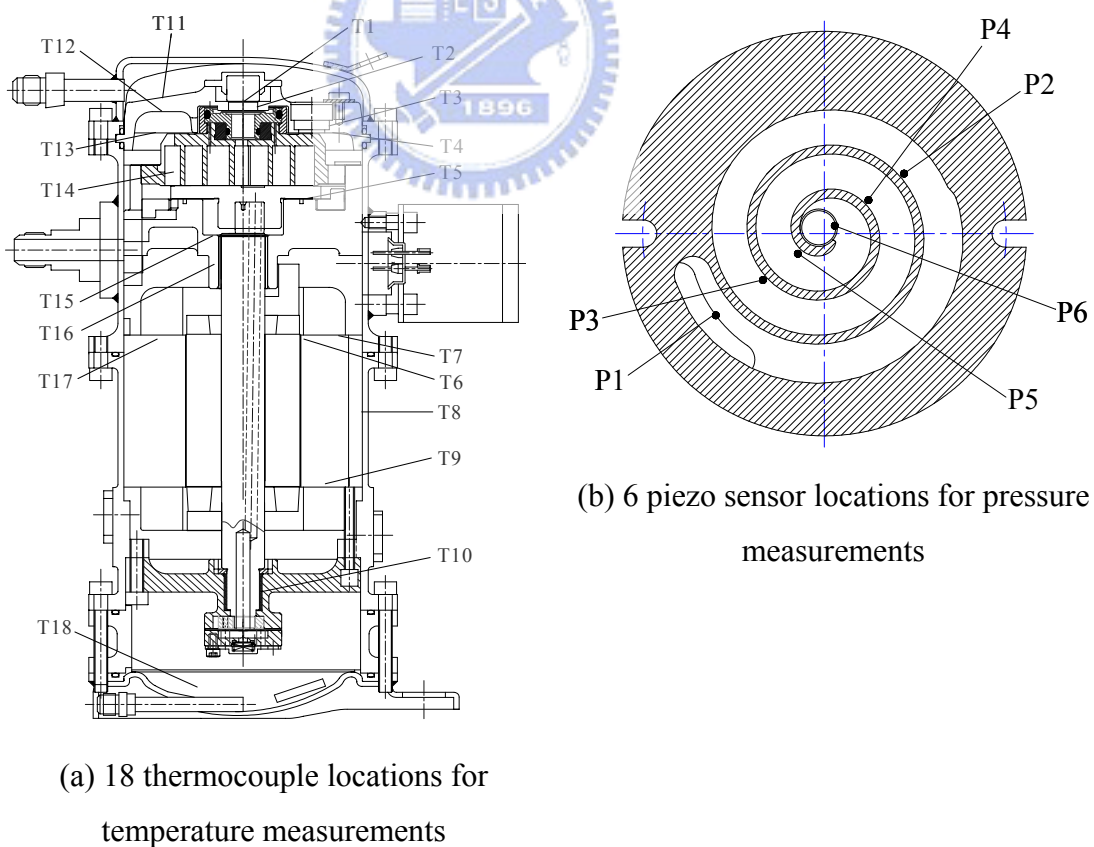
Fig. 3.2 Temperatures and pressures measuring locations for experimental validations
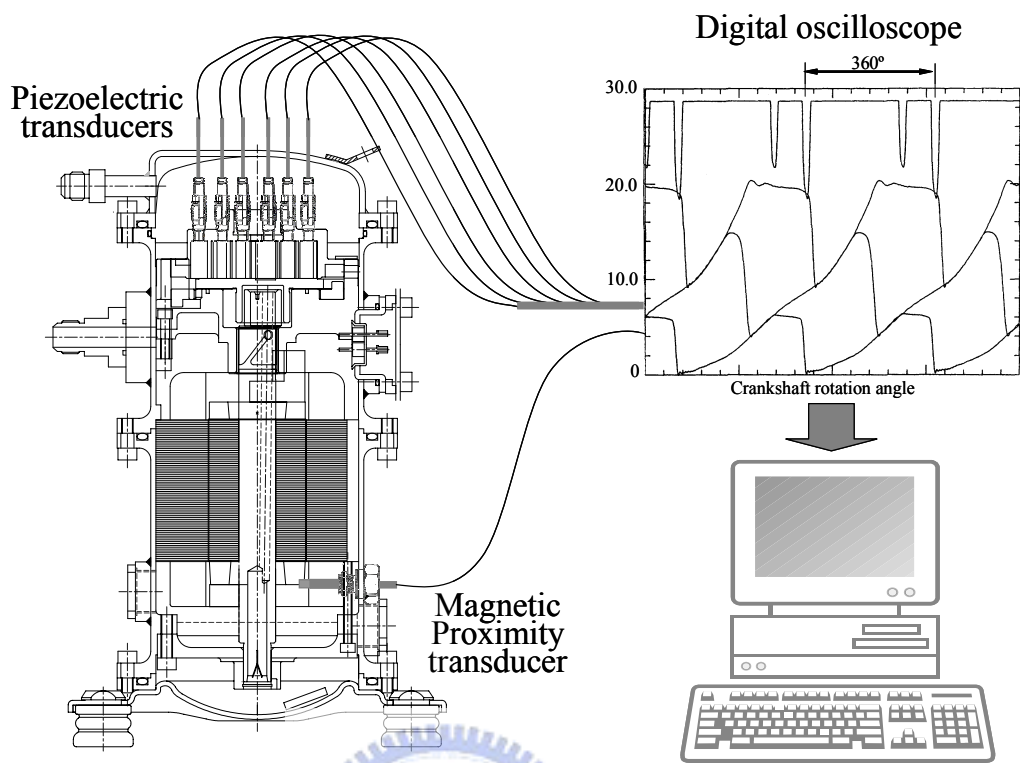
Fig, 3.3 Experimental schematic for measuring STC instantaneous pressures

(a) Laboratory STC assembly
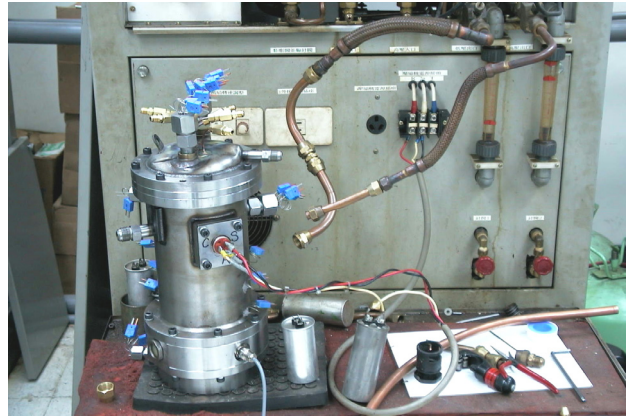
(b) Laboratory STC located in test bench
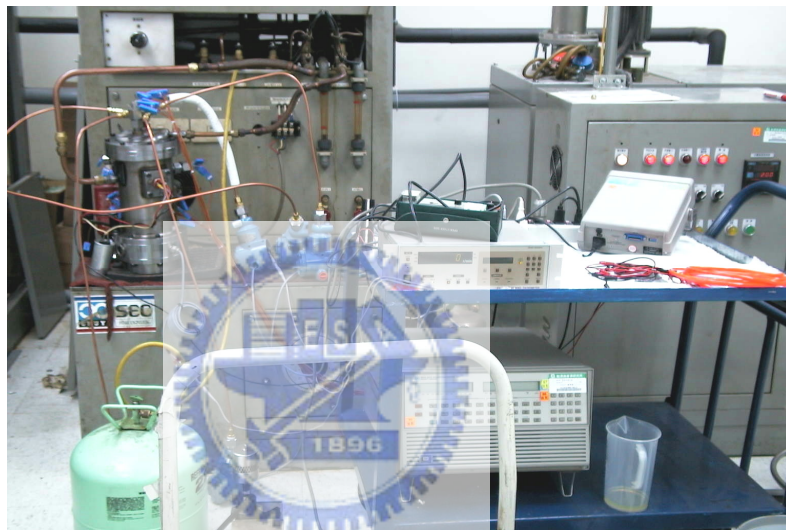
(c) Testing feature

Fig. 3.4 Photos of laboratory STC used for validation test in this study
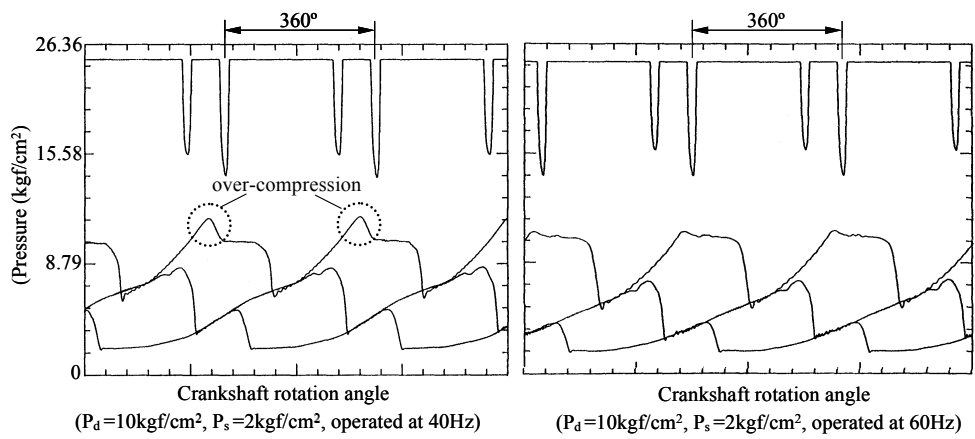
(a) The results of operating conditions 1 and 2
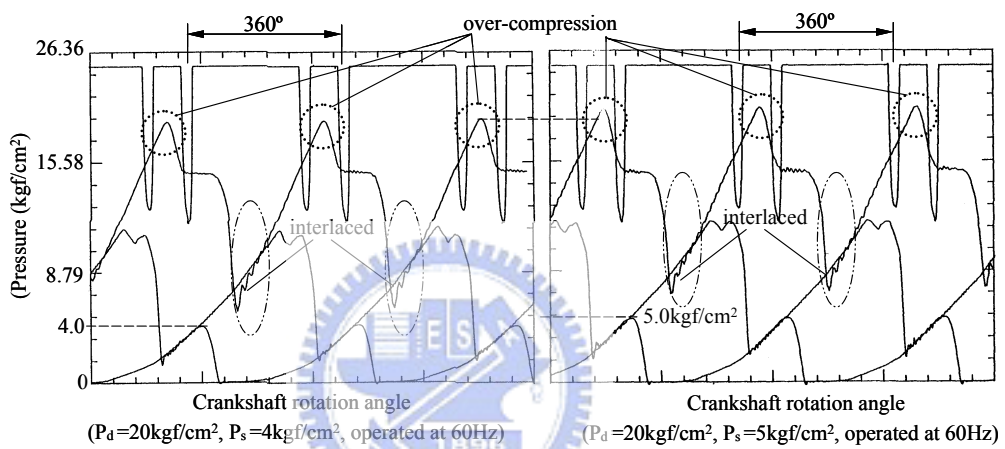
(b) The results of operating conditions 3 and 4
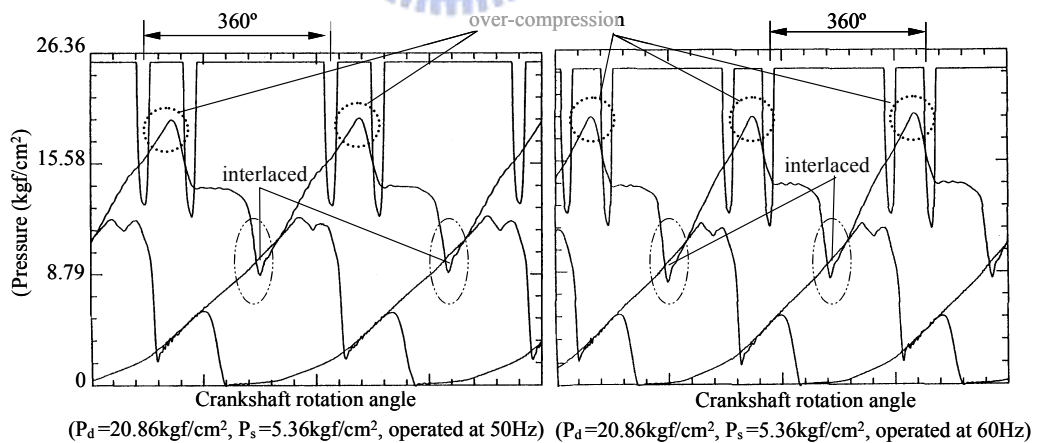
(c) The results of operating conditions 5 and 6

Fig. 3.5 The experimental results at first stage validation
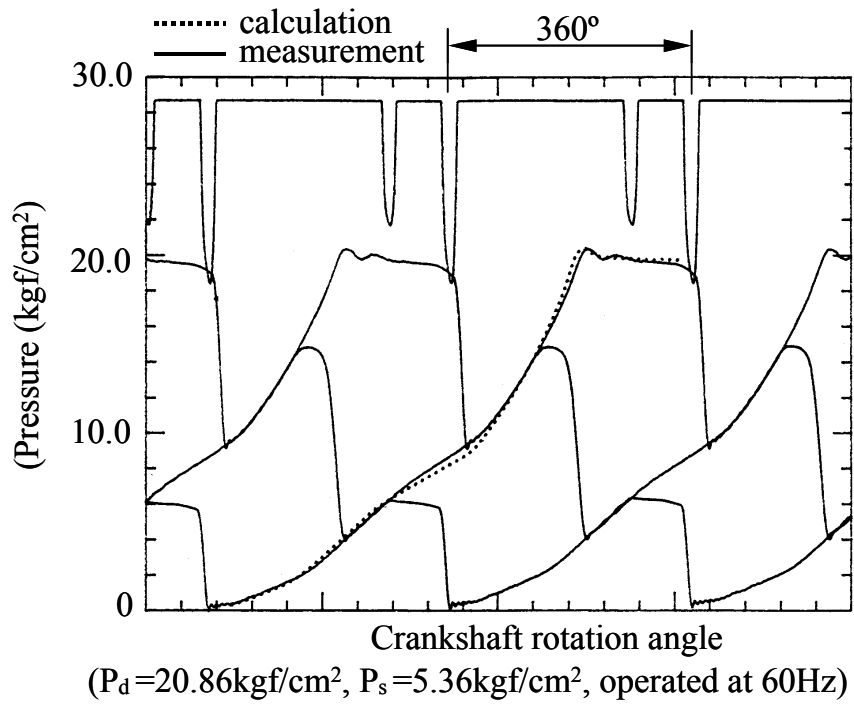
Fig. 3.6 The comparison between calculated results and measuring results

Symbols	Units	Condition No.					
		1	2	3	4	5	6
p_s/p_d	kgf/cm^2	2/10	2/10	4/20	5/20	5.36/20.86	5.36/20.86
f_m	Hz	40	60	60	60	50	60
T1	℃	74.00	75.21	103.20	96.11	104.60	105.56
T2	℃	68.11	70.22	92.10	84.33	91.50	92.11
T3	℃	58.89	60.12	79.01	72.11	78.09	78.89
T4	℃	67.33	72.23	89.20	81.56	89.10	89.78
T5	℃	51.72	52.12	58.20	55.72	59.30	60.44
T6	℃	63.89	65.41	83.20	72.78	84.00	85.00
T7	℃	44.44	45.12	61.01	57.22	61.80	62.78
T8	℃	62.78	63.12	80.21	71.11	81.21	82.22
T9	℃	44.44	45.12	55.21	50.00	57.22	57.22
T10	℃	43.44	43.89	51.20	50.33	51.92	53.94
T11	℃	58.89	61.12	79.12	72.11	78.10	78.89
T12	℃	53.67	54.18	65.78	60.56	65.01	65.56
T13	℃	48.22	49.20	53.12	51.22	54.12	55.39
T14	℃	33.67	33.91	35.01	34.44	35.89	36.67
T15	℃	55.28	56.10	60.21	59.89	64.21	64.94
T16	℃	48.72	49.11	51.50	53.33	56.41	57.44
T17	℃	43.39	44.17	51.20	48.78	52.12	53.22
T18	℃	42.78	43.12	50.20	49.61	51.91	53.22
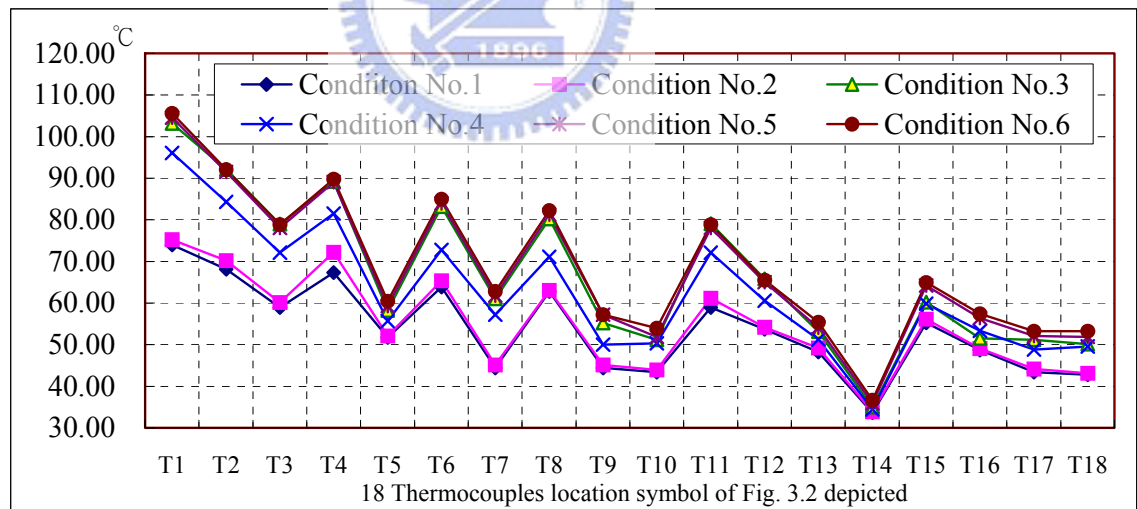
Fig. 3.7 The 18 temperatures measurement data at 6 operating conditions

CHAPTER 4

STC FAMILY DESIGN WITH OPTIMIZATION METHOD

One critical problem in the mass production of commercial STC is that their key components—including fixed scroll, orbiting scroll, Oldham ring, mainframe and crankshaft—all require the use of very high precision machining skills. To help in lowering the complexity, cost and lead-time of product development, a systematic design method with optimization for developing a family of STC is proposed. Such a family design needs to meet two goals: (i) a series of STC with multi-specified cooling capacities should have the same outside shell diameter and use common key parts or casting molds, (ii) the performance of each specified capacity of the developed STC should meet market requirements.

In addition to using the general design optimization model which includes multi-variable, direct search and inequality constraints, both interactive session and discrete variable design optimization skills have also been employed in this study. Meanwhile, based on the balance between cost, manufacturing effectiveness and product performance, the STC family design used for a series of air-conditioners, has been carried out, and the STC family with a range of 5200W~9800W in four models has been implemented. The performance of each model is also verified and satisfies the required objectives.

4.1 Literatures review

From a technical point of view, Etemad and Nieter (1989) provided a simple and easily understood optimization design approach to evaluate the effect of three relevant

physical parameters on manufacturing, design limitations and energy losses for STC. Ooi (2005) presented a design optimization algorithm coupled with a mathematical model of the rolling piston compressor by employing multi-variables, direct search and constrained optimization technique. Although these two studies could provide some guides for STC optimization design algorithm and design procedure, the details of optimum design to put in practice were not demonstrated.

Kota *et al.* (2000) has introduced the use of commonality components in product family design to help in lowering the complexity, cost and lead-time of product development. In addition, Hernandez *et al.* (2001) described a mathematical decision model to carrying out a family design evaluation for absorption chiller development that provided a guideline for the systematic design of a product family.

This paper proposes a family design procedure that combines with the optimization method (Arora, 2004) and the STC simulation package that this study developed to use in STC commercial product development.

4.2 Description of the design process

Fig. 2.9 lists the cross section and major components of a hermetic STC used in this study. This STC's structure consists of a low-pressure-shell design with a solid axial compliance mechanism. The details of the STC design structure and the design model, have been described in Chapter 2 of this dissertation.

In STC family design, the first decision of the design process is to select a common outside diameter for the main shell of the STC. This selection is made based on the inside space constraints of specified air-conditioners and the motor size that can meet the torque requirements for the developed STC.

After the decision is made on the common outside diameter, the most important

design process is to define the objective functions for the optimization approach. In this study, the requirement is to obtain the maximum coefficient of performance based on electrical power input (COP_{el}) for each model of the developing STC family. Therefore, the COP_{el} is selected as the objective function and defined as the ratio of useful cooling capacity, $\dot{Q}_c$, to the overall power consumption of the motor, P_{motor} :

$$COP_{el} = \frac{\dot{Q}_c}{P_{motor}} \tag{4-1}$$

The next process is to define the design variables and related constraints, and then evaluate the feasible dimensions and performance for each specified STC to meet these requirements. To realize the controllable design variables and the constraint functions, the following steps are carried out.

Step 1: Define the design variables that have the most effect on the cooling capacity, $\dot{Q}_c$, and the overall power consumption of the motor, P_{motor} .

$$\dot{Q}_c = \left\{ \eta_v \cdot \omega_c \cdot (h_{in} - h_{out}) \cdot \rho_s \right\} \cdot \left\{ [2 \cdot (\frac{\phi_r}{360} - \frac{1}{4}) - 1] \cdot \pi \cdot p_t \cdot (p_t - 2t) \cdot h_e \right\} \tag{4-2}$$

$$P_{motor} = \frac{P_{shaft}}{\eta_{motor}} = \frac{T_{shaft} \cdot \omega_c}{\eta_{motor}} = \frac{\left[F_{B\theta} \cdot (\frac{p_t}{2} - t) + \sum M_B \right] \cdot \omega_c}{\eta_{motor}} \tag{4-3}$$

Because the refrigerant properties, operation conditions and suction paths can all be specified in the same family, the cooling capacity, $\dot{Q}_c$, can be evaluated from four major design variables: ϕ_r, p_t, t and h_e. In the meantime, the journal bearings and the Oldham coupling used in the developed STC family are the same, so it should be noted that this model makes it possible to obtain the motor efficiency and compressor speed. Several work losses and the overall power consumption, P_{motor}, can all be evaluated while the design variables of p_t and t are defined.

Step 2: Set up the design constraints in order to meet the practical requirements of the scroll wrap manufacture and STC assembly.

To communicate with the engineering experts, three constraints should be considered. The rigidities of the scroll wrap and the cutting tool are the constraints for scroll wrap manufacturing, and the outside diameter limits of the scroll is the constraint for STC assembly. The correlations between design variables and constraints are defined respectively as follows:

$$G_w = \frac{h_e}{t} \tag{4-4}$$

$$G_c = \frac{h_e}{(p_t - t)} \tag{4-5}$$

$$D_{o\_max} = D_{o\_motor} - \delta_a \tag{4-6}$$

From involute spiral definition (Ikegawa *et al.*, 1984), the outmost curve coordinates that define the minimum required outside diameter D_{ob_min} of the orbiting scroll are formulated as

$$\begin{aligned} x_{ob\_o} &= r_b \left[\cos(\phi_r) + \phi_r \sin(\phi_r) \right] \\ y_{ob\_o} &= r_b \left[\sin(\phi_r) - \phi_r \cos(\phi_r) \right] \end{aligned} \tag{4-7}$$

where $r_b = \dfrac{p_t}{2\pi}$, and Eq. (4-7) gives the limitation for ϕ_r, p_t as

$$D_{ob\_min} = 2 \cdot \sqrt{x_{ob\_o}^2 + y_{ob\_o}^2} = 2 \cdot r_b \sqrt{1 + (\phi_r)^2} = \frac{p_t}{\pi} \sqrt{1 + (\phi_r)^2} \le D_{o\_max}, \tag{4-8}$$

$$p_t \sqrt{1 + \phi_r^2} \le \pi \cdot D_{o\_max} \tag{4-9}$$

From Morishita *et al.*'s (1984) derivation and Eq. (2-12), the roll angle of the scroll wrap is roughly obtained as

$$\phi_r \approx \frac{v_r \cdot (3 - \dfrac{\theta_d}{180^\circ}) + 1}{2} \cdot 360^\circ \tag{4-10}$$

where the built-in volumetric ratio v_r can be derived from the polytropic compression laws,

$$v_r = \left(\frac{v_s}{v_d}\right) = \left(\frac{p_d}{p_s}\right)^{\frac{1}{n}}$$ (4-11)

in which p_s and p_d are the suction and discharge pressures defined by the operation conditions depicted in Table 4.1 and Fig. 2.11. The polytropic index n can be measured by the laboratory experiment (DeBlois and Stoeffler, 1988), which 1.11 is selected for this study.

Eqs. ((4-4) to (4-11)) clearly define the constraints of ϕ_r, p_t, t and h_e for the STC family design.

Step 3: Select a proper and robust optimization algorithm to perform detailed simulation and iteration, and to obtain the optimum solutions for practical applications.

Summarize the Eq. (4-2) ~ Eq. (4-9), the objective function requirement can be defined as:

$$\max imize \quad COP_{el} = f(\phi_r, p_t, t, h_e)$$ (4-12)

and subjected to the constraints:

$$LowerLimits \leq G_w, G_c, D_{o\_\max} \leq UpperLimits$$ (4-13)

Since the objective function and constraints are non-linear, the suitable optimization technique was a direct search method (Ooi, 2005). Meanwhile, the design variables must monitor the progress and be selected from a given set of values with practical experience. An algorithm combined with interactive session and discrete variable design optimization (Arora, 2004), has been employed in the current study. Fig. 4.1 depicts the optimization process.

Interactive design optimization algorithms are based on utilizing the designer's input during the iterative process. They must be implemented into an interactive environment to report the status of the calculation results and then the designer can specify what needs to be done depending on the current design conditions. In this study, an analysis module of STC simulation package and graphical display to draw conclusions play a part in the decision making during the interactive optimization process. Fig. 4.2 shows the basic simulation flowchart of the developed STC computer package.

A design variable is called discrete if its value must be selected from a given finite set of values to meet the parametric design requirements, fabrication limitations and cost effectiveness. Therefore, ϕ_r, p_t, t and h_e of the four design variables is given as discrete variables to put in practice. In the meantime, the Equal Interval Search technique (Arora, 2004) is used in this approach.

By using the optimization algorithm combined with the graphical solution method, the feasible region of each design variable can be identified. Finally, the optimum solutions for this family design are obtained.

4.3 Case study of STC family design

The required operation conditions and specifications used in the case study of STC family evaluation are given in Tables 4.1 and 4.2. The design constraints, defined in Table 4.3, are based on the facility limitations and capabilities of manufacturing and assembling STCs. An outside diameter of 139 mm for the motor stator is selected as the design base.

4.3.1 Initial design

First, the motor performance data must be collected from the motor supplier or from experiments using the dynamometer. Under the specified operational conditions (as defined in Table 1), the R22 refrigerant properties can be obtained from REFPROP 6.01 (1998). Thereafter, the theoretical pressure ratio, mass flow rate and displacement can be roughly calculated from Eqs. ((2-1) to (2-3)). Based on the suggestion of the scroll manufacturer, $t = 2.5mm$ and $\phi_r = 1050°$ are selected as initial design values. Given the limitations of the outside motor diameter and assembly tolerance, 100 mm is selected as the maximum outside diameter of the scroll set.

Table 4.4 shows the initial design data in this STC family development. The four design variables can be evaluated from the equations outlined above using an iterative process.

4.3.2 Search direction approach

The optimization approach used in this study first requires is that a search direction for the multiple design variable variations should be identified. Figs. 4.3 and 4.4 illustrate the direction of the scroll wrap height, the sizes resulting from the different steps in the search direction approach to meet cooling capacity requirements under the constraints of D_{o_max}, G_w and G_c based on the initial design data of $t = 2.5mm$ and $\phi_r = 1050°$. These results underscore three important outcomes of using this approach:

(1) On the basis of one set of thickness t and a roll angle ϕ_r of the scroll wrap selections, Eq. (4-2), subjected to a change in the search direction of scroll height h_e matched with pitch p_t of the scroll wrap, can fit to each required cooling

capacity requirement.　　The allowances are listed in Table 4.4.

(2) For a specified cooling capacity requirement, increasing h_e, G_w and G_c will increase, but D_{ob_min} reduce.　　To meet the constraints of $D_{ob\_min} \leq D_{o\_max} \leq 100mm$, $G_w \leq 8.5$, $G_c \leq 2.5$, the feasible region of h_e can be given.　　In this initial design case, the feasible region of h_e is between 16 mm and 21.3 mm.　　Fig. 4.3 has presented the approach results clearly.

(3) At specified cooling capacity, increasing h_e can improve COP_{el} as Fig. 4.4 shows.

4.3.3 Optimization process

Once the search direction of the four design variables of ϕ_r, p_t, t and h_e have been tuned to meet the objective requirements for each specified cooling capacity with interactive process, the optimization approach with a detailed simulation and iteration is carried out.

1. First phase evaluation:

In the first-phase evaluation, the basic data variations of t are 2.5mm ~ 3.3mm with a step size of 0.05mm ~ 0.1mm, and ϕ_r is $1050°$~$1250°$ with a step size of $20°$ ~$50°$, respectively.　　As shown in Table 4.4, by individually applying a search direction approach to each specified set of t and ϕ_r, a maximum COP_{el} can be arrived at for every required cooling capacity subject to practical design limits.　　Fig. 4.5 shows the simulation data and depicts the following optimum results:

(1) Except in the case of 5200W, the maximum COP_{el} of each required cooling capacity in this STC family occurs at $\phi_r = 1150°$, despite various thicknesses of scroll wrap.　　Moreover, even though the maximum COP_{el} for 5200W is located at $\phi_r = 1120°$, the COP_{el} deviation between 1120º and 1150º is within 0.1%.

(2) The optimum points of scroll wrap thickness are 3.2mm, 3.3mm, 2.6mm and 2.6mm for 9800W, 8100W, 6800W and 5200W, respectively. Nevertheless, for 8100W, the COP_{el} deviation between 3.3mm and 3.2mm is within 0.1%. Table 4.5 shows the detailed design variable data for achieving the maximum COP_{el}.

(3) As a result of the above data, two thicknesses of scroll wrap are proposed to meet the objective function requirements—2.6mm for 5200 and 6800W, 3.2mm for 8100W and 9800W. At the same time, 1150° of roll angle is selected as the optimum value. Thereafter, only the two design variables h_e and p_t need to be tuned continuously.

2. Second phase evaluation

As already discussed, increasing h_e can improve the COP_{el} at specified t and ϕ_r, but G_w and G_c will limit the increment of h_e. In addition, the orbiting radius of $r_{or} = \dfrac{p_t}{2} - t$ must also be considered because the r_{or} will influence the decision on the crankshaft dimension. Therefore, the following two approaches are carried out in this second-phase evaluation for this STC family design:

(1) The first approach uses the same orbiting radius for the STC family. Under a maximum height of scroll wrap with G_w, G_c constraints (see Table 4.6(a) for the solutions), the COP_{el} cannot meet the objective requirement of 5200W.

(2) The second approach opens the restraint of the orbiting radius by drawing on the two thicknesses defined in the first-phase evaluation to propose two types of orbiting radius for this STC family. As Table 4.6(b) shows, all result data can satisfy the COP_{el} objective requirements under specified constraints and present the final optimum solutions for this study.

4.3.4 Prototyping and experimental validations

Subsequent to finding the optimum solutions for the STC family, this study implements four family prototypes.　A calorimeter with a semi-anechonic chamber (a background noise of 40dBA) and a sound level meter are used to measure the cooling capacity, COP_{el} and noise level of the developed STC series under investigation. Table 3.3 has presented the specifications and measuring method of this calorimeter.

Fig. 4.6 shows one hermetic sample of the developed STC family prototype and its major components.　Figure 4.7 shows the comparisons of cooling capacity and COP_{el} between the experimental and calculated results.　The maximum deviations for cooling capacity and COP_{el} are under 2.53% and 1.69%, respectively, suggesting that the research has successfully achieved its desired results.

Table 4.7 illustrates the common sharing of each major component in this STC series.　In all, 58% of shared components are identical, with a total cost share of 26.85%, while 26% of shared parts are made with the same mold but have partially different dimensions, with a cost share of 62.08%.　Only 16% of components, with a cost share of 11.07%, are wholly different for each specified STC in this family.

4.4 Results and Discussion

This study has demonstrated a systematic and practical process for optimization of STC family design that allows the COP_{el} for each specified capacity to meet the objective requirements of commercialization.　Seven important aspects of this research are summarized below:

(1) The study implemented a practical optimization algorithm combined with interactive session and discrete variables techniques.　Meanwhile, the developed

STC simulation package and graphical display method play a part in the decision making during the interactive optimization process.

(2) This investigation selected as its design variables the four geometrical factors of scroll wrap—ϕ_r, p_t, t and h_e—that can define the major dimensions of the developed STC family.

(3) Based on manufacturing and assembling expertise input, and after the COP_{el} was defined as the objective function, one case study of an STC family was developed. The calculated COP_{el} for each specified capacity of this STC family are 3.027, 3.173, 3.230, 3.296 for 5200, 6800, 8100, 9800W, respectively.

(4) All STC models developed for this study met the target requirements and performance objectives. Comparisons between measured and calculated results show that the maximum deviation of cooling capacity and the COP_{el} deviation are below 2.53% and 1.69%, respectively.

(5) Two sets of scroll wrap thickness are designated, 2.6mm for 5200W and 6800W and 3.2mm for 8100W and 9800W, but the dimension of the outside diameter for each specified STC in this family is identical.

(6) A common share percentage of over 80% is achieved for major components in this family design, and only 16% of components are wholly different for each specified STC.

(7) As the case study results of STC family development proved, by following the design procedure and considering the manufacturing constraints, the STC products with good performance, can be developed logically and easily.

Table 4.1 Compressor operation conditions

Condensing temperature	Evaporating temperature	Degree of Subcooling	Degree of Superheating
54.4℃	7.2℃	8.3℃	27.8℃

Table 4.2 Specifications of the STC family used in this study

Refrigerant	R-22			
Input power	220V, single phase			
Lubricants	Mineral oil			
Shell type	Low pressure			
Compliant mechanism type	Solid axial compliant mechanism			
Motor outside diameter (mm)	139			
Specified capacity (W)	5200	6800	8100	9800
Objective of COP_{el} (W/W)	3.00	3.10	3.15	3.20

Table 4.3 Design constraints

Item no.	Design constraint	Notes
1	$D_{ob\_min} \leq D_{o\_max} \leq 100 \ mm$	$D_{o\_motor} = 139 \ mm$ $\delta_a \approx 40 \ mm$
2	$1 \leq G_w \leq 8.5$	From finite analysis of stress deflection and wrap machining capability
3	$1 \leq G_c \leq 2.5$	From cutter catalog and machining expertise

Table 4.4 Initial data definitions in this STC family

Required cooling capacity (W)	5200	6800	8100	9800
Displacement volume (cc)	25.4	32.3	37.4	45
Motor operating torque (N·m)	3.8~4.8	4.8~5.8	5.5~6.7	6.5~8.2
Motor efficiency (%)	87	88	89	90
Cooling capacity allowance	±2%			
Motor operating speed (rpm)	3490			
Theoretical compression ratio	3.43			
Polytropic exponent	1.11			
Initial design data	$t = 2.5mm, \ \phi_r = 1050°$			

Table 4.5 Optimum results of first-phase evaluation.

Required cooling capacity (W)	5200	6800	8100	9800
Objective of COP_{el} (W/W)	3.00	3.10	3.15	3.20
Calculated cooling capacity (W)	5224.73	6689.15	8151.13	9817.72
Calculated COP_{el} (W/W)	3.093	3.172	3.253	3.292
Thickness of scroll wrap t (mm)	2.6	2.6	3.3	3.2
Height of scroll wrap h_e (mm)	22.0	22.0	25.6	26.8
Pitch of scroll wrap p_t (mm)	11.730	12.629	13.596	14.135
Orbiting radius of crankshaft r_{or}	3.265	3.714	3.635	3.867
Roll angle of scroll wrap ϕ_r (°)	1120	1150	1150	1150
D_{ob_min}	73.083	80.784	86.972	90.416
$G_w = h_e / t$	8.462	8.462	7.758	8.375
$G_c = h_e / (p_t - t)$	2.41	2.19	2.49	2.45

Table 4.6 Second-phase evaluation results.

(a) Used with the same orbiting radius

Calculated cooling capacity (W)	5273.15	6697.32	8181.60	9813.60
Objective of COP_{el} (W/W)	3.00	3.10	3.15	3.20
Calculated COP_{el} (W/W) of first-phase	3.093	3.172	3.253	3.292
Calculated COP_{el} (W/W)	2.999	3.149	3.230	3.296
Thickness of scroll wrap t (mm)	2.6	2.6	3.2	3.2
Roll angle of scroll warp (°)	1150			
Height of scroll wrap h_e (mm)	16.524	20.952	22.605	27.2
Pitch of scroll wrap p_t (mm)	12.860	12.860	14.061	14.061
Orbiting radius $r_{or} = p_t/2 - t$	3.83			
D_{ob_min}	73.083	80.784	84.880	90.416
$G_w = h_e/t$	6.355	8.059	7.064	8.500
$G_c = h_e/(p_t - t)$	1.61	2.04	2.08	2.50

(b) Final optimum solutions used with two types of orbiting radius

Calculated cooling capacity (W)	5266.15	6688.37	8181.60	9813.60
Objective of COP_{el} (W/W)	3.00	3.10	3.15	3.20
Calculated COP_{el} (W/W) of first-phase	3.093	3.172	3.253	3.292
Calculated COP_{el} (W/W)	3.027	3.173	3.230	3.296
Thickness of scroll wrap t (mm)	2.6	2.6	3.2	3.2
Roll angle of scroll warp (°)	1150			
Height of scroll wrap h_e (mm)	17.427	22.100	22.605	27.200
Pitch of scroll wrap p_t (mm)	12.608	12.608	14.061	14.061
Orbiting radius $r_{or} = p_t/2 - t$	3.704		3.830	
D_{ob_min}	80.651	80.648	89.946	89.944
$G_w = h_e/t$	6.703	8.500	7.064	8.500
$G_c = h_e/(p_t - t)$	1.74	2.21	2.08	2.50

Table 4.7 Common sharing status of each major component of this STC family.

Component items	Common sharer	Cost share	Notes
Top cover include outlet port	∨	3.74%	One type for this series of compressor
Check valve mechanism	∨	1.50%	One type for this series of compressor
Oldham ring	∨	1.50%	One type for this series of compressor
Main frame	∨	11.97%	One type for this series of compressor
Driving bushing	∨	0.15%	One type for this series of compressor
Main journal bearing	∨	0.22%	One type for this series of compressor
Terminal	∨	0.15%	One type for this series of compressor
Bottom frame	∨	2.24%	One type for this series of compressor
Lower journal bearing	∨	0.15%	One type for this series of compressor
Oil pump	∨	2.24%	One type for this series of compressor
Bottom cover	∨	2.99%	One type for this series of compressor
Back pressure mechanism and isolating member	△	5.24%	One type of casting mold but different hole diameter for different back pressure required
Fixed scroll	△	20.19%	Two types of scroll wrap but used with same outside diameter
Orbiting scroll	△	19.45%	Two types of scroll wrap but used with same outside diameter
Main shell include inlet port and suction baffle	△	13.46%	One type of pressing mold but different length with different capacity required
Motor	△	3.74%	One type of pressing mold but different stack height with different capacity
Upper balancer	X	0.30%	Different type for each specified capacity
Crankshaft	X	10.47%	Same shaft diameter with two types of orbiting radius and a different length for each specified capacity
Lower balancer	X	0.30%	Different type for each specified capacity

Notes:

1. " ∨ " means this series of STC family uses the same component.

2. " △ " means the dimension of this component has been somewhat modified.

3. "X" means this component is different for each specified STC.
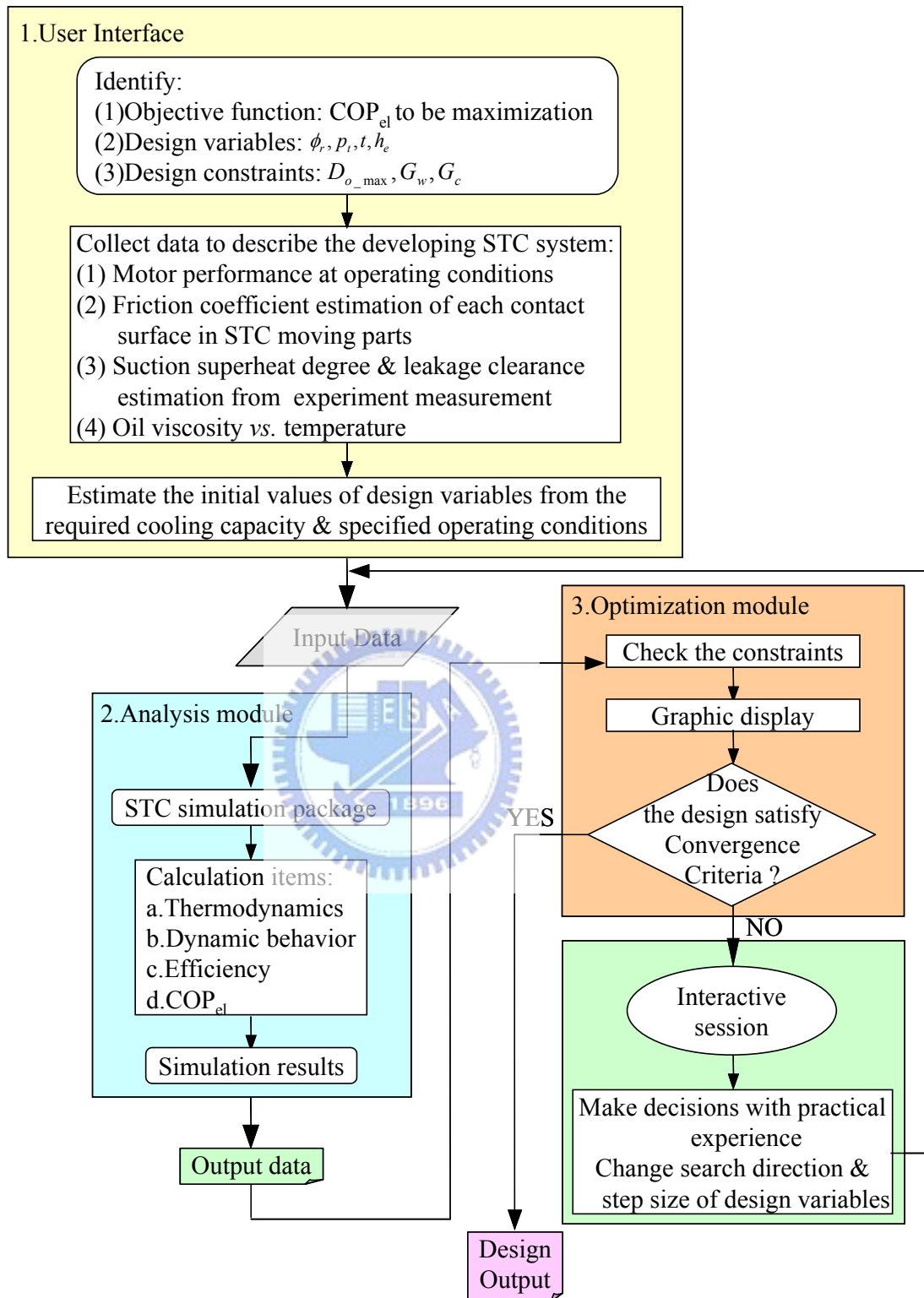
Fig. 4.1 The optimization process used in this study
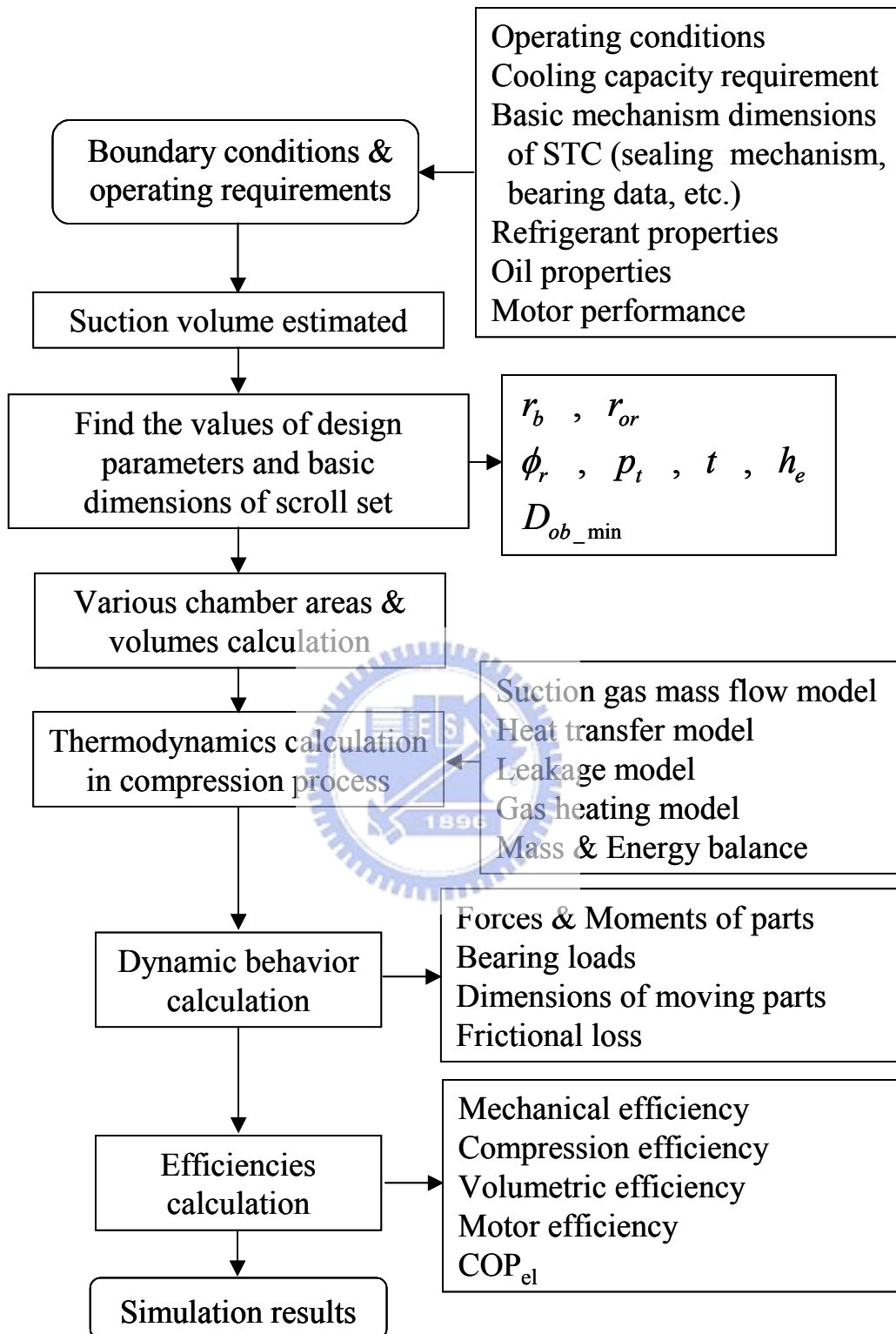
Fig. 4.2 The design flowchart of STC simulation package used in this study
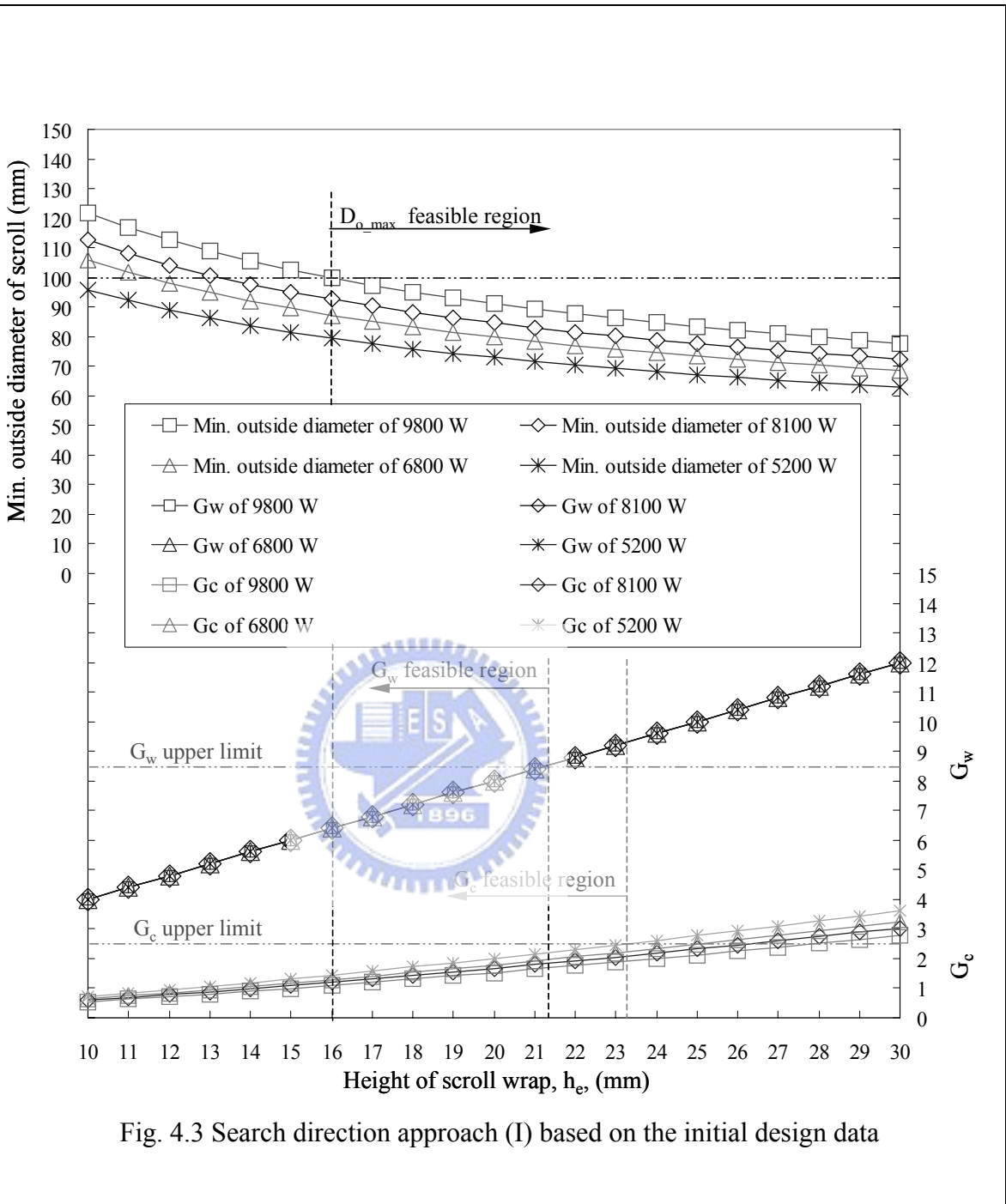
Fig. 4.3 Search direction approach (I) based on the initial design data
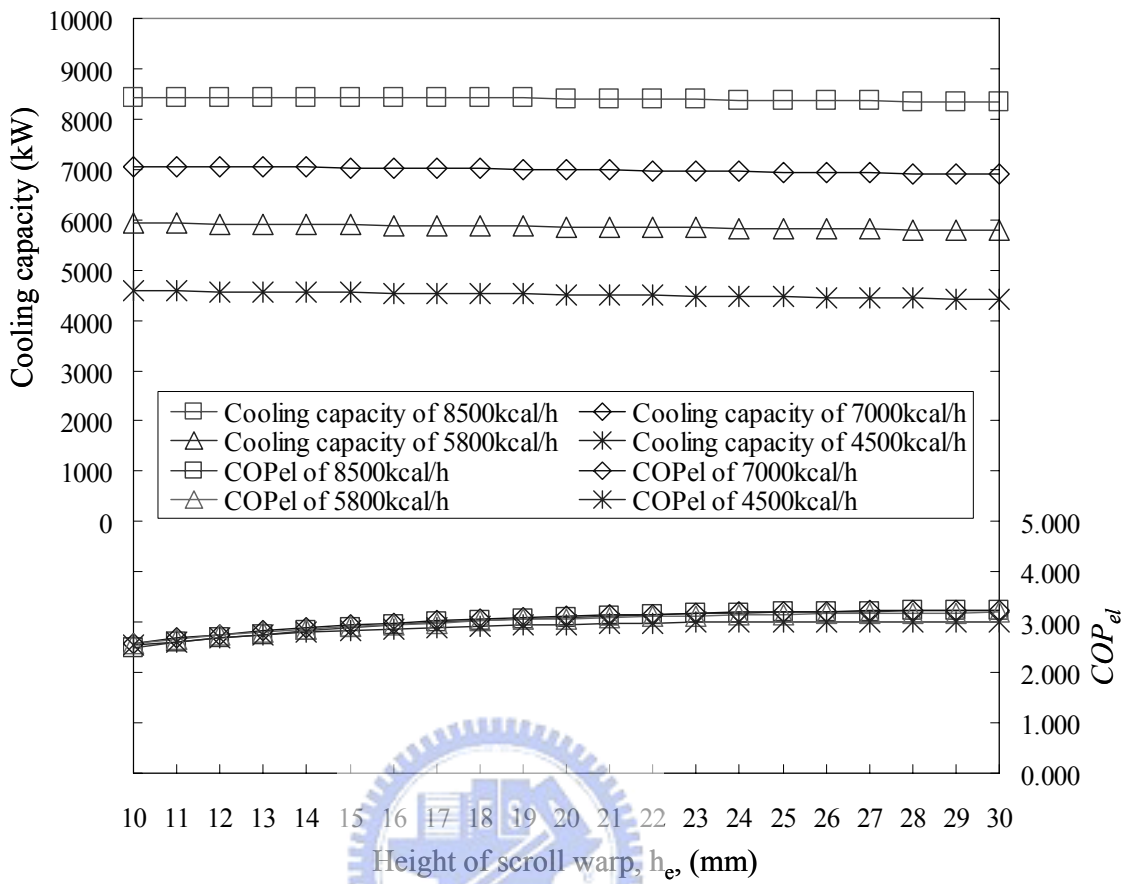
Fig. 4.4 Search direction approach (II) based on the initial design data.
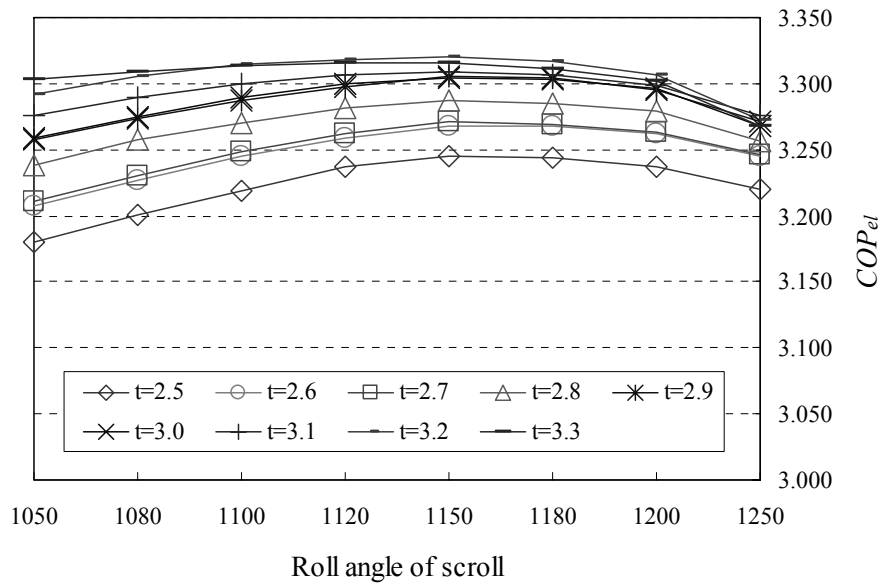
(a) 9800W
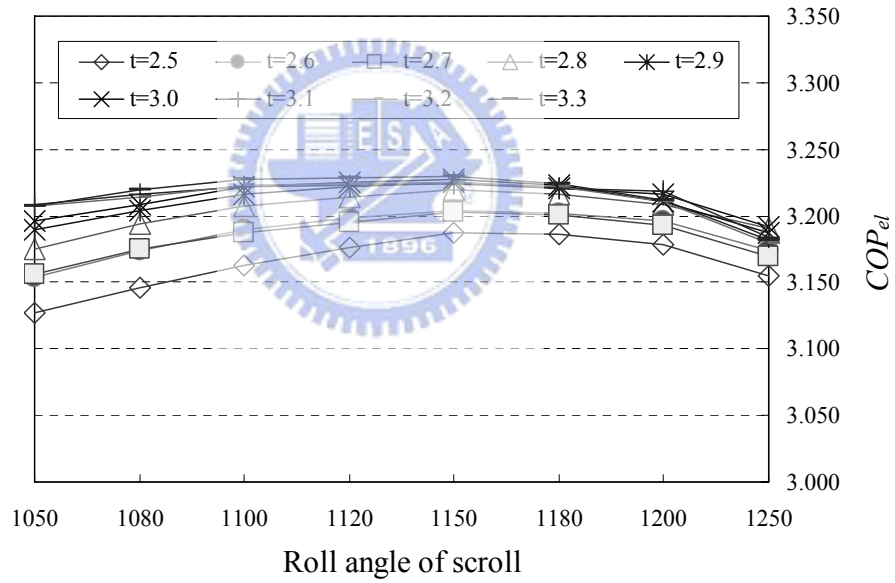
(b) 8100W

Fig. 4.5 Optimization results in the first-phase evaluation
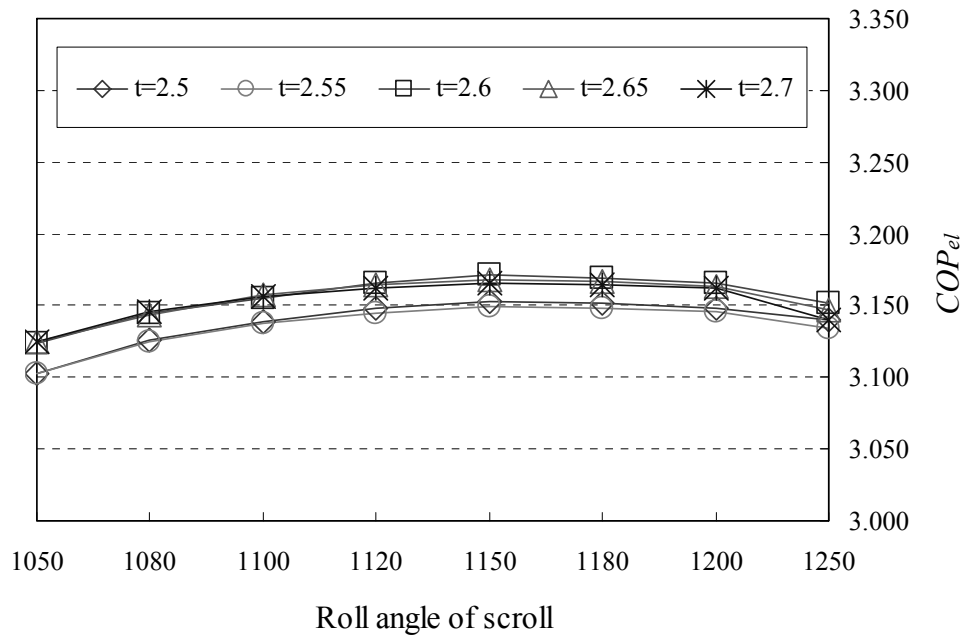
(c) 6800W
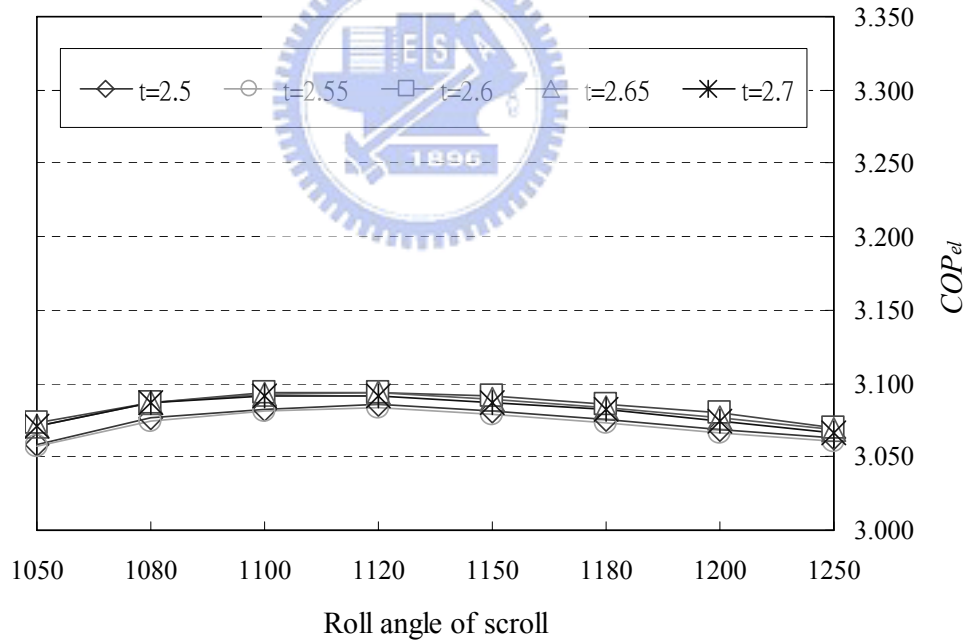
(d) 5200W

Fig. 4.5 Optimization results in the first-phase evaluation (continued)

(a) Hermetic STC family sample

(b) Major components of the STC family prototype

(c) Scroll family of four models

Fig. 4.6 The sample of the developed STC
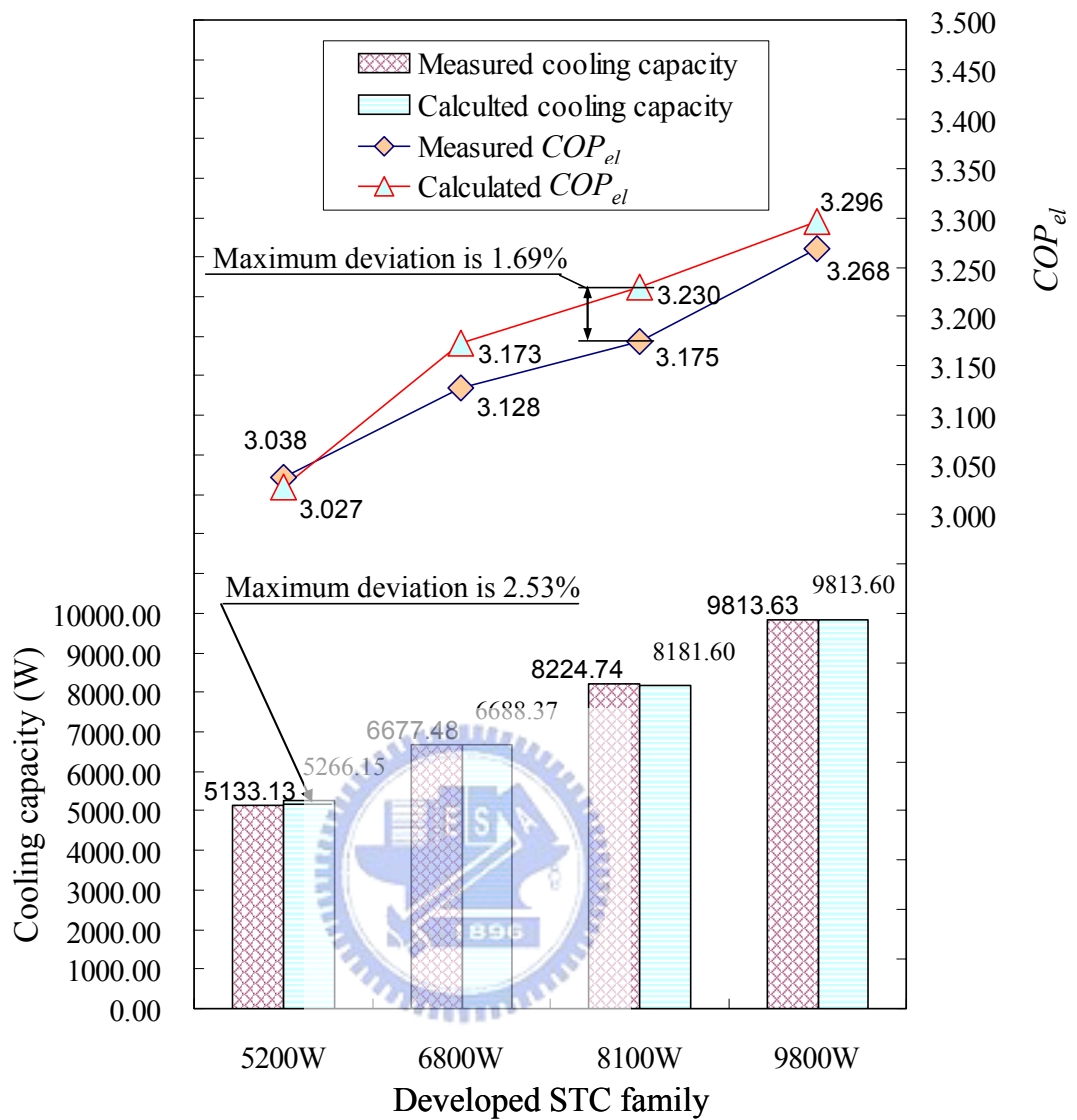
Fig. 4.7 The comparisons of cooling capacity and COP_{el} between the experimental and calculated results

CHAPTER 5

VARIABLE-SPEED STC DESIGN WITH OPTIMIZATION

Based on the required specifications of the developed STC family in this dissertation, one variable-speed STC is investigated. At different specified rotation speed, the variable-speed STC can supply various definite cooling capacities required to cover the developed STC family. It means the developed variable-speed STC combined with inverter-fed controller can replace a series of constant-speed STC such as the four models of the STC family that this study implemented.

Three types of variable-speed motor, which are the three-phase AC induction motor, the brushless DC motor with surface permanent magnet (SPM) and the interior permanent magnet synchronous motor (IPMSM), are used with the same scroll mechanism to implement the prototypes. Meanwhile, the performance comparison between these three types of variable-speed STC, has been observed.

While developing the IPMSM in this study, a patent survey and innovative skill have been used to create a new configuration as Appendix 1 presents in this dissertation. In the meantime, a new IPMSM patent that this study innovated has been granted in Taiwan, mainland China and United States of America, respectively.

5.1 Literatures review

Twenty-five years ago, Danfoss Group, the biggest compressor manufacturer in Europe, presented the first paper about hermetic piston-type compressors used with brushless DC motor in small refrigerators (Sorensen, 1980). In 1982, Toshiba Corp., the most famous rotary compressor manufacturer in Japan, depicted the study of a

frequency-controlled compressor used with AC two-poles and three-phases induction motor in air-conditioner applications (Itami *et al.*, 1982). According to the experimental results, it shows that when equipped with the frequency-controlled compressor, the COP_{el} of air-conditioner can be improved by 20% ~ 40% in comparison to the general ON/OFF controlled (constant-speed) compressor. Daikin Industries Ltd., the other world-class compressor manufacturer in Japan, introduced other research results in 1998, that based on the same size of variable-speed motor applied for air-conditioners, the IPMSM can be derived to larger torque and operate at higher efficiency than AC induction motor and brushless DC motor as Fig. 5.1 shows (Igata *et al.*, 1998).

Some papers have presented the performance and experimental analysis of scroll compressor varying its speed when applied for air-conditioners, heat-pumps and water chilling systems (Ishii *et al.*, 1990; Morimoto *et al.*, 1996; Kim *et al.*, 1998; Park *et al.*, 2001; Li *et al.*, 2002; Cho *et al.*, 2002; Aprea *et al.*, 2006). But up to now, very few papers in the world have conducted research related to the variable-speed STC design with scroll geometrical evaluation.

Therefore, based on the minimum design change, the optimum design process and STC design model that this dissertation developed, one variable-speed STC to meet the specification requirements of the original STC family with constant-speed as Chapter 4 introduced, has been implemented. Meanwhile, the performance comparisons between the STC family with a constant speed motor, the variable-speed STC with AC induction motor and permanent magnet (PM) motor, have also been evaluated in this study.

5.2 Design Simulation

For commercialization purposes, the required operation conditions, specifications and basic design constraints are given as Tables 4.1, 4.2 and 4.3.   The other required constraint is used with the same orbiting radius for the developing scroll set so that the crankshaft and Oldham ring of the STC can be the same also.   Therefore, the major work will focus on the design changes of fixed scroll and orbiting scrolls only.

Five steps are carried out in the design evaluation to search for the optimum design data of this variable-speed STC as follows:

(1) Initial design: define the related specifications for this developing variable-speed STC from original STC family requirements with constant-speed and engineering decisions

(2) First-phase design approach: Based on the original scroll geometrical data and motor operating efficiency that Chapter 4 developed for STC family with constant-speed, reduce the scroll height only to meet the rated cooling capacity requirement and evaluate the design parameters availability.

(3) Second-phase design approach: fixed on the two types of orbiting radius that the STC family used, the optimization algorithm combined with a graphical solution method to search the maximum COP_{el} for the developing variable-speed STC is calculated.   Set in the same design base, the motor efficiency is also assumed the same as the STC family with constant-speed in this phase approach.

(4) Prototyping: combined with above optimum approach results and practical engineering experience, the prototypes that include three type of motors, two controllers and one variable-speed STC will be implemented and the operating performance will be measured at specified conditions also.

(5) Performance evaluation: the comparisons between measured results and

calculated results have been discussed.   In advance, the STC simulation package receives the real motors operating efficiency and recalculates the operation performance for the STC to perform in variable-speed conditions.   Thereafter, the deviation between recalculated results and measured results has been introduced. Finally, the performance evaluation between constant-speed STC family prototypes and variable-speed prototypes is discussed to make sure the optimum design process meets the practical engineering requirements.

5.2.1 Initial design

The initial design for this developing variable-speed STC has been defined as Table 5.1 and summarized as below:

(1) The rated cooling capacity, 7700W, which is operated at 3600rpm, and is decided from the mean-value of four capacities of the STC family required as Table 4.4 shows.   The allowance of cooling capacity is also ±2%.

(2) Based on the same compression ratio, the displacement can be roughly calculated from Eqs. ((2-1) to (2-3)) as 34cc, and the Polytropic exponent selected as the same value, 1.11.

(3) Because the rotation speed of the variable-speed STC can be controlled exactly by inverter-fed controller, the required cooling capacities of the original STC family supplied can be met easily from different rotation speeds.

(4) The motor operating torque and efficiency in different required cooling capacity is defined as the same between constant-speed and variable-speed STC.   At the rated cooling capacity requirement of 7700W, the motor efficiency is defined as 89% because the operating torque is near 8100W.

(5) Table 4.6 has depicted two sets of scroll wrap thickness and orbiting radius that

have been designated in the developed STC family, they are $t = 2.6mm$, $r_{or} = 3.704mm$ for 5200W and 6800W, and $t = 3.2mm$, $r_{or} = 3.83mm$ for 8100W and 9800W, respectively. For minimum design change requirements, the scroll geometry parameters should follow these two scroll sets data as the design base.

5.2.2 First-phase design approach

Table 5.2 shows the comparison between original STC family data and the first-phase evaluation results and underscore two important outcomes:

(1) On the basis of scroll parameters, $t = 2.6mm$, $r_{or} = 3.704mm$, $\phi_r = 1150°$, subjected to a scroll height $h_e = 22.1mm$, can fit to rated cooling capacity 7700W. But $G_W = 9.116$ is over the design constraint of $G_W \leq 8.5$. It means this original STC model, $t = 2.6mm$, $r_{or} = 3.704mm$, $\phi_r = 1150°$, can not meet the required variable-speed STC by tuning the wrap height only.

(2) On the other scroll parameters, $t = 3.2mm$, $r_{or} = 3.83mm$, $\phi_r = 1150°$, subjected to a scroll height $h_e = 20.55mm$, can fit the rated cooling capacity of 7700W and all data is under the design constraints. Table 5.2 shows the calculated COP_{el} of required cooling capacities with various rotation speeds as Table 5.1 defined. For 5200W and 6800W, the calculated COP_{el} are higher than the original data, but for 8100W and 9800W, the calculated COP_{el} are lower than the original data. Moreover, the calculated COP_{el} of 9800W can not meet the objective requirement.

Therefore, tuning scroll height only from the original scroll design parameters can not satisfy this study's required target, so the following approach should be carried out with an optimization algorithm to develop the optimum variable-speed STC in this study.

5.2.3 Second-phase design approach with optimization

Since only one set of variable-speed STC has been developed to cover the cooling capacity range, which is not same as the STC family with constant-speed that develops a series of STC models to meet the required specified range of cooling capacity by using more common components as investigated in Chapter 4.   Therefore, the discrete variables optimization approach has some differences, but the optimization algorithm combined with a graphical solution method, such as Chapter 4 described, is the same. The newly approach process is introduced as.

The objective function requirement is also defined as Eq. (4-12) and subjected to the constraints as Eq. (4-13):

$$\max imize \quad COP_{el} = f(\phi_r, p_t, t, h_e) \tag{4-12}$$

$$LowerLimits \quad \leq \quad G_w, G_c, D_{o\_max} \quad \leq \quad UpperLimits \tag{4-13}$$

The other major design consideration in this design approach is the orbiting radius that also sets as a restraint in two types: (1) $r_{or} = 3.704mm$, (2) $r_{or} = 3.83mm$, so that the crankshaft can be the same as the original STC family.   Meanwhile, each motor efficiency at a specified rotation speed, is assumed the same as the STC family with constant-speed.

1. First-stage simulation:

This stage focuses on developing a variable-speed STC to operate at 3600rpm and with a cooling capacity of 7700W to search for the maximum objective function (maximum COP_{el}) by drawing on the variation of scroll thicknesses from 2.6mm to 3.2mm.   Table 5.3 and Fig. 5.2 depict the simulation results.

(1) As the orbiting radius is fixed, the basis of one set of thickness t with pitch p_t

of the scroll wrap, from Eq. (4-2) can be subjected to a change of scroll height h_e matched with a roll angle, ϕ_r, which fit the required cooling capacity requirement.

(2) As Chapter 4 introduced, increasing h_e can improve the COP_{el} at specified t and ϕ_r, but G_w and G_c will limit the increment of h_e. Therefore, selecting $G_w = 8.5$, means increasing h_e to the limit value, as researched in this study.

(3) Based on the above decisions, to increase wrap thickness, the pitch and the wrap height are increased, and the roll angle is reduced. Finally, the calculated cooling capacity can fit the defined data with a small variation and the COP_{el} is higher than 3.2 and over the objective target.

(4) The maximum COP_{el} occurs at $t = 2.9mm$, $\phi_r = 1077.694°$, $h_e = 24.65mm$ and the orbiting radius is the type 1, $r_{or} = 3.704mm$. The calculated cooling capacity is 7728.26W and the COP_{el} is 3.309. Moreover, at $t = 2.8mm$, $\phi_r = 1119.40°$, $h_e = 23.80mm$ the orbiting radius is the same as 3.704mm, the COP_{el} is 3.308 and the calculated cooling capacity is 7746.57W. These two points all meet the object requirement, and the deviation between the two points is very little.

(5) Based on the type 2 orbiting radius, $r_{or} = 3.83mm$, the maximum COP_{el} is located at $t = 2.7mm$, $\phi_r = 1118.49°$, $h_e = 22.95mm$. The calculated cooling capacity is 7752.45W, and the COP_{el} is 3.299, which is lower than the optimum point of type 1 of orbiting radius, but the deviation is within 0.3%.

(6) As a result of the above data, the optimum value can be searched at $t = 2.9mm$ in $r_{or} = 3.704mm$, but the simulated variable-speed STC is operated at 3600rpm only. Furthermore, in the range of operating speed as defined in Table 5.1, the optimum searching point should be approached and evaluated continuously.

2. Second-stage simulation:

Subsequent to finding the optimum solutions for the variable-speed STC in the

whole operating speed range, the search direction of four design variables of ϕ_r, p_t, t and h_e have been evaluated for each specified cooling capacity at definite rotation speed with an interactive process.   Following on the first-stage approach, the orbiting radius also fixed on two types as type 1, $r_{or} = 3.704mm$, and type 2, $r_{or} = 3.83mm$, and also set $G_w = 8.5$ in this stage investigation.   The optimum approach with detailed simulation and iteration has been carried out.

(1) As the orbiting radius r_{or} and G_w are fixed, one thickness of scroll wrap is selected, subjected to a change of scroll height h_e and matched with a roll angle ϕ_r of the scroll wrap, which fits each required cooling capacity requirement at the defined rotation speed.   Meanwhile, the COP_{el} can be calculated by STC simulation package that Chapter 2 introduced.

(2) Figure 5.3 presents the calculated results for type 1 orbiting radius, $r_{or} = 3.704mm$, operated at five rotation speeds, 2450rpm, 3200rpm, 3600rpm, 3800rpm and 4600rpm, and fit the five required cooling capacities as 5200W, 6800W, 7700W, 8100W, 9800W, respectively.   Figure 5.4 shows the simulation results for the developed STC used with a type 2 orbiting radius, $r_{or} = 3.83mm$, and operated at the same conditions as mentioned above.

(2) Fig. 5.3 and Fig. 5.4 depict, not any one set of scroll design parameters can all give the maximum COP_{el} of each required operating speed:

 (a) In type 1 orbiting radius, $r_{or} = 3.704mm$, operated at 2450rpm and 3200rpm, the maximum COP_{el} can be obtained at $t = 2.8mm$, but operated at 3600rpm, 3800rpm and 4600rpm, the maximum COP_{el} occurred at $t = 2.9mm$.

 (b) In type 2 orbiting radius, $r_{or} = 3.83mm$, operated at 2450rpm, 3200rpm and 3600rpm, the maximum COP_{el} can be obtained at $t = 2.7mm$, but operated at 3800rpm and 4600rpm, the maximum COP_{el} occurred at $t = 2.8mm$.

 (3) Combining two types of orbiting radius simulation, as Fig. 5.5 shows, the

maximum COP_{el} occurred at type 1 orbiting radius $r_{or} = 3.704mm$ but is located at two thickness of scroll wrap as depicted above. Operated at 2450rpm and 3200rpm, the thickness of scroll wrap, $t = 2.8mm$, has a maximum COP_{el}. But when operated at 3600rpm, 3800rpm and 4600rpm, the thickness $t = 2.9mm$ can give the maximum COP_{el}.

(4) Therefore, two sets of optimum design data disappear in this study. The 1st set optimum design parameter is defined as $r_{or} = 3.704mm$, $t = 2.8mm$, $h_e = 23.80$, $p_t = 13.008$, $\phi_r = 1119.402°$. Mmeanwhile, the 2nd set optimum design parameter is $r_{or} = 3.704mm$, $t = 2.9mm$, $h_e = 24.65$, $p_t = 13.208$ and $\phi_r = 1077.694°$.

(5) Table 5.4 displays the comparisons of the calculated result between original STC family design with constant-speed and the new developed variable-speed STC with optimum design:

(a) Although in large capacities (8100W and 9800W) with higher operating speed, the COP_{el} of the developed variable-speed STC has little decrease with 0.08% to 2.08%, but the COP_{el} is over the maximum objective target requirement of 3.2. In small cooling capacities such as 5200W and 6800W, this new developed optimum design presents better COP_{el} than the original STC family design. The improvement is from 4.86% to 7.23%, which provides very good performance.

(b) The COP_{el} deviation between 1st and 2nd set optimum design parameters is in the range of 0.04%~0.32% only. The 2nd set optimum design parameter presents a little better COP_{el} than 1st set in the whole operating speed range.

(6) Because only one set at design parameters can be selected for the final result, the 2nd set optimum design parameter, $r_{or} = 3.704mm$, $t = 2.8mm$, $h_e = 23.80$, $p_t = 13.008$, $\phi_r = 1119.402°$, has been decided to prototype and evaluate the

practical performance combined with various variable-speed motors in continuous study.

5.2.4 Prototype implementation

Three types of variable-speed motor have been applied in the developing variable-speed STC prototype.   They are the three-phase (3Φ) AC induction motor, the brushless DC motor with surface permanent magnet (SPM) and the interior permanent magnet synchronous motor (IPMSM).   These motor prototypes were supported by EEL of ITRI, but the IPMSM developed by this study that include patent around survey, new configuration innovation and applied to the patent in the world. Appendix 1 has introduced the IPMSM development records in detail.

Figure 5.6 shows these motor prototypes and their operating efficiencies curve at whole operating speed range.   The IPMSM that this study innovated, presents the best efficiency, especially when operated at lower speed.   Running at 1000rpm, the efficiency of IPMSM exceeds the AC induction motor and the SPM brushless motor by 17.53% and 4.85% respectively.   Table 5.5 has listed the real efficiency of each motor prototype at the required operating conditions.

Figure 5.7 (a) and (b) introduced two controllers, one is used for driving the 3Φ AC induction motor, the other is for the SPM and IPMSM motors, and both are supported by EEL of ITRI.   Operated at 2450rpm to 4500rpm, the efficiencies of these two controllers can achieve from 88% to 92% and provide very better performance.

To easily change the motor based on the same scroll pump mechanism, a semi-hermetic STC has been implemented as Fig. 5.7 (c) shows.   Meanwhile, the two scroll prototypes which are implemented with the 2nd set optimum design parameter that this

study developed, has been presented also.

5.2.5 Performance evaluation

Based on the original AC motor efficiency operated at STC family with constant-speed to meet specified cooling capacities requirements, the comparisons of cooling capacities and COP_{el} between measured and calculated results have been drawn on Fig. 5.8. Each cooling capacity deviation of the developed variable-speed STC driven by a different motor, is under 2%. The reason is that the operating speed of each variable-speed motor can be driven by a controller in the required speed exactly. Meanwhile, following on the STC family developed experience, the engineering implementation for variable-speed STC presents much better controllability in this study.

Figure 5.8 also presents the COP_{el} deviations between measured and calculated results of the real STC prototype. The deviation has reached to 6.04% because the real motor efficiency makes a large difference with the design value. When only used with 3 φ AC induction motor, the COP_{el} shows less than the simulated results because the real motor efficiency is 2%~7% lower than the original simulation data, and the maximum deviation between the simulated and measured results is 4.94%. By contrast, the STC prototype used with IPMSM, the COP_{el} presents much better performance, the maximum improvement achieved is 6.04% with the developed STC operated at 3800rpm. In addition, the STC used with the SPM brushless motor presents smaller amount of difference between the calculated and measured result, the maximum deviation under 2.33%.

The STC simulation package receives the feedback of the real motor efficiencies with variable-speed operation, reveals the variable-speed STC performance needs to be recalculated. Figure 5.9 and Table 5.5 introduce the performance comparisons and

the deviations between the measured and recalculated results respectively:

(1) The maximum deviation between measured and recalculated result has been narrowed down to under 3.35%.   It proves that this study with optimum design has grasped the major design parameters.

(2) Only one measured point is below the recalculated data, which is the variable-speed STC prototype operated at 2450rpm and used with the AC 3φ induction motor.   But the deviation is 1.82% only.   In the meantime, the measured results of the STC prototype used with AC 3φ induction motor present very little difference to recalculated results.   The maximum error is just 2.27%.

(3) When used with the SPM brushless motor and IPMSM, the deviation between measured and recalculated results of this STC prototype are 1.06%~3.30% and 1.06%~3.36%, respectively.   The measured data is all higher than recalculated data but the difference is small.

5.2.6 Final results

Table 5.6 has summarized the prototype performance comparisons between the STC family with constant-speed that Chapter 4 studied and the new developed variable-speed STC:

(1) This newly developed STC with IPMSM can increase the COP_{el} by about 11.85%, 10.17%, 7.78% and 5.02%, which is respective to STC family used with AC 1φ induction motor to provide four required cooling capacities of 5200W, 6800W, 8100W and 9800W.   Meanwhile, this new developed STC when used with the SPM brushless motor also obtains good performance improvement of about 7.79%, 6.71%, 3.65% and 1.44%, respectively.   They all present much better design implementation, especially for operating at a lower speed.

(2) When the new developed STC is used with the AC 3φ induction motor, the COP_{el}

is not increased so high. Although the *COP_el* has increased 1.45%, 3.74% and 0.57%, by which the STC is operated at 2450rpm, 3200rpm and 3800rpm, respectively, but when operated at highest speed of 4600rpm, with the cooling capacity at 9800W, the *COP_el* is 0.70%lower than the constant-speed STC as .

5.3 Results and Discussion

This study has proven the systematic algorithm for STC design optimization that Chapter 4 developed to be used for variable-speed STC implementation. Meanwhile, the *COP_el* of this newly developed variable-speed STC can be improved for each specified capacity respective to the STC family with constant-speed. The important contributions of this research are summarized below:

(1) This study enhanced the STC systematic algorithm with optimization developed in Chapter 4 to apply a variable-speed STC implementation. The new variable-speed STC has been prototyped and the performance evaluated with three types of motor as the AC $3\,\varphi$ induction motor, the SPM brushless motor and the IPMSM. Meanwhile, the IPMSM is an innovation and has been applied for a patent by this study. The innovated contents have been recorded in the Appendix of this dissertation.

(2) This investigation also selected the four geometrical factors of scroll wrap—ϕ_r, p_t, t and h_e as design parameters, but for commercialization requirement, the orbiting radius, r_{or}, has played the key design constraint. Thereafter, the original two set design parameters, $\phi_r = 1150°$, $p_t = 12.608$, $t = 2.6mm$, $r_{or} = 3.704mm$, and $\phi_r = 1150°$, $p_t = 14.061$, $t = 3.2mm$, $r_{or} = 3.830mm$, with different wrap height, h_e, that is used for the STC family requirement, have been modified to only one set design parameter, $\phi_r = 1077.694°$, $p_t = 13.208$, $t = 2.9mm$,

$r_{or} = 3.704mm$ with one scroll wrap height, $h_e = 24.65mm$, for the variable-speed STC.

(3) The newly developed variable-speed STC prototype with three types of motor, can all meet the target requirements and performance objectives.   The best result is the STC used with the IPMSM motor.   It presents the COP_{el} over the objective target of 7.25~13.27%.   Respective to the original STC family which used the AC 1 φ induction motor, this newly developed STC with the IPMSM motor can increase COP_{el} by about 11.85%, 10.17%, 7.78% and 5.02%, which is relative to provide the four required cooling capacities of 5200W, 6800W, 8100W and 9800W, respectively.

(4) Comparison between the measured prototypes and this study's calculated results, show that the maximum deviation of cooling capacity and the COP_{el} deviation are below 1.63% and 3.36%, respectively.   From the case study result of variable-speed STC development, the systematic optimum design procedure combined with the engineering experiences that this study conducted, the STC products performed well and can be predicted logically and easily.

(5) Only two scrolls, the fixed scroll and orbiting scroll, and the motor should be changed in the newly developed variable-speed STC prototype. The other components can all be the same as the original STC family with constant-speed. It means the design of the original STC family developed in Chapter 4 only change a little, and can be implemented in variable-speed STC easily with the family design skill of this study development.   In the meantime, the original STC family has been enhanced to the application range.

Table 5.1 Initial data definitions in variable-speed STC

Items	Rated	Original STC family			
Required cooling capacity (W)	**7700**	5200	6800	8100	9800
Motor operating speed (rpm)	**3600**	2450	3200	3800	4600
Motor operating torque (N·m)	**5.1~6.3**	3.8~4.8	4.8~5.8	5.5~6.7	6.5~8.2
Motor efficiency (%)	**89**	87	88	89	90
Cooling capacity allowance	±2%				
Theoretical compression ratio	3.43				
Displacement volume (cc)	34.0				
Polytropic exponent	1.11				
Initial scroll design data	$t = 2.6mm$, $\phi_r = 1150°$, $r_{or} = 3.704$ $t = 3.2mm$, $\phi_r = 1150°$, $r_{or} = 3.830$				

Table 5.2 The comparisons between original data of STC family with constant-speed
and first-phase evaluation data of the variable-speed STC

Constant-speed STC family	Original data			
Calculated cooling capacity (W)	5266.15	6688.37	8181.60	9813.60
Calculated COP_{el} (W/W)	**3.027**	**3.173**	**3.230**	**3.296**
Thickness of scroll wrap t (mm)	2.6	2.6	3.2	3.2
Height of scroll wrap h_e (mm)	17.427	22.100	22.605	27.200
Pitch of scroll wrap p_t (mm)	12.608	12.608	14.061	14.061
Orbiting radius $r_{or} = p_t / 2 - t$	3.704		3.830	
D_{ob_min}	80.651	80.648	89.946	89.944
$G_w = h_e / t$	6.703	8.500	7.064	8.500
$G_c = h_e /(p_t - t)$	1.74	2.21	2.08	2.50
Set 1 of Variable-speed STC	$t = 2.6$, $r_{or} = 3.704$, $h_e = 22.1$ $D_{ob\_min} = 85.112$ $G_w = \underline{9.116}$, $G_c = 2.368$			
Set 2 of Variable-speed STC	$t = 3.2$, $r_{or} = 3.83$, $h_e = 20.55$ $D_{ob\_min} = 89.946$, $G_w = 6.422$, $G_c = 1.892$			
Calculated cooling capacity (W)	5281.90	6852.30	8195.03	9937.34
Calculated COP_{el} (W/W)	**3.20**	**3.27**	**3.17**	**3.18**

Table 5.3 The first-stage simulation results of second phase design approach for variable-speed STC operated at 3600rpm

Type 1 of orbiting radius (mm)	3.704						
Thickness of scroll wrap t (mm)	2.6	2.7	2.8	2.9	3.0	3.1	3.2
Height of scroll wrap h_e (mm)	22.1	22.95	23.8	24.65	25.50	26.35	27.20
Pitch of scroll wrap p_t (mm)	12.608	12.808	13.008	13.208	13.408	13.608	13.808
Roll angle of scroll wrap ϕ_r (°)	1213.76	1164.62	1119.40	1077.694	1018.91	1003.37	970.17
Calculated cooling capacity (W)	7780.32	7763.89	7746.57	7728.26	7708.84	7688.20	7666.27
Calculated COP_{el} (W/W)	3.266	3.298	**3.308**	**3.309**	3.294	3.277	3.259
D_{ob_min}	85.112	82.969	81.001	79.19	77.521	75.979	74.552
$G_w = h_e / t$				8.50			
$G_c = h_e /(p_t - t)$	2.208	2.270	2.232	2.391	2.450	2.508	2.564

Type 2 of orbiting radius (mm)	3.830						
Thickness of scroll wrap t (mm)	2.6	2.7	2.8	2.9	3.0	3.1	3.2
Height of scroll wrap h_e (mm)	22.1	22.95	23.8	24.65	25.50	26.35	27.20
Pitch of scroll wrap p_t (mm)	12.86	13.06	13.26	13.46	13.66	13.86	14.06
Roll angle of scroll wrap ϕ_r (°)	1164.83	1118.49	1075.85	1036.50	1000.10	966.352	934.995
Calculated cooling capacity (W)	7769.67	7752.45	7734.19	7714.78	7694.11	7672.13	7648.52
Calculated COP_{el} (W/W)	3.283	**3.299**	3.297	3.282	3.266	3.247	3.223
D_{ob_min}	83.321	81.259	79.366	77.625	76.021	74.540	73.171
$G_w = h_e / t$				8.50			
$G_c = h_e /(p_t - t)$	2.154	2.215	2.275	2.334	2.392	2.449	2.505

98

Table 5.4 The calculated result comparisons between original STC family and the optimum calculation of variable-speed STC

Items	Rated	Required operating conditions			
Required cooling capacity (W)	7700	5200	6800	8100	9800
Motor operating speed (rpm)	3600	2450	3200	3800	4600
Original STC family design data operated at constant-speed					
Optimum design parameters	==	$r_{or} = 3.704mm,$ $t = 2.6mm,$ $p_t = 12.608,$ $\phi_r = 1150°$		$r_{or} = 3.830mm,$ $t = 3.2mm,$ $p_t = 14.061,$ $\phi_r = 1150°$	
		$h_e = 17.427$	$h_e = 22.100$	$h_e = 22.605$	$h_e = 27.200$
Calculated cooling capacity (W)	==	5266.15	6688.37	8181.60	9813.60
Calculated COP_{el} (W/W)	==	**3.027**	**3.173**	**3.230**	**3.296**
1st set of optimum design parameters $(r_{or} = 3.704mm, \quad t = 2.8mm, \quad h_e = 23.80, \quad p_t = 13.008, \quad \phi_r = 1119.402°)$ $(D_{ob\_min} = 81.001mm, \quad G_w = 8.5, \quad G_c = 2.332)$					
Calculated cooling capacity (W)	7746.57	5245.6	6817.03	8135.91	9870.99
Calculated COP_{el} (W/W)	3.308	3.246	3.331	3.223	3.228
COP_{el} improvement (%)	==	7.23	4.97	-0.23	-2.05
2nd set of optimum design parameters $(r_{or} = 3.704mm, \quad t = 2.9mm, \quad h_e = 24.65, \quad p_t = 13.208, \quad \phi_r = 1077.694°)$ $(D_{ob\_min} = 79.190mm, \quad G_w = 8.5, \quad G_c = 2.391)$					
Calculated cooling capacity (W)	7728.26	5230.58	6802.29	8113.78	9848.31
Calculated COP_{el} (W/W)	3.309	3.242	3.327	3.227	3.239
COP_{el} improvement (%)	==	7.12	4.86	-0.08	-1.73
The COP_{el} deviation between 1st and 2nd sets of optimum design parameters (%)	0.04	0.11	0.10	0.14	0.32

Table 5.5 The deviations between calculated result and measured result of the STC prototypes with variable-speed motor

Items	Rated	Required operating conditions			
Motor operating speed (rpm)	3600	2450	3200	3800	4600
Required cooling capacity (W)	7700	5200	6800	8100	9800
Driven by 3Φ induction motor					
Real motor efficiency (%)	86.47	80.24	85.16	86.83	88.15
Calculated cooling capacity (W)	7728.26	5230.58	6802.29	8113.78	9848.31
Measured cooling capacity (W)	7768.54	5302.12	6772.15	8142.69	9975.26
Cooling capacity Deviation	0.52%	1.37%	0.44%	0.36%	1.29%
Calculated COP_{el}	3.215	3.139	3.220	3.149	3.173
Measured COP_{el}	3.268	3.082	3.245	3.193	3.245
COP_{el} Deviation	1.66%	-1.82%	0.76%	1.39%	2.27%
Driven by SPM motor					
Real motor efficiency (%)	88.10	85.21	87.35	88.52	90.26
Calculated cooling capacity (W)	7728.26	5230.58	6802.29	8113.78	9848.31
Measured cooling capacity (W)	7772.11	5312.10	6775.18	8159.29	9986.52
Cooling capacity Deviation	0.57%	1.56%	0.40%	0.56%	1.40%
Calculated COP_{el}	3.275	3.175	3.303	3.210	3.249
Measured COP_{el}	3.361	3.280	3.338	3.291	3.315
COP_{el} Deviation	2.63%	3.30%	1.06%	2.53%	2.00%
Driven by IPMSM					
Real motor efficiency (%)	91.13	88.24	90.18	91.87	92.52
Calculated cooling capacity (W)	7728.26	5230.58	6802.29	8113.78	9848.31
Measured cooling capacity (W)	7773.22	5315.97	6781.25	8162.17	9990.32
Cooling capacity Deviation	0.58%	1.63%	0.34%	0.60%	1.44%
Calculated COP_{el}	3.388	3.288	3.410	3.332	3.330
Measured COP_{el}	3.477	3.398	3.446	3.422	3.432
COP_{el} Deviation	2.62%	3.36%	1.06%	2.70%	3.07%

Table 5.6 The prototype performance comparisons between the STC family with

constant-speed STC and the developed variable-speed STC

Required cooling capacity (W)	5200	6800	8100	9800
Required COP_{el} objective	3.00	3.10	3.15	3.20
Constant-speed STC family	$r_{or}=3.704mm,$ $t=2.6mm,$ $p_t=12.608,$ $\phi_r=1150°,$		$r_{or}=3.830mm,$ $t=3.2mm,$ $p_t=14.061,$ $\phi_r=1150°$	
Height of scroll wrap h_e (mm)	17.427	22.100	22.605	27.200
AC 1φ motor efficiency (%)	87.0	88.0	89.0	90.0
Measured cooling capacity (W)	5133.13	6677.48	8224.74	9813.63
Measured COP_{el} (W/W)	3.038	3.128	3.175	3.268
Over objective percentage (%)	1.27%	0.90%	0.79%	2.12%
Variable-speed STC	$r_{or}=3.704mm,\ \ t=2.9mm,$ $p_t=13.208,\ \ \phi_r=1077.694°,$ $h_e=24.65mm$			
AC 3φ motor efficiency (%)	80.24	85.16	86.83	88.15
Measured cooling capacity (W)	5302.12	6772.15	8142.69	9975.26
Measured COP_{el} (W/W)	3.082	3.245	3.193	3.245
Improvement (%)	1.45%	3.74%	0.57%	-0.70%
Over objective percentage (%)	2.73%	4.68%	1.37%	1.41%
SPM brushless motor efficiency (%)	85.21	87.35	88.52	90.26
Measured cooling capacity (W)	5312.10	6775.18	8159.29	9986.52
Measured COP_{el} (W/W)	3.280	3.338	3.291	3.315
Improvement (%)	7.97%	6.71%	3.65%	1.44%
Over objective percentage (%)	9.33%	7.68%	4.48%	3.59%
IPMSM efficiency (%)	88.24	90.18	91.87	92.52
Measured cooling capacity (W)	5315.97	6781.25	8162.17	9990.32
Measured COP_{el} (W/W)	3.398	3.446	3.422	3.432
Improvement (%)	11.85%	10.17%	7.78%	5.02%
Over objective percentage (%)	13.27%	11.16%	8.63%	7.25%
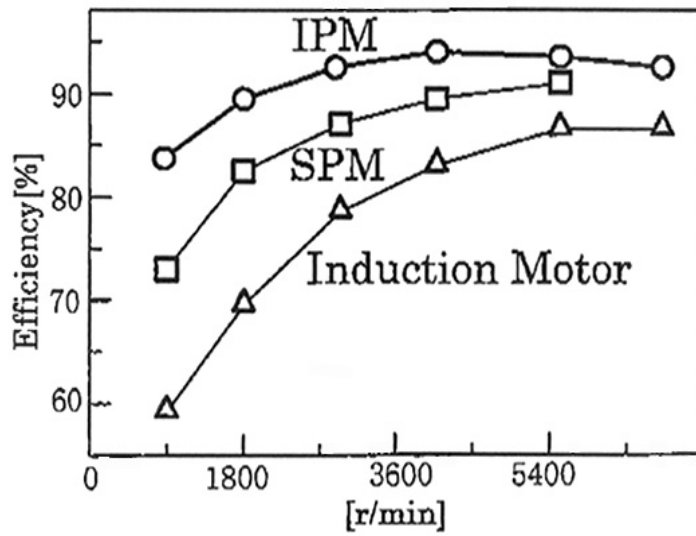
(b) Efficiency comparison of each motor used for compressor
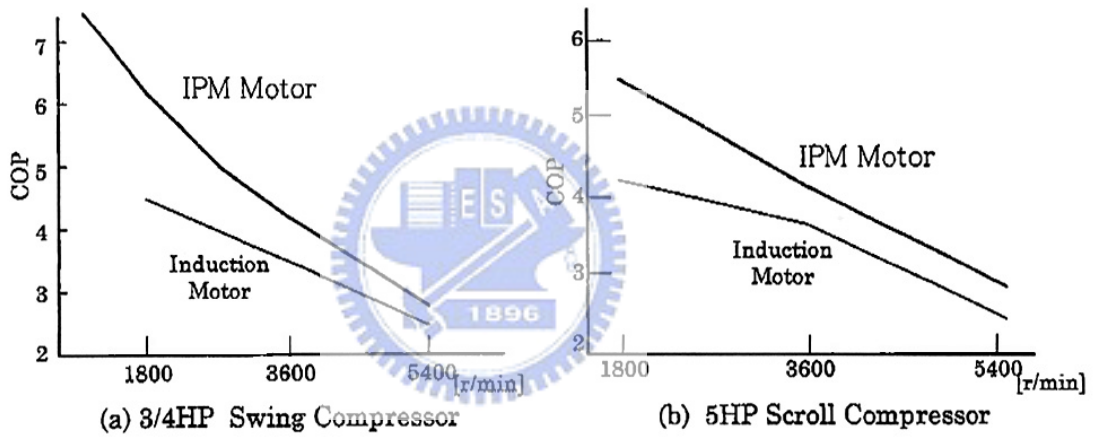
(a) 3/4HP Swing Compressor

(b) 5HP Scroll Compressor

(c) COP comparisons of compressors

Fig. 5.1 Comparisons of each motor used in compressors (Igata *et al.*, 1998)
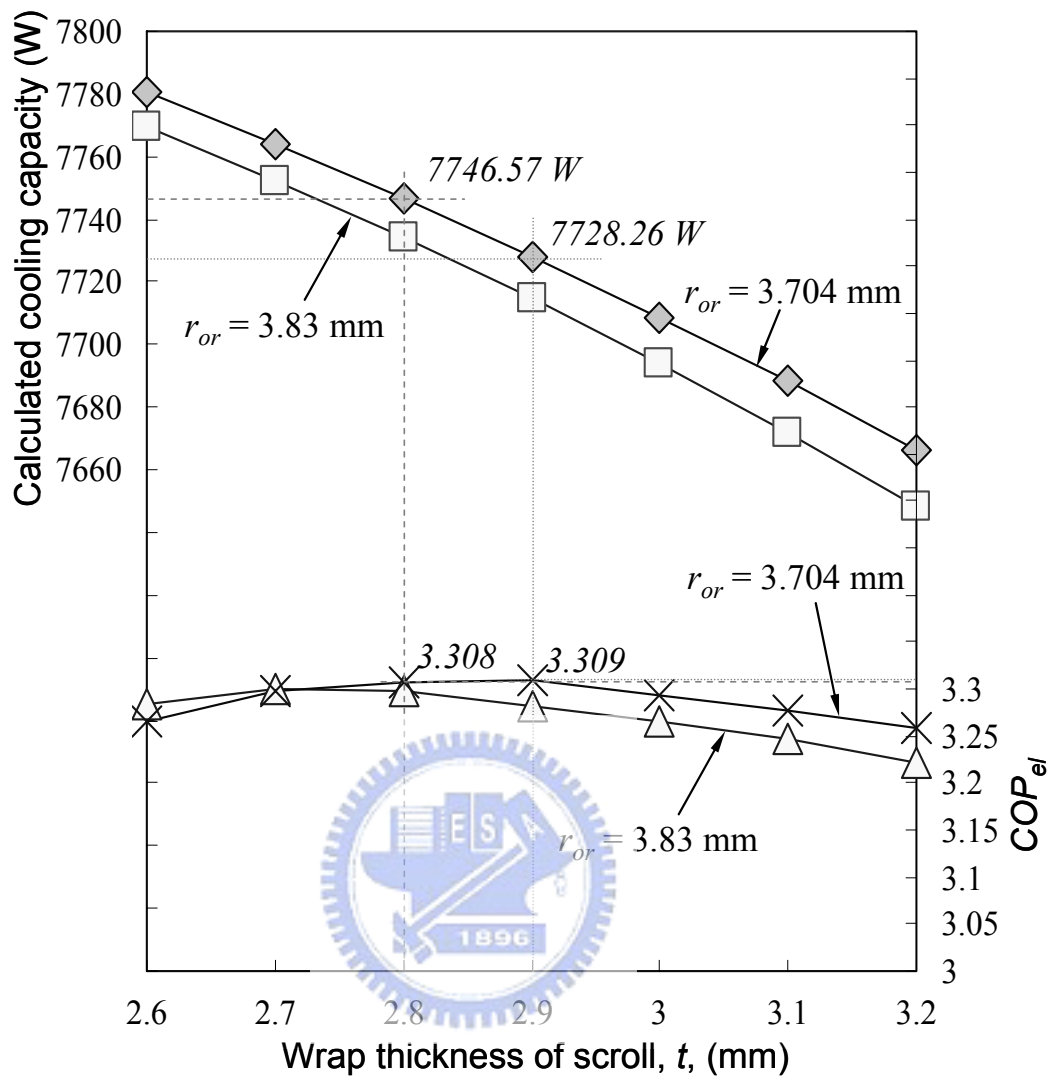
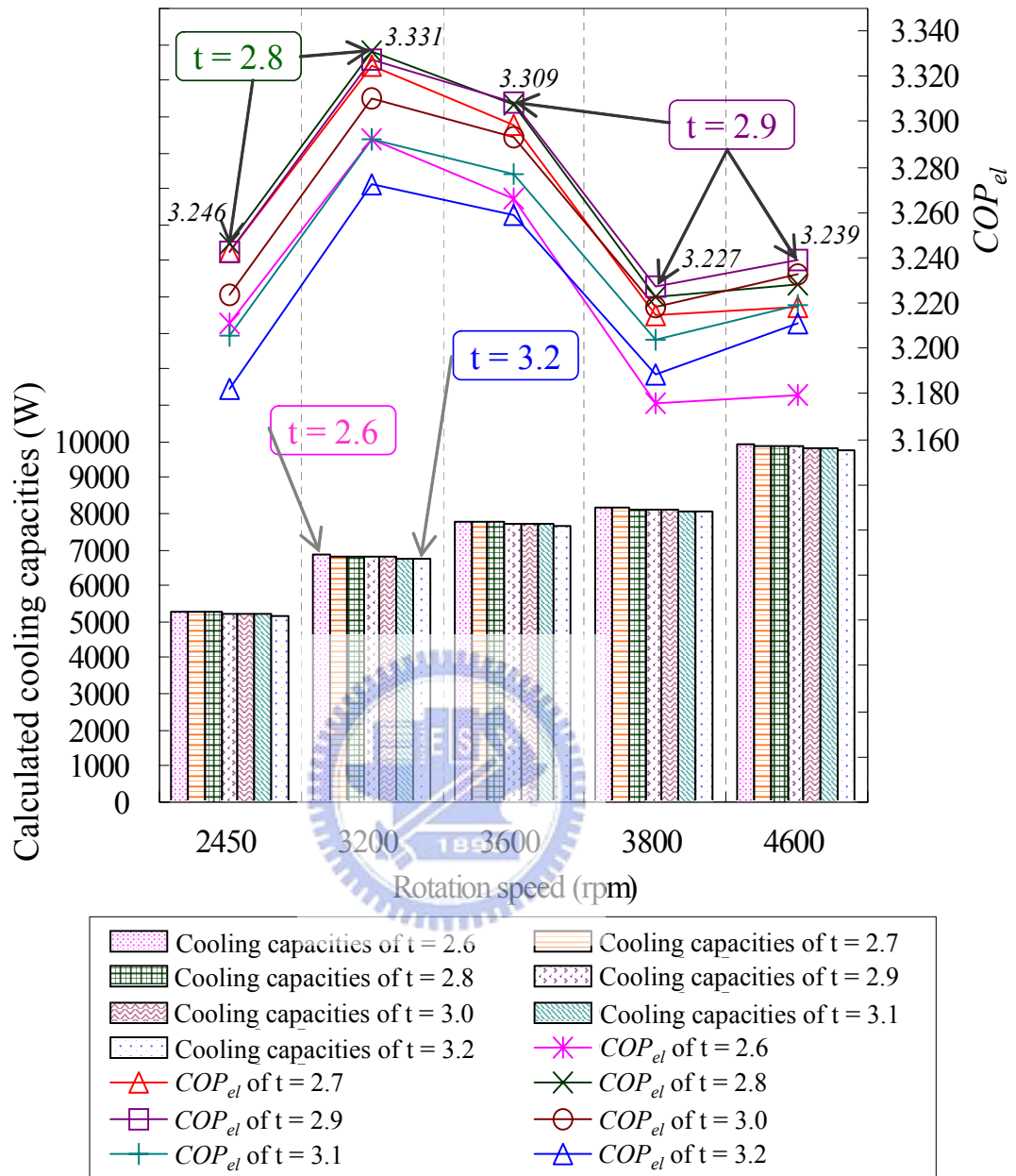Fig. 5.2 The first-stage simulation results for searching maximum COP_{el}

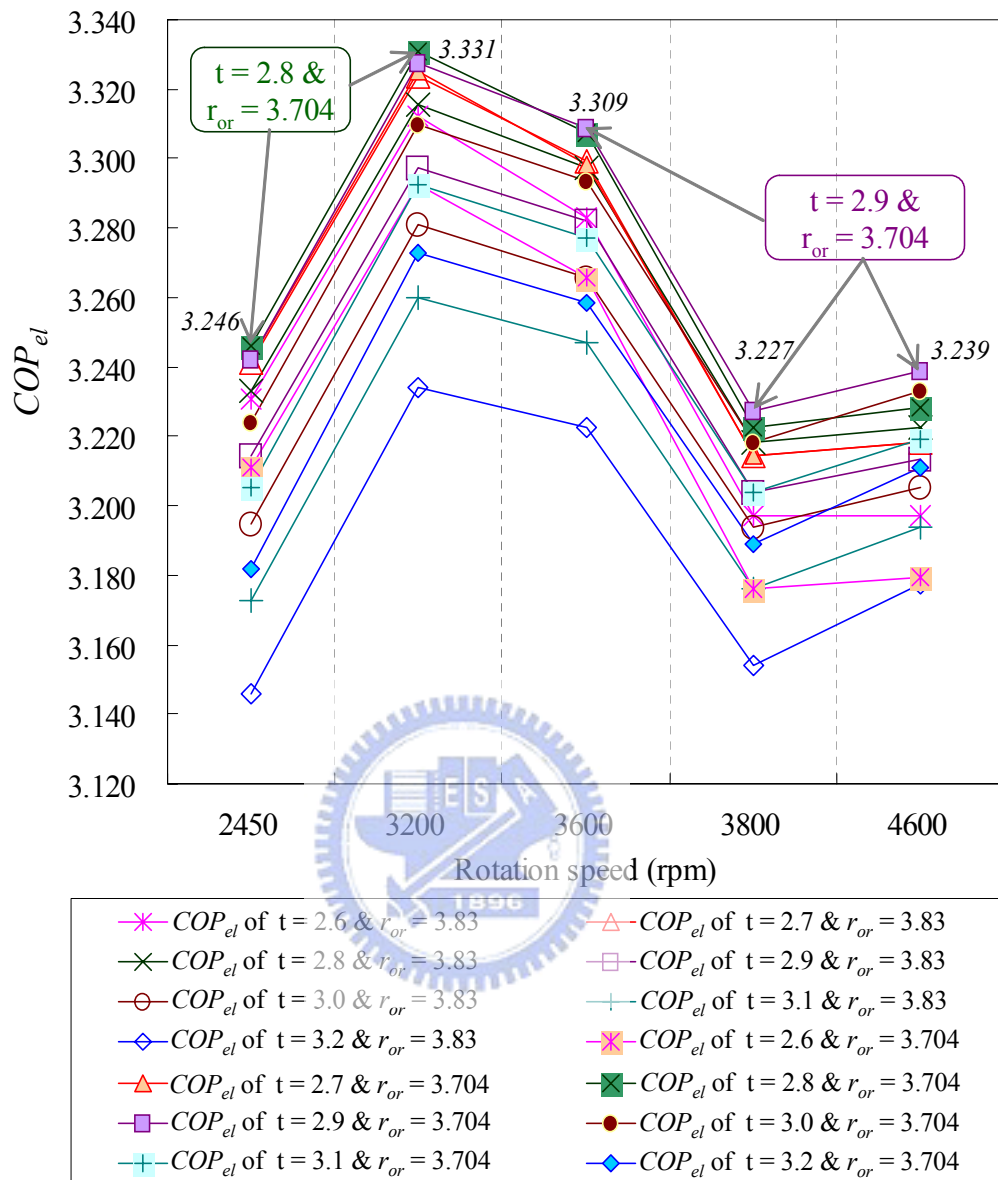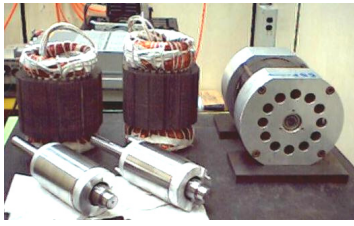Fig. 5.3 The second-stage simulation for type 1 orbiting radius
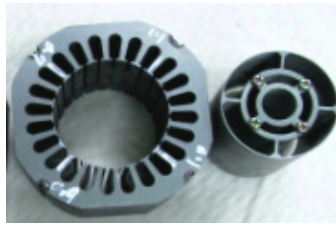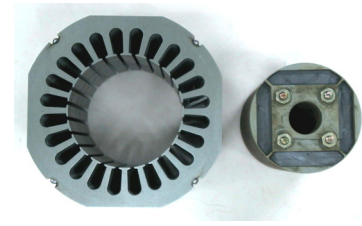
Fig. 5.4 The second-stage simulation for type 2 orbiting radius

Fig. 5.5 *COP$_{el}$* comparisons of the second-stage simulaion
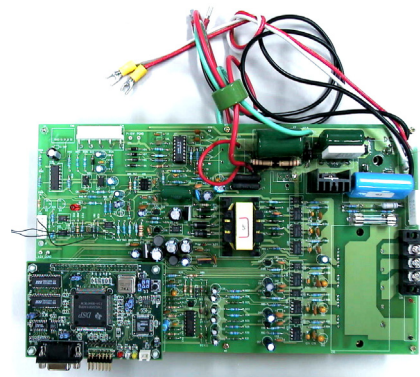
(a) 3Φ induction motor   (b) SPM brushless motor   (c) IPMSM
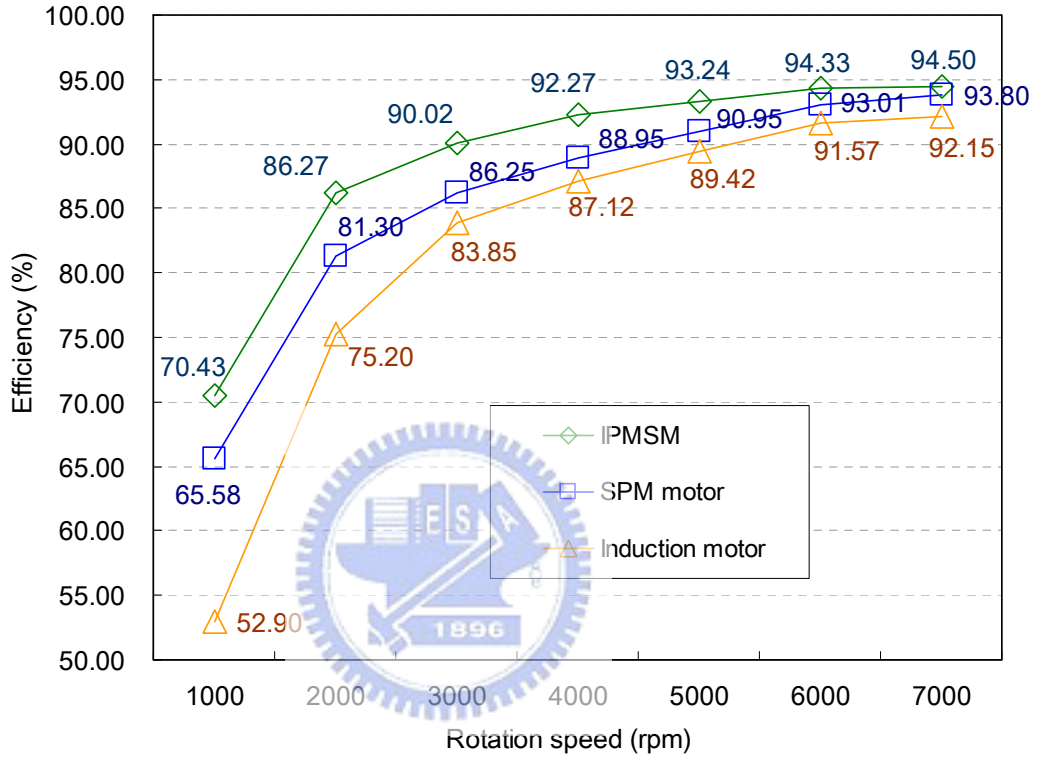
(d) Efficiency comparison between different motor

Fig. 5.6 The variable-speed motor prototypes and their efficiencies
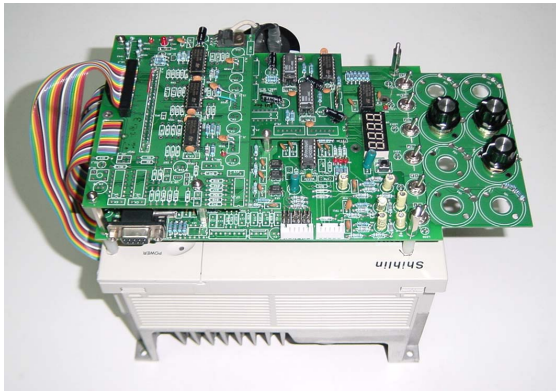
(a) AC inverter controller

(b) SPM & IPMSM motor controller

(c) Semi-hermetic prototype and scroll components of variable-speed STC

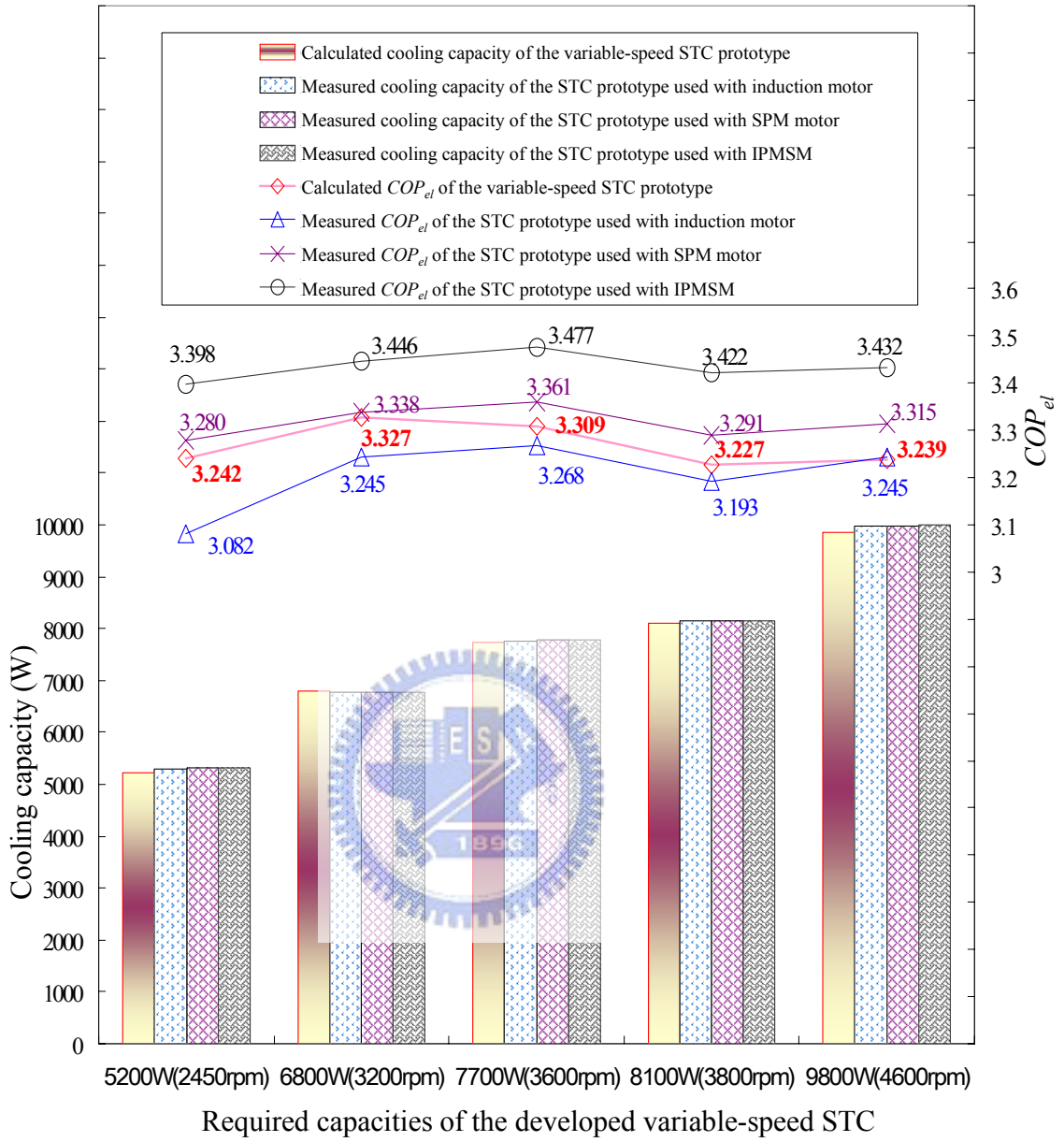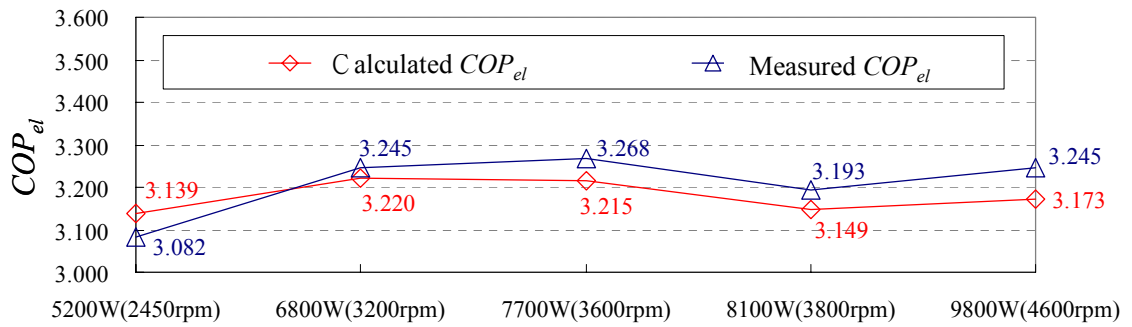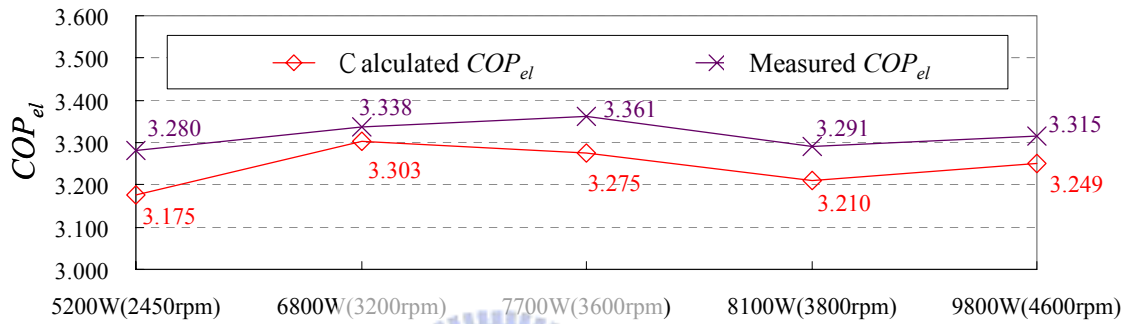Fig. 5.7 The variable-speed STC controllers and compressor prototype

Fig. 5.8 The comparisons of cooling capacity and COP_{el} between measured and calculated results based on the original AC motor efficiencies
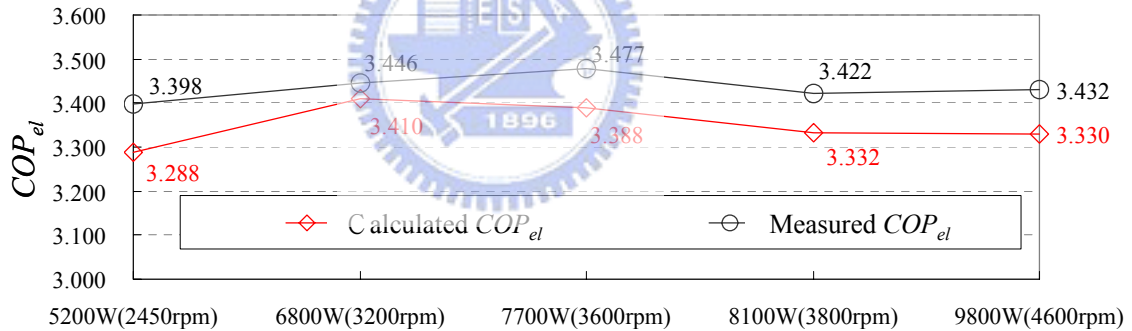
(a) Driven by 3ϕ AC induction motor

(b) Driven by SPM Brushless motor

(c) Driven by IPMSM

Fig. 5.9 The comparisons of COP_{el} between the measured and calculated results

based on the real variable-speed motor efficiencies

CHAPTER 6

CONCLUSIONS

6.1 Conclusions

Using discrete variables and interactive session approach, the optimum design with non-linear & multi-objectives problem can be implemented very practically. This dissertation has created a practical scroll-type compressor (STC) family design process with systematic and optimization algorithm for the first time in the world. In addition, two case studies of STC family design have been implemented, prototyped and the performance verified. One case is used for constant-speed STC application, the other is applied for variable-speed requirement. The results show that the developed STC families present a high potential for commercialization.

The design process of this dissertation conducted to include objective function definition, critical design parameters selection, constraints identification that relate to manufacturing and assembling limitations, an iterative process approach with interactive session, the discrete variable make decision with engineering experience. A STC simulation tool has been developed and experimental validation. Thereafter, the design results are able to meet a series of performance requirements of commercial STC.

The major contributions of this dissertation research are summarized as:

(1) The detailed critical patents, mathematical model and design structure of STC, have all been introduced in Chapter 2. Meanwhile, a new design structure that this study proposed and one simulation package of STC has been built-up. One international conference paper (Proceedings of the 4th International Conference on Compressor and Refrigeration, Xi'an City, China, pp189-196, October, 2003) and

one domestic engineering journal paper (機械月刊, 第廿八卷第十一期, 文 41-54 頁, 2002 年 11 月) have been presented.

(2) Chapter 3 depicts the approach results of the experimental validation for the STC simulation tool, the deviation of the verified STC's performance between predicted results and experimental measured results is under 4%, and shows the validated STC simulation package that this study developed can be used in the practical STC design works.   The research results of this topic have been introduced in one SCI journal paper (Applied Thermal Engineering Vol. 25, Aug. 2005, pp. 1724-1739), one international conference paper (Proceedings of the 18th International Compressor Engineering Conference at Purdue, USA, C016, July, 2004) and one domestic engineering journal paper (機械月刊, 第三十一卷第九期, 文 34-43 頁, 2005 年 9 月). The Appendix 1 of this dissertation has introduced the detailed calculation inputs and outputs of the developed STC simulation package.

(3) Two case studies of STC family design have been carried out in Chapter 4 and Chapter 5.   One study is for a constant-speed STC family requirement, the other is applied for an inverter-fed control STC with variable-speed motors.   Following on the proposed optimum design process, these two case studies have been prototyped and performance verified by compressor's calorimeter.   The design results meet the target requirements.   Based on these two case studies, one SCI journal paper (Journal of Applied Thermal Engineering, Vol. 26, Issue 10, July 2006, pp. 1074-1086), three international conference papers (Proceedings of the 3rd International Compressor Technique Conference, Wuxi City, China, pp200-207, August, 2001; Proceedings of the 17th International Compressor Engineering Conference at Purdue, USA, C24-3, July, 2002; International Conference on Compressors and their Systems 2005, I Mech E, U. K., Sep., 2005, pp. 413-422) and one domestic

scientific conference paper (Proceedings of the 2nd Symposium on Air-Conditioning, Refrigeration and Energy Engineering at National Chin-Yi Institute of Technology, Taichung, Taiwan, No. 20, July, 2004) have published the related investigation results.

(4) In STC optimum design, four geometrical parameters of scroll wrap—ϕ_r, p_t, t and h_e—have been selected by this study to define the major dimensions of the developed STC family, and the COP_{el} has been defined as the objective function. In constant-speed STC family design results, the comparisons between measured and calculated results show that the maximum deviation of cooling capacity and COP_{el} are below 2.53% and 1.69%, respectively. In variable-speed STC development, the maximum deviation of cooling capacity and COP_{el} deviation are below 1.63% and 3.36%, respectively. It has been proven the optimum design process and the calculated capability are very close to the practice requirements.

(5) From a commercialization point of view, this dissertation has achieved to get the benefits of using a common components share with the developed STC family. Two sets of scroll wrap thickness are designated for constant-speed STC family, but the dimension of the outside diameter for each specified STC in this family is identical. The common components share of over 80% is achieved for the major components in this family design, and only 16% of the components are wholly different for each specified STC. Based on the developed STC family, only fixed scroll, orbiting scroll and motor are design changed, the variable-speed STC with performance improvement has been implemented.

(6) As for the needs of higher efficiency STC products, three types of variable-speed motors, which are the three-phase AC induction motor, the brushless DC motor with surface permanent magnet (SPM) and the interior permanent magnet

synchronous motor (IPMSM), are used with the same scroll mechanism to implement the variable-speed prototypes. The best result is the STC used with the IPMSM, which presents the COP_{el} over the objective target of 7.25~13.27%. Meanwhile, an IPMSM has been operated with patent survey and innovative skill. Finally, a new IPMSM patent has been applied and granted in Taiwan, mainland China and United States of America, respectively. (中華民國專利, 新型第 200822 號, 2003 年 2 月, 中國大陸專利, 實用新型第 ZL01267457.5 號, 2002 年 7 月, U.S. Patent 6,987,341, Jan. 17, 2006). The Appendix 2 of this dissertation has described the innovation records.

As the above descriptions, a whole systematic design procedure combined with a practical optimization algorithm and engineering expertise, has been conducted by this dissertation. Following on the design procedure, any engineering product can be predicted to perform well and easily.

REFERENCES

American Society of Heating, Refrigerating and Air-Conditioning Engineers (ASHRAE), "Compressors", Chapter 34 in Heating, Ventilating, and Air-Conditioning SYSTEMS AND EQUIPMENT of 2000 ASHRAE Handbook, ASHRAE, 2000.

Anderson, G. J. and Bush, J. W., "Scroll machine with floating seal", Unite States Patent Number: 5,156,539, Oct. 20, 1992.

Aprea, C., Mastrullo, R. and Renno, C., "Experimental analysis of the scroll compressor performances varying its speed", Applied Thermal Engineering, Vol. 26, pp. 983-992, 2006.

Arora, C. P., Refrigeration and air conditioning, McGraw-Hill Co., 2001.

Arora, J. S., Induction to optimum design, McGraw-Hill Co., 2004.

Arora, J. S. and Tseng, C. H. "Interactive design optimization", Engineering Optimization, Vol. 13, pp. 173-188, 1988.

Asano, Y., Shinto, M., Ito, H., Morishige, T., Honda, Y., Murakami, H., Kadoya, N. and Yokote, S., "Motor using a rotor including an interior permanent magnet", Unite States Patent Number: 6,008,559, Dec. 28, 1999.

Bailey, R. S. and Cutts, D. G., "Journal bearing experimental evaluations and data correlation", Proc. of the 1996 Int. Compressor Engineering Conference at Purdue, pp.295-302, Aug., 1996.

Beseler, F., "Scroll compressor technology comes of age", Heating, Piping and Air Conditioning, Vol. 59, No. 7, pp.67-70, 1987.

Bloch, H. P., **Cameron, J. A., Danowski, F. M., James, R., Swearingen, J. S. and Weightman, M. E.** "Compressors and expanders – selection and application for the process industry", Marcel Dekker, Inc., 1979.

Bush, J. W., Cailiat, J. L. and Seibel S. M., "Dimensional optimization of scroll compressor", Proc. of the 1986 Int. Compressor Engineering Conference at Purdue, pp.840-855, Aug., 1986.

Bush, J. W. and Elson, J. P., "Scroll compressor design criteria for residential air conditioning and heat pump applications", Proc. of the 1988 Int. Compressor Engineering Conference at Purdue, pp.83-97, July, 1988.

Butterworth, A. L., "Scroll machine with flex member pivoted swing link", Unite States Patent Number: 4,413,959, Nov. 8, 1983.

Caillat, J. L., Ni, S., and Daniels,M., "A computer model for scroll compressors", Proc.

of the 1988 Int. Compressor Conference at Purdue, pp.47-55, 1988.

Caillat, J. L. and Seibel, S. M., "Scroll compressor with lubricated flat driving surface", Unite States Patent Number: 4,954,057, Sep. 4, 1990.

Caillat, J. M., Weatherston, R. C. and Bush, J. W., "Scroll-type machine with axially compliant mounting", Unite States Patent Number: 4,767,293, Aug. 30, 1988.

Cengel, Y. A. and Boles M. A., Thermodynamics – an engineering approach, McGraw-Hill Co., 1998.

Chang, Y. C., Tseng, C. H., Tarng, G. D. and Chang, L. T., "Scroll compressor with solid axial sealing mechanism", Proceedings of the 4th International Conference on Compressor and Refrigeration, Xi'an City, China, pp189-196, October, 2003.

Chang, Y. C., Tsai, C. E., Tseng, C. H., Tarng, G. D. and Chang, L. T., "Computer simulation and experimental validation of scroll compressors", Proceedings of the 18th International Compressor Engineering Conference at Purdue, USA, C016, July, 2004.

Chen, J. L. and Tseng, C. H., "A study on the integration of methods and strategies for patent-based product design", A dissertation for the degree of doctor of philosophy in mechanical engineering, National Chiao-Tung University, Taiwan, 2002.

Chen, Y., Halm, N. P., Groll, E. A. and Braun, J. E., "Mathematical modeling of scroll compressors-part I: compression process modeling", International Journal of Refrigeration, 25, pp.731-750, 2002.

Chen, Y., Halm, N. P., Braun, J. E. and Groll, E. A., "Mathematical modeling of scroll compressors-part II: overall scroll compressor modeling", International Journal of Refrigeration, 25, pp.751-764, 2002.

Cho, N. K., Youn, Y., Lee, B. C. and Min, M. K., "The characteristics of tangential leakage in scroll compressors for air conditioners", Proc. of the 2000 Int. Compressor Conference at Purdue, pp.807-814, 2000.

Chu, T., Ishijima, K. and Sakaino, M., "Analysis of the rolling-piston type rotary compressor", Proc. of the 1978 Int. Compressor Conference at Purdue, pp.219-224, 1978.

DeBlois, R. L., and Stoeffler, R.C., "Instrumentation and data analysis techniques for scroll compressors", Proc. of the 1988 Int. Compressor Conference at Purdue, pp.182-188, 1988.

Dossat, R. J., Principles of refrigeration, Prentice-Hall, Inc., 1991.

Ekelöf, J., "Rotary pump of compressor", Unite States Patent Number: 1,906,142, Dec. 05,1933.

Engelmann, R. H. and Middendorf and W. H., Handbook of electric motors, Marcel Dekker, Inc., 1995.

Etemad, S. and Nieter, J., "Design optimization of the scroll compressor", International Journal Refrigeration, Vol. 12, pp.146-150, May, 1989.

Fraser, H. H. and Etemad, S., "Slider block radial compliance mechanism", Unite States Patent Number: 5,017,107, May 21, 1991.

Hayano, M., Sakata, H., Nagatomo, S. and Murasaki, H., "An analysis of losses in scroll compressor", Proc. of the 1988 Int. Compressor Conference at Purdue, pp.189-197, July, 1988.

Hendershot, J. R., Design of brushless permanent magnet motors, Magna Physics Corp., 1991.

Hernandez, G., Allen, J. K., Woodruff, G. W., Simpson, T. W., Bascaran, E., Avila, L. F. and Salinas, F., "Robust design of families of products with production modeling and evaluation", Journal of Mechanical Design of ASME, Vol. 123, pp.183-190, June, 2001.

Hidden, W. P., Mason, N. H. and McCullough, J. E., "Liquid immersible scroll pump", Unite States Patent Number: 4,160,629, Jul. 10, 1979.

Hitachi Co., Catalog No. HG-460(H) (in Japanese), 2000-Winter.

Honda, Y., Higaki T., Morimoto, S. and Takeda, Y., "Rotor design optimisation of a multi-layer interior permanent-magnet synchronous motor", IEE Proceedings-Electric Power Applications, Vol. 145, No. 2, pp.119-124, March, 1998.

Honda, Y., Murakami, H., Narazaki, K., Itoh, H., Shinto, M., Asano, Y. and Kadoya, N., "Motor with built-in permanent magnets", Unite States Patent Number: 5,945,760, Aug. 31, 1999.

Igegawa, M., Sato, E., Tojo, K., Arai, A. and Arai, N., "Scroll compressor with self-adjusting back-pressure mechanism", ASHRAE Transactions, No. 2846, pp.314-326, 1984.

Igata, M., Kitaura, H., Ogawa, Y., Nawatedani, K., Matsuno, S. and Yamagiwa, A., "High efficiency hermetic compressor operated by IPM motor and inverter system", Proc. of the 1998 Int. Compressor Engineering Conference at Purdue, pp.385-390, 1998.

Iizuka, K., Uzuhashi, H., Kano, M., Endo, T. and Mohri, K., "Microcomputer control for sensorless brushless motor," IEEE Transactions on Industry Applications, Vol. 21, No. 4, pp. 595-601, 1985.

Ishii, N., "The study of rolling piston rotary compressor dynamic behavior when stopping to reduce noise and vibration level", Proc. of the 1984 Int. Compressor Engineering Conference at Purdue, pp.259-266, July, 1984.

Ishii, N., Fukushima, M., Sano, K. and Sawai, K., "A study on dynamic behavior of a scroll compressor", Proc. of the 1986 Int. Compressor Engineering Conference at Purdue, pp.901-96, Aug., 1986.

Ishii, N., Fukushima, M., Sawai, K., Sano, K. and Imaichi, K., "Dynamic behavior of a scroll compressor (dynamic analysis)", JSME International Journal, Series III, Vol. 31, No. 1, pp.58-67, 1988

Ishii, N., Yamamura, M., Morokoshi, H., Fukushima, M., Yamamoto, S. and Sakai, M., "On the superior dynamic behavior of a variable rotating speed scroll compressor", Proc. of the 1988 Int. Compressor Conference at Purdue, pp.75-82, July, 1988.

Ishii, N., Yamamura, M., Muramatsu S., Yamamoto, S. and Sakai, M., "Mechanical Efficiency of a variable speed scroll compressor", Proc. of the 1990 Int. Compressor Conference at Purdue, pp.192-199, July, 1990.

Itami, T., Okoma, K., Misawa, K., "An experimental study of frequency-controlled compressors", Proc. of the 1988 Purdue Compressor Technology Conference, pp.297-304, July, 1982.

Jones, D. W., "Method of making a permanent magnet rotor", Unite States Patent Number: 4,570,333, Feb. 18, 1986.

Kim, T. D., "Rotor core having slots for receiving permanent magnets", Unite States Patent Number: 5,929,547, Jul. 27, 1999.

Kim, Y., Seo, K. J. and Park, H. H., "Modeling on the performance of an inverter driven scroll compressor", Proc. of the 1998 Int. Compressor Conference at Purdue, pp.755-760, July, 1998.

Kota, S., Sethuraman, K. and Miller, R., "A metric for evaluating design commonality in product families", Journal of Mechanical Design of ASME, Vol. 122, pp.403-410, Dec., 2000.

Lee, G. H. and Kim, G. W., "Performance simulation of scroll compressors", IMechE Conference Transactions, International Conference on Compressors and Their Systems, C591/051/2001, Sep., 2001.

Lee, S. C., "Brushless DC motor capable of preventing leakage magnetic flux", Unite States Patent Number: 6,031,311, Feb. 29, 2000.

Li, H., Liao, Q., Wang, R., "Research and development of variable-speed scroll compressor", Proc. of the 2002 Int. Compressor Conference at Purdue, C24-4, July, 2002.

Lin, C. C., Chang, Y. C., Liang, K. Y., Hung, C. H., "Temperature and thermal deformation analysis on scrolls of scroll compressor", Applied Thermal Engineering Vol. 25, Aug. 2005, pp. 1724-1739.

Léon Creux, Unite States Patent Number: 801,182, Oct. 03, 1905.

Matsunobu, Y., Tajima, F., Kawamata, S., Kobayashi, T., Shibukawa S. and Koizumi, O., "Permanent magnet type dynamo electric machine and electric vehicle using the same", Unite States Patent Number: 6,034,459, Mar. 7, 2000

McCullough, J. E., "The scroll machine", Mechanical Engineering, pp.46-51, Dec., 1979.

McCullough, J. E., "Fluid-cooled, scroll-type, positive fluid displacement apparatus", Unite States Patent Number: 3,986,799, Oct. 19, 1976.

McCullough, J. E., "Scroll member and scroll-type apparatus incorporating the same", Unite States Patent Number: 3,994,635, Nov. 30, 1976.

McCullough, J. E. and Shaffer, R. W., "Axial compliance means with radial sealing for scroll-type apparatus", Unite States Patent Number: 3,994,636, Nov. 30, 1976.

McCullough, J. E., "Scroll-type apparatus with hydrodynamic thrust bearing", Unite States Patent Number: 4,065,279, Nov. 30, 1976.

McCullough, J. E., "Scroll-type apparatus with fixed throw crank drive mechanism", Unite States Patent Number: 4,082,484, Nov. 30,1976.

McCullough, J. E., "Coupling member for orbiting machinery", Unite States Patent Number: 4,121,438, Nov. 30, 1976.

McCullough, J. E., "Scroll-type liquid pump with transfer passages in end plate", Unite States Patent Number: 4,129,405, Nov. 30, 1976.

McDermott, C. M., and Stock, G. N., "The use of common parts and designs in high-tech industries: a strategic approach", Production and Inventory Management Journal, Vol. 35, No. 3, pp.65-68, 1994.

Miller, T. J. E., Brushless permanent-magnet and reluctance motor drives, Oxford University Press, Inc., 1989.

Mistree, F., Hughes, O. F. and Bras, B. A., "The compromise decision support problem and the adaptive linear programming algorithm", Structural Optimization: Status and Promise, AIAA, Washington, D. C., pp.247-286, 1993.

Mita, M., Sasaki T., "Permanent magnet field-type rotating machine", Unite States Patent Number: 5,684,352, Nov. 4,1997.

Mohan, N., Undeland, T. M. and Robins, W. P., <u>Power electronics-converters applications and design</u>, John Wiley & Sons, Inc., 1995.

Moore, R. W., Shaffer, R. W. J. and McCullough, E., "A scroll compressor for shipboard helium liquefier systems", Proc. of the 1976 Int. Compressor Conference at Purdue, pp.417-422, 1976.

Morimoto, T., Yamamoto, S., Hase, S., Yamada, S. and Ishii, N., "Development of a high SEER scroll compressor", Proc. of the 1996 Int. Compressor Conference at Purdue, pp.317-322, 1996.

Morishita, E., Sugihara, M., Inaba, T., Nakamura T. and Works, W., "Scroll compressor analytical model", Proc. of the 1984 Int. Compressor Conference at Purdue, pp.487-495, July, 1984.

Morishita, E. and Sugihara, M., "Geometrical theories of scroll compressor", Pump Machine (in Japanese), Vol. 13, No. 4, pp.23-33, 1985.

Morishita, E., Sugihara, M. and Nakamura, T., "Scroll compressor dynamics (1st report, The model for the fixed radius crank)", Bulletin of JSME, Vol. 29, No. 248, pp.476-482, 1986.

Morishita, E., Sugihara, M., Inaba, T. and Kimura T., "Scroll compressor dynamics (2nd report, The compliant crank and the vibration model)", Bulletin of JSME, Vol. 29, No. 248, pp.483-488, 1986.

Morishita, E. and Sugihara, M., "Some design problems of scroll compressor", Bulletin of JSME, Vol. 29, No. 258, pp.4139-4146, 1986.

Muir, E. B., Griffith, R. W. and Lilienthal, G. W., "Scroll-type machine with rotation controlling means and specific wrap shape", Unite States Patent Number: 4,609,334, Sep. 2, 1986.

Morakami, H., Ito, H., Asano, Y., Narazaki, K., and Hasegawa, S., "Highly efficient double layer IPM (Interior Permanent Magnet) motor", Matsushita Technical Journal (in Japanese), Vol. 44, No. 2, pp.37-42, 1998.

Narita, K., Suzuki, T., Okudera, H., Kawai, Y., Souma, Y., Kawanishi K. and Fukuda, Y., "Permanent magnet rotor type electric motor", Unite States Patent Number: 5,990,593, Nov. 23, 1999.

Narita, K., Suzuki, T., Okudera, H., Kawai, Y., Souma, Y., Kawanishi K. and Fukuda, Y., "Permanent magnet rotor type electric motor", Unite States Patent Number:

5,962,944, Oct. 5, 1999.

National Institute of Standards and Technology (NIST), REFPROP 6.01, U.S. Department of Commerce, Gaitherburg, MD 20899, 1998.

Nieter, J. J. and Barito T., "Dynamics of compliance mechanisms in scroll compressor Part I: axial compliance, Part II: radial compliance", Proc. of the 1976 Int. Compressor Conference at Purdue, pp.308-326, 1976.

Ooi, K. T., "Design optimization of a rolling piston compressor for refrigerators", Applied Thermal Engineering, Vol. 25, pp.813-829, 2005.

Otto, O. K., "Variable-speed compressor performance", ASHRAE Transaction, Vol. 94, Part2, pp.1215-1228, 1988.

Ozisik, M. N., Basic heat transfer, McGraw-Hill Co., 1977.

Park, Y. C., Kim, Y. C. and Min, M. K., "Performance analysis on a multi-type inverter air conditioner", Energy Conversion and Management, Vol. 42, pp.1607-1621, 2001.

Park, Y. C., Kim, Y. C. and Cho, H. H., "Thermodynamic analysis on the performance of a variable speed scroll compressor with refrigerant injection", International Journal of Refrigeration, Vol. 25, pp.1072-1082, 2002.

Pandeya, P. N., "A simplified procedure for designing hermetic compressors", Proc. of the 1986 Int. Compressor Conference at Purdue, pp.415-427, Aug., 1986.

Qureshi, T. Q. and Tassou, S. A., "Variable-speed capacity control in refrigeration systems", Applied Thermal Engineering, Vol. 16, pp.103-113, 1996.

Richardson, H. and Gatecliff, G., "Comparison of the high side vs. low side scroll compressor design", Proc. of the 1992 Int. Compressor Conference at Purdue, pp. 603-608, July, 1992.

Richardson, H. and Gatecliff, G., "Scroll compressor stabilizer ring", Unite States Patent Number: 5,383,772, Jan. 24, 1995.

Sanderson, S. and Uzumeri, M., "Managing product families: The case of the Sony Walkman", Research Policy, Vol. 24, pp.761-782, 1995.

Schein, C. and Radermacher, R., "Scroll compressor simulation model", Journal of Engineering for Gas Turbines and Power, Vol. 123, pp.217-225, Jan., 2001.

Shao, S. Q., Shi, W. X., Li, X. T. and Chen, H. J., "Performance representation of variable-speed compressor for inverter air conditioners based on experimental data", International Journal Refrigeration, Vol. 27, pp.805-815, 2004.

Shimma, Y., Tateuchi, T. and Sugiura, H., "Inverter control systems in a residential heat-pump air-conditioner", ASHRAE Transactions Paper, HI-85-31, No. 2, pp.1541-1552, 1988.

Shon, J. C. and Hwang, D. Y., "Brushless DC motor with a two-layered permanent magnet rotor structure", Unite States Patent Number: 6,072,256, Jun. 6, 2000.

Sorensen, F., "Hermetic compressor with brushless DC motor", Proc. of the 1980 Purdue Compressor Technology Conference, pp. 223-226, July, 1980.

Suefuji, K. and Shiibayashi, M., "Performance analysis of hermetic scroll compressor", Proc. of the 1992 Int. Compressor Conference at Purdue, pp. 75-84, July, 1992.

Sundgren, N., "Introducing interface management in new product family development", Journal of Product Innovation Management, Vol. 16, pp.40-51, 1999.

Tanimoto, S. and So, M., "Permanent magnet motor", Unite States Patent Number: 5,510,662, Apr. 23, 1996.

Tassou, S. A., Marquand, C. J. and Wilson, D. R., "Comparison of the performance of capacity-controlled and conventional-controlled heat-pumps", Applied Thermal Engineering, Vol. 14, pp.241-256, 1988.

Terauchi, K. and Hiraga, M., "Scroll fluid compressor unit with axial end surface sealing means", Unite States Patent Number: 4,437,820, Mar. 20, 1984.

Tojo, K., Hosoda, T., Ikegawa, M. and Shiibayashi, M., "Scroll compressor provided with means for pressing an orbiting scroll member against a stationary scroll member and self-cooling means", Unite States Patent Number: 4,365,941, Dec. 28, 1982.

Uchikawa, N., Terada, H. and Arata, T., "Scroll compressors for air conditioners", Hitachi Review, Vol. 36, No. 3, pp.155-162, 1987.

Ulrich, K., "The role of product architecture in the manufacturing firm", Research Policy, Vol. 24, pp.419-440, 1995.

Wang, C. C. and Chiang, C. S., "Two-Phase Heat Transfer Characteristics for R-22/R-407C In a 6.5-mm Smooth tube", Int. J. of Heat and Fluid Flow, Vol. 18, No. 6, pp.550-558, 1997.

Yanagisawa, T. and Shimizu, T., "Leakage losses with a rolling piston type rotary compressor II: leakage losses through clearances on rolling piston faces", Int. J. of Refrigeration, Vol. 8, No. 3, pp.152-158, 1985.

Young, N. O., Mason, N. H. and McCullough, J. E., "Scroll-type positive fluid displacement apparatus", Unite States Patent Number: 3,884,599, May 20, 1975.

Youn, Y., Cho, N. K., Lee, B. C. and Min, M. K., "The characteristics of tip leakage in scroll compressors for air conditioners", Proc. of the 2000 Int. Compressor Conference at Purdue, pp.797-806, 2000.

APPENDIX 1

THE INTRODUCTIONS OF STC SIMULATION PACKAGE

A STC computer simulation package has been developed by the author and the colleagues of ITRI in Taiwan. This computer model can predict the power consumptions, capacity, various efficiencies and COP_{el} of a STC for given operating conditions and the scroll designs. The design structure and the calculation flowchart developed by this study have been shown in Fig. 2.13 and Fig. 2.14, respectively.

The detailed input data include:

(1) Common design parameters of scroll: thickness, pitch, height, roll angle, tip leakage clearance, flank leakage clearance, material density.

(2) Dimension data of orbiting scroll and fixed scroll: suction port and discharge port coordinates, relative location between orbiting scroll and Oldham ring, other geometrical definition data.

(3) Oldham ring design data: mean diameter, keyway dimensions, material density.

(4) Crankshaft design data: bearing locations, counter-balancer location, material density, other geometry data.

(5) Bearings data: weight, height, inside and outside diameters, assembly clearance, thrust bearing diameter.

(6) Coefficients of friction between each contact pair that has relative motion: the contact pairs include orbiting scroll and Oldham ring, Oldham ring and main frame, orbiting scroll and fixed scroll, orbiting and main frame.

(7) Other components data: motor dimensions (height, inside and outside diameters, material density), upper and lower counter-balancer diameters and their mass center locations.

(8) Operation conditions: polytropic index, condensing and evaporating temperatures, STC suction temperature, import temperature of the expansion device.

(9) Other data: motor operating performance curve data (torque, efficiency), superheat temperature at suction port of scroll pump, power loss estimation of oil disturbance, individual bearing operating temperature, leakage coefficients estimation, step size definition of each design parameter, iteration number and convergence tolerance definitions.

Figure A1.1~A1.8 introduce the calculation outputs in this developed STC computer package. The detailed contents comprise:

(1) Figure A1.1 shows the animation of the scroll pump in compression process. It means that the geometrical model of the simulated scroll pump has been created.

(2) Figure A1.2 describes the simulation of initial design which does not include the leakage effects between orbiting scroll and fixed scroll. Six diagrams have been shown to depict the variation of pressure, temperature, density, viscosity, compression chamber volume and discharge area, respectively. It shows that the whole refrigerant and lubricant properties related to different pressure and temperature during compression process have been calculated in this program.

(3) Figure A1.3 presents the simulation of the property variations of working fluid that operate at compression and discharge process with leakage effects. Meanwhile, the leakage mass variations have also been calculated.

(4) Figure A1.4 introduces the dynamic balance and various power losses. The individual acting force that worked on the orbiting scroll as equation (2-15) defined, has all been described in the diagrams. It depicts that the total real compression work has been calculated.

(5) Figure A1.5 shows one embodiment of analysis results of the driving bushing. It

presents the maximum lubricant pressure, friction power losses, lubricant mass flow rates and the bearing load.   The other bearings as Fig. 2.8 depicted, will all be shown the calculated results in this diagram.

(6) Figure A1.6 ~ A1.8 display the simulation results of various power consumptions, capacity, COP_{el}, volumetric efficiency, motor efficiency, compression efficiency, mechanical efficiency and other important calculation outputs.

An overview of the developed computer package for STC simulation is introduced as above.   Moreover, the validation work with R22 refrigerant has been carried out in Chapter 3, the deviation between calculated and measured data of the verified STC is under 4%.

Table A1.1 lists one embodiment of the calculation output used with this computer package for searching the maximum COP_{el} subjected to a change of scroll height on the basis of $t = 2.6mm$, $\phi_r = 1150°$.   By following the optimization process and STC design flowchart of Fig. 4.1 and Fig. 4.2 depicted, the STC family design approach has been implemented in this dissertation and the results have been present very practical.

Table A1.1 One calculation output datasheet of STC family approach

h_e	p_t	r_{ob}	t	h_e/t	$h_e/(p_t-t)$	D_{o_max}
(mm)	(mm)	(mm)	(mm)	(-)	(-)	(mm)
10.0	15.735	5.267	2.6	3.846	0.761	100.654
11.2	15.041	4.920	2.6	4.308	0.900	96.211
12.4	14.451	4.625	2.6	4.769	1.046	92.440
13.6	13.942	4.371	2.6	5.231	1.199	89.186
14.8	13.498	4.149	2.6	5.692	1.358	86.344
16.0	13.105	3.953	2.6	6.154	1.523	83.833
17.2	12.756	3.778	2.6	6.615	1.694	81.595
18.4	12.441	3.621	2.6	7.077	1.870	79.585
19.6	12.157	3.478	2.6	7.538	2.051	77.766
20.8	11.898	3.349	2.6	8.000	2.237	76.110
22.0	11.661	3.231	2.6	8.462	2.428	74.596
h_e	η_v	η_m	η_c	Q_c	P_{motor}	COP_{el}
(mm)	(%)	(%)	(%)	(W)	(W)	(-)
10.0	0.934	0.711	0.898	4660.79	2027.024	2.674
11.2	0.932	0.739	0.896	4653.78	1954.433	2.769
12.4	0.931	0.761	0.893	4646.5	1900.248	2.844
13.6	0.929	0.78	0.89	4639.02	1856.704	2.906
14.8	0.928	0.795	0.887	4631.36	1824.278	2.953
16.0	0.926	0.808	0.884	4623.56	1798.598	2.990
17.2	0.925	0.821	0.881	4615.62	1774.431	3.025
18.4	0.923	0.83	0.877	4607.57	1758.217	3.048
19.6	0.921	0.838	0.874	4599.43	1744.906	3.066
20.8	0.92	0.845	0.871	4591.19	1733.965	3.080
22.0	0.918	0.851	0.867	4582.86	1725.618	3.089
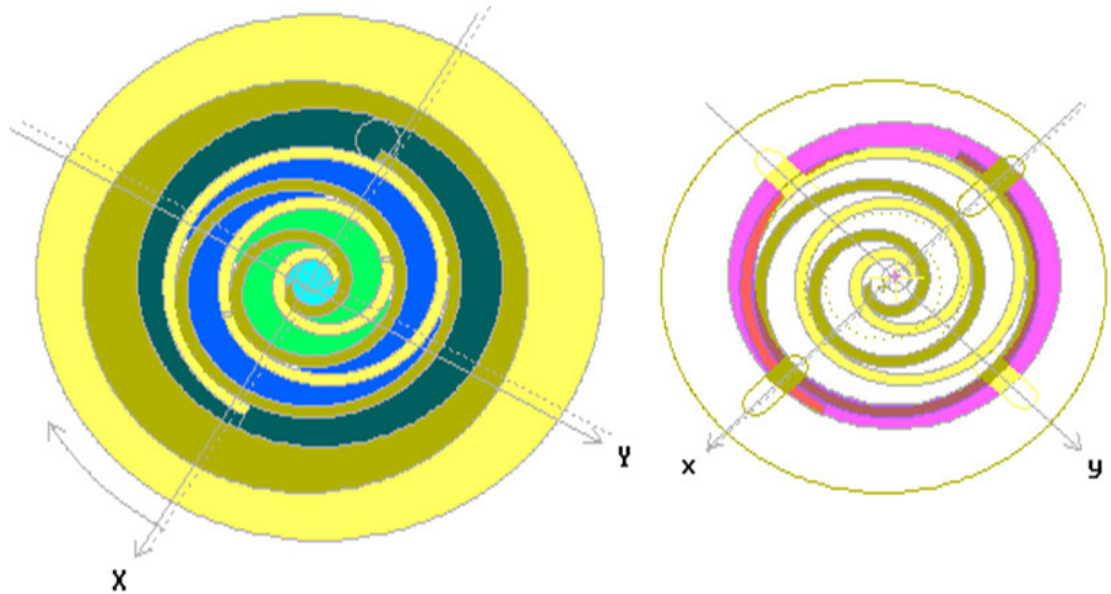
Fig. A1.1 The animation of the scroll pump in compression process
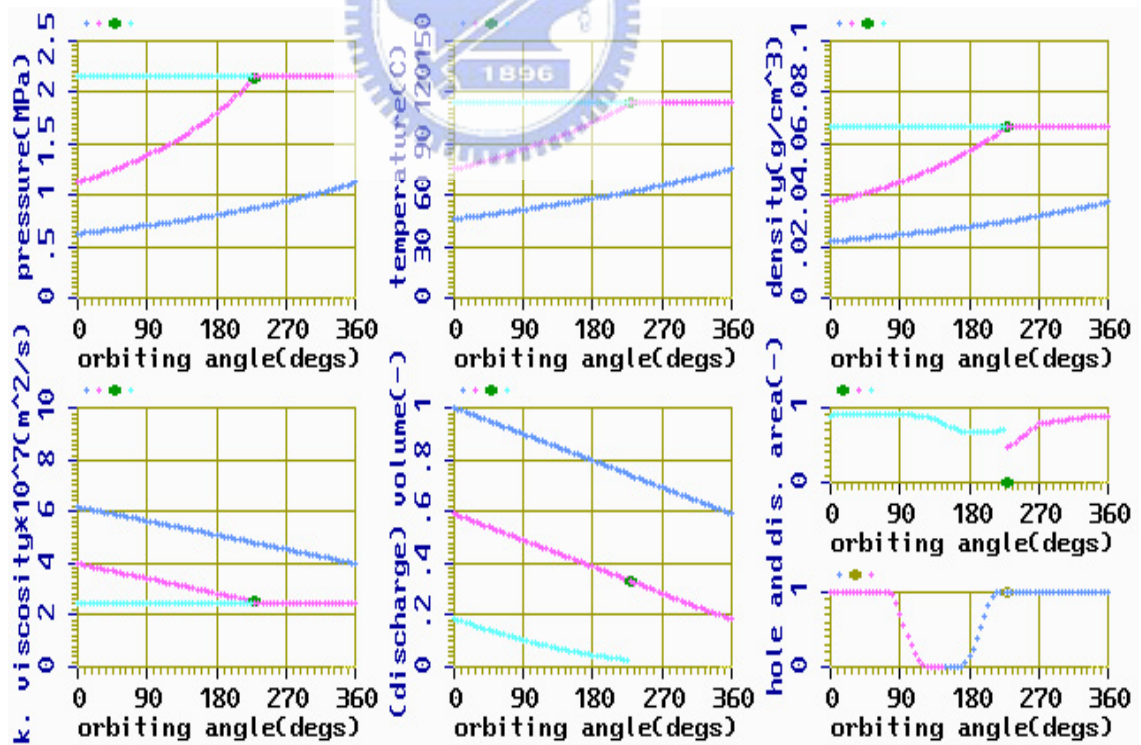
Fig. A1.2 The initial design simulation (leakage effects not include)
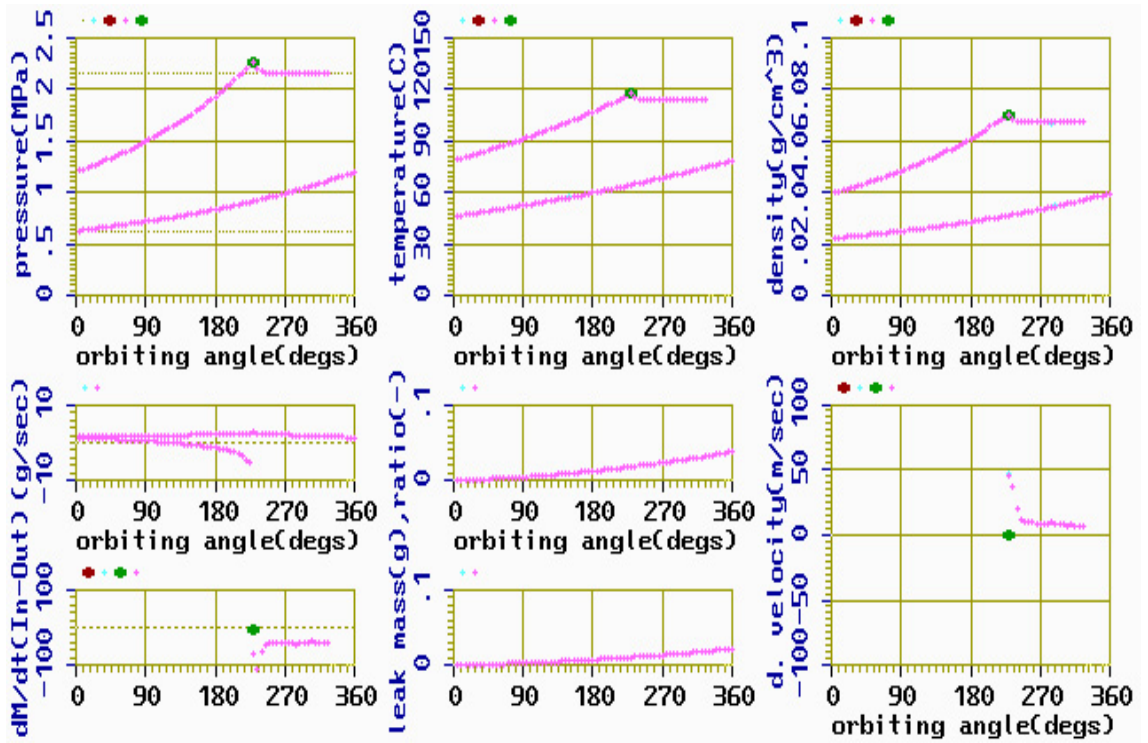
Fig. A1.3 The design simulation in compression and discharge process
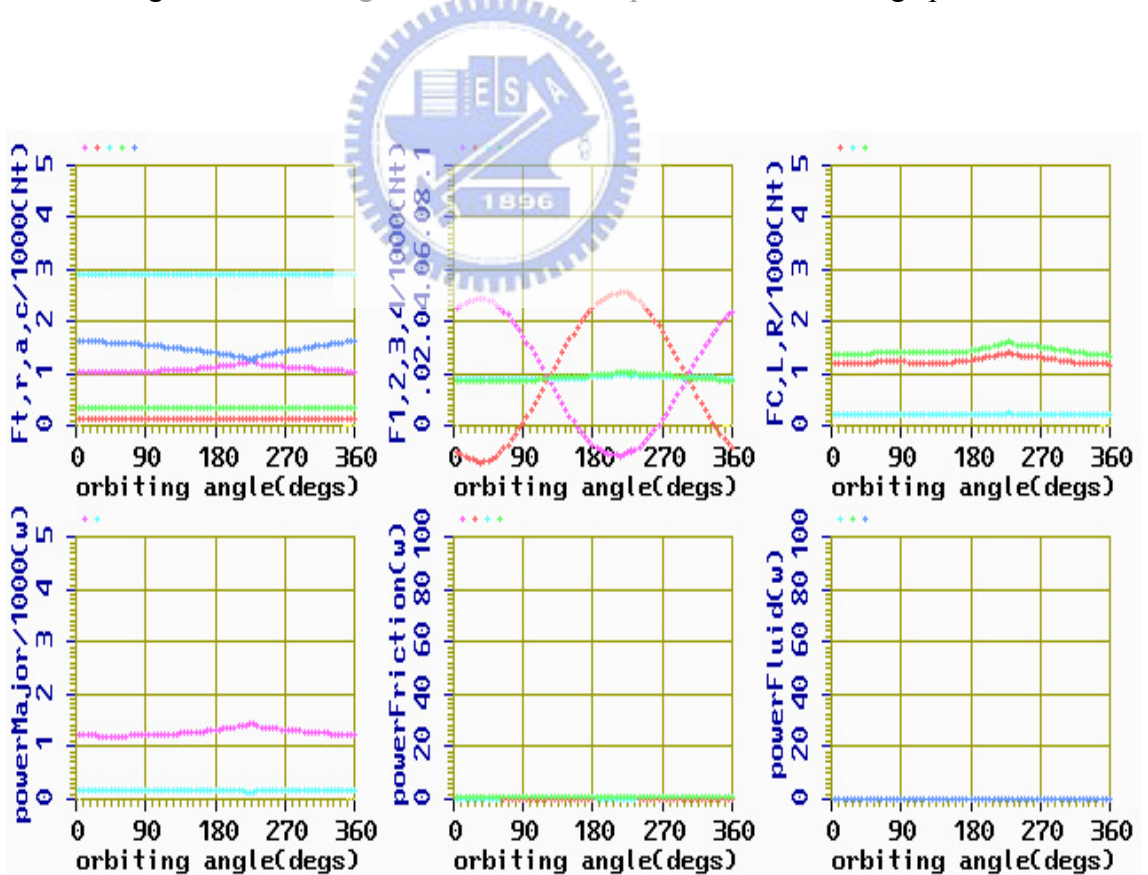
Fig. A1.4 The simulation of dynamics balance and power losses
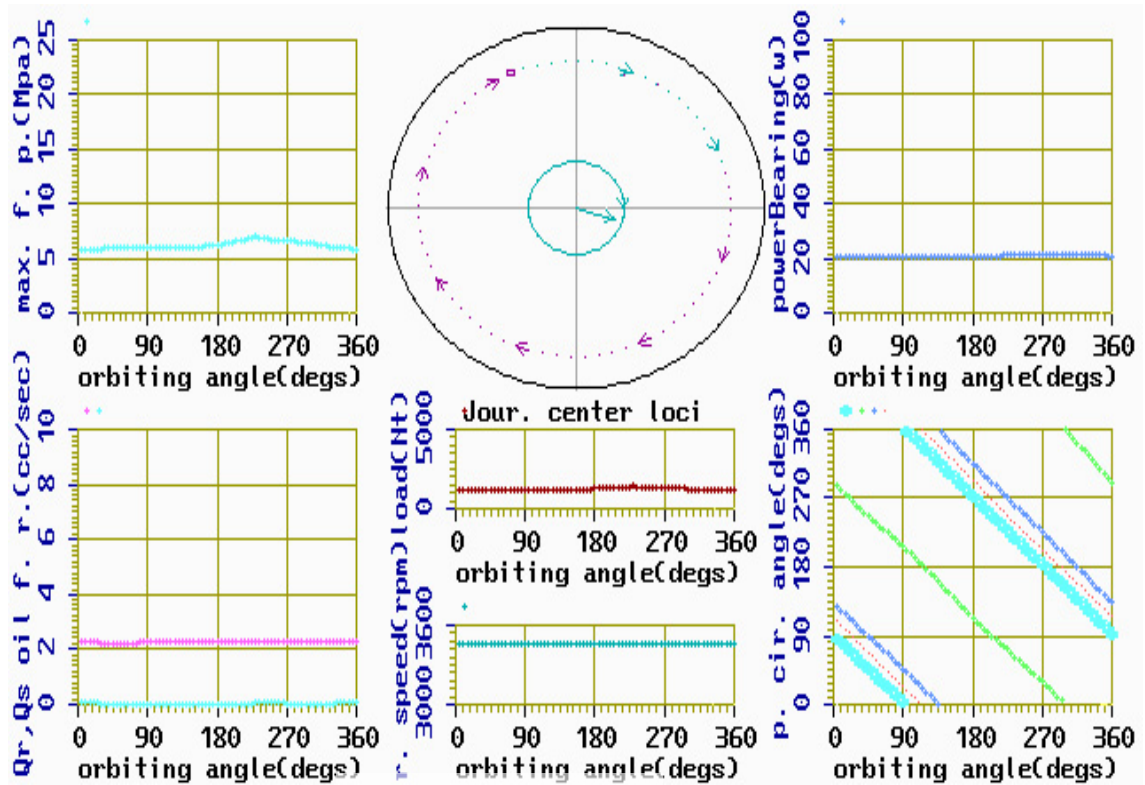
Fig. A1.5 The simulation of each bearing working status

P. of Friction between Scroll and Thrust	119.2(w)	5.8(%)	55.6(%)
P. of Friction between Scroll and Oldham	0.5(w)	0.0(%)	0.2(%)
P. of Friction between Oldham and Thrust	0.01(w)	0.0(%)	0.0(%)
P. of Friction between Oldham and Frame	0.49(w)	0.0(%)	0.2(%)
P. of Friction between Shaft and Thrust	0.38(w)	0.0(%)	0.2(%)
P. of Friction of Crank journal bearing	34.3(w)	1.7(%)	16.0(%)
P. of Friction of Upper journal bearing	42.4(w)	2.1(%)	19.8(%)
P. of Friction of Lower journal bearing	10.8(w)	0.5(%)	5.1(%)
P. of Fluid of turbulering oil	0.0(w)	0.0(%)	0.0(%)
P. of Fluid of pumping oil	6.8(w)	0.3(%)	3.2(%)
P. of Mechanical Loss (summing above all)	214.4(w)	10.5(%)	100.0(%)
P. of Gas Compression	1837.1(w)	89.5(%)	********
P. of Mechanical Total(summing above two)	2051.6(w)	100.0(%)	********

Fig. A1.6 The output of power consumptions

```
                    EER and EFF result

  EER(kcal/hr-w)                               2.75
  COP(-)                                       3.19
  motor input power(w)                      2390.20
  refrigerating capacity(kcal/hr)           6567.94

  motor rotating speed(rpm)                 3470.00
  refrigerant mass flow rate(kg/hr)          160.97
  Volumetric efficiency of gas   Heat(%)      95.02
  Volumetric efficiency of mass  Loss(%)      96.13

  Volumetric  efficiency(%)                   91.35
  Motor       efficiency(%)                   86.21
  Compression efficiency(%)                   86.57
  Mechanical  efficiency(%)                   89.55
```

Fig. A1.7 The output of various operating efficiencies

```
                    Else result

  internal superheat temperature              12.00
  pump suction    temperature(C)              47.00
  pump discharge temperature(C)              116.38

  discharge angle(degs)                      185.51
  suction    volume(cc)                       36.60
  discharge volume(cc)                        12.83
  volume ratio(-)                              2.85
  shape design compression ratio(-)            3.22
  T.E.C design compression ratio(-)            3.43
  operating compression ratio(-)               3.43
```

Fig. A1.8 The output of other important calculation results

APPENDIX 2
IPMSM INNOVATION RECORDS

According to the study results, the STC used with IPMSM (Interior Permanent Magnet Synchronous Motor) and applied in inverter-fed air-conditioning system, has more energy-saving effect. But the IPMSM used for compressor has many patents in the world. Therefore, the first investigation should be to do the patent around of an IPMSM motor used for an inverter-fed STC.

As for the patent around, Chen and Tseng (2002) have introduced the overall structure to justify the importance of a patent database because of the judgment of patent infringement and technological innovations.

In this appendix, an implemented case of the patent innovation process used for the developing IPMSM is introduced. The records of IPMSM developing in this appendix include patent survey, a built-up abstract list and a function matrix analysis of the major related patents, concept design, performance predictions and comparisons with prior arts. Finally, a new design of IPMSM has been proposed, in the meantime, an innovative concept has been applied to patent and the prototype put into practice with the performance comparisons between the new IPMSM design, the traditional SPM (surface permanent magnet) of brushless motor and the three-phase AC induction motor used in the developed STC, are also presented respectively.

A2.1 Patent Survey of IPMSM Applied For Compressor

A search of the US patent of IPMSM from the USPTO (United States Patent and Trademark Office) patent database from 1976 to 2003, show that 52 patents are judged to relate to compressor applications. Through detailed review of the patents, 10

patents have been selected to do a patent abstract in advance because these patents are major obstacles to overcome. Table A2.1 shows the patent numbers and the titles of these 10 selected patents. The IPMSM rotor configuration of each selected patent has been described in Fig. A2.1.

Table A.2 shows the summarized functional decomposition results of the selected patents used with a function matrix table which is the basic method of QFD (quality function deployment), and depicts four important design directions:

(1) A rotor built-in with one layer of permanent magnets with a rectangular shape is easy to manufacture and assemble, but the performance needs to be verified.

(2) The leaking of magnetic flux can be avoided due to the flux barrier holes or non-permeability regions that deposed in rotor, but the manufacturing and assembling process will be more complex.

(3) Narrowing the space between the permanent magnets and the contour of rotor, and by putting the side face between each permanent magnet as closely as possible will reduce the leaking of magnetic flux.

(4) An arc-shaped cross section with its convex portion directed toward the rotor axis, has better performance (Murakami *et al.*, 1998), but the manufacturing and assembling process will be more complex.

A2.2 Bench Marking Analysis

To verify the above summarizations described in A.1, four Japanese commercial products of the PMSM (permanent magnet synchronous motor) used in compressor, have been collected from DC inverter-fed air-conditioners. The computer package of Maxwell 2D developed by ANSOFT Corp. is used to receive the detailed dimension of each motor component, so that the magnetic flux and related performance can be

analyzed.

One type of SPM and three types of commercialized IPMSMs have been studied. The SPM brushless DC motor is produced by MHI (Mitsubishi Heavy Industries, Ltd.), the IPMSMs are the products of Toshiba co., Matsushita electric industrial co. and G.E. (General Electric Co.), respectively. These four types of PMSM, all have 3-phases, 4-poles, 24-slots configurations. Table A2.2 shows the specifications of these PMSM for the bench marking approach.

Figures A2.2~A2.5 show the simulation results of these four types of PMSM, which include air-gap magnetic flux, maximum output torque and maximum cogging torque. Both the Toshiba and Matsushita IPMSMs use a rotor with arc-shape magnets which results in better performance than either MHI SPM brushless motor or the traditional IPMSM with a rectangular-shape magnet such as G.E. product. But the manufacturing costs of the rotor with an arc-shaped magnet are higher and require a more complex process to assemble than the rotor with rectangular flat-plate type magnet. Therefore, an innovation study about the IPMSM has been carried out in this study.

A2.3 Innovation of IPMSM

A2.3.1 Concept Design

The product commercialization requirements are: easy manufacturing and assembly, a common rotor's magnet and stator's core materials and higher performance. These are the innovative objectives also.

Therefore, the summarized innovative directions are:

(1) Cross section magnet with a rectangular-shape, single layer and no flux-barrier holes: to allow easier manufacture for the rotor.

(1) Narrowing the space between the permanent magnets and the contour of rotor and by putting the side face between each permanent magnet as closely as possible: to reduce the leakage of magnetic flux and to get higher performance.

(2) The Rotor's magnets and stator's core material are the same as the bench marking products: to get the same base of material properties and cost.

Thereafter, four types of the new IPMSM concept design have been innovated as Fig. A2.6 introduces.

A2.3.2 Performance simulations and comparisons

Based on the same specifications as Table A2.3 shows, Fig A2.7~Fig. A2.10 have presented the simulated results of these four innovated concept designs.

Table A2.4 shows the comparisons between the bench marking products and the concept designs. The simulation results can be summarized as:

(1) The air-gap flux density of these four concept designs have the same results as the Toshiba and Matsushita products that have the maximum output torque based on the previous study.

(2) The concepts of design 1 and design 3, which have the smallest cogging torque mean these two designs will have low operating noise.

(3) To compromise between maximum output torque and cogging torque, design 1 and design 2 are both feasible solutions, with the concept of design 2 having the best torque output performance. In addition, these two types of magnet configuration obtain an effective manufacturing cost that will compete with the benchmarked products. Meanwhile, the performance solutions meet the innovative objectives defined in this study.

(4) Therefore, based on the design concepts of 1 and 2, one patent has been applied for Taiwan, mainland China and the USA.

A2.4 Patent Design of the Innovated IPMSM

A2.4.1 Invention Abstract

The present invention is a motor that includes an annular stator and a rotor. The rotor is with a built-in permanent magnet. The annular stator has a cylindrical interior into which the rotor is inserted. A space is formed between a circumference surface of the cylindrical interior and rotor. The rotor further includes a rotor core, and a plurality of openings that are formed surrounding the rotor core. Each opening has two parallel surfaces, a top surface and a bottom surface, and each of them is a flat plate figure. A suitable distance is between the two side surfaces and an outer circumference of the rotor, and the two side surfaces of adjacent openings are spaced by a channel of suitable width. A plurality of permanent magnets are arranged in openings by way of interlaced magnetic poles, and the shape of permanent magnet matches with the shape of the opening.
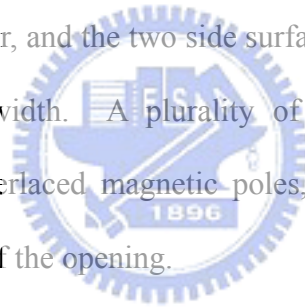
A2.4.2 Invention Descriptions

As shown in the Fig. A2.11, when the rotor radius of the innovated IPMSM rotor R_o is determined, in order to meet the requirement of magnetic flux reduction, and due to the constraints of assembly, the minimum $\triangle R$ will be obtained. According to the practical experiences in manufacturing, $\Delta R \leq 0.7mm$ will provide the optimal solution. Therefore the radius R_m of the maximum arc (shown as AB and A'B') of the magnet can be obtained, which means $\triangle R = (R_o - R_m) \leq 0.7mm$.

Next, the thickness, t, has to be determined, according to the drawing, $t = t_1 + t_2$, wherein t_1 and t_2 can be 0, so, the length of AA' (define as L_1) is equal to $2(R_m \cdot \sin\theta_1)$,

Which means $L_1=2(R_m \cdot sin\,\theta_1)$ and $L_3=2[(R_m \cdot sin\,\theta_2)-(t_2\,tan\,\theta_2)]$, wherein $L_3=CC'$ and $t_1=R_m \cdot (cos\,\theta_1 - cos\,\theta_2)$.

As the drawing of Fig. A2.11 depicts, $d=R_m \cdot con\,\theta_2$, θ_2 is determined depending on the number of magnets of the IPMSM and the requirement of the performance, when the number of magnets, $P\geqq4$, $\theta_2=(360/P)-\varDelta\,\theta$, wherein $\varDelta\,\theta$ is the angle between the gap of two adjacent magnets toward the axis of the rotor, which means the gap is around $R_m \cdot \Delta\,\theta$, in the experimental testing, the gap$\leqq0.7mm$ will produce the best performance, which also means $\Delta\,\theta \leqq[(0.7\ R_m)-(360/\pi)]$. And when $P\leqq4$, θ_2 will not be limited, the value will be determined by the performance desired and the outer radius of the rotor of the motor.

From the above derivation, when $t_2=0$, $L_2=L_3$, the shape of magnet can be changed to concept design 1 as Fig. A2.6(a) shows. It means by modifying these geometrical design parameters, the magnet shape can be changed to many types.

As the aforesaid mention, the rotor with built-in permanent magnet of the present invention is with the functions of flexible design and easy formation. The motor runs with low cogging torque and high output torque to promote efficiency and decreases vibration noise, and the cost is also low. Thus, the present invention totally figures out the shortcomings of the earlier designs.

The details of this patent, can be seen from the issued patent of US 6,987,341 (2006), TW200822 and ZL01267457.5.

A2.5 Prototyping and Performance Verification

Based on the concept of design 2 as Fig. A2.6(b) shows, the prototyping and performance verification have been carried out. Figure A2.12 shows the components

of this new IPMSM motor prototype and the Fig. A2.13 shows the efficiency comparisons between the AC induction motor, the SPM brushless motor of commercial products, and the new IPMSM motor that was developed by this study.   The dimension of these tested motors is identical and all is operated at constant torque of 2.0 N-m. The results depict the new IPMSM design has a higher efficiency of about 3%~5% more than the SPM brushless motor while operating under 5000rpm.

A2.6 Conclusions

A new IPMSM has been innovated and granted the patent in the world.   The present invention has better effectiveness of flexible design, easy formation, low cogging torque and high output torque.   Meanwhile, the prototyping and performance verification has been implemented.   The results show that the new IPMSM design has a higher efficiency than either the SPM brushless motor of the AC induction motor.
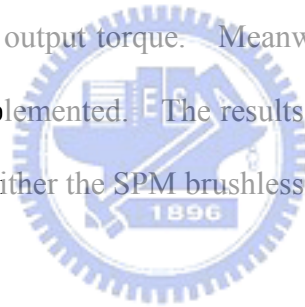
Table A2.1 Ten selected patents of IPMSM to analyze in this study

Patent no.	Titles	Assignee
US 5,510,662	Permanent Magnet Motor	Kabushiki Kaisha Toshiba, Kanagawa, Japan
US 6,072,256	Brushless DC Motor with a Two-Layered Permanent Magnet Rotor Structure	SamSung Electronics Co., Ltd., Kyungki-do,
US 5,962,944	Permanent Magnet Rotor Type Electric Motor	Rep. of Korea
US 5,990,593	Permanent Magnet Rotor Type Electric Motor	Fujitsu General Limited, Kawasaki, Japan
US 6,031,311	Brushless DC Motor Capable of Preventing Leakage of Magnetic Flux	Fujitsu General Limited,
US 6,034,459	Permanent Magnet Type Dynamo Electric Machine and Electric Vehicle using the Same	Kawasaki, Japan
US 5,945,760	Motor With Built-in Permanent Magnets	Samsung Electronics Co. Ltd., Suwon,
US 4,570,333	Method of Making a Permanent Magnet Motor	Rep. of Korea
US 5,684,352	Permanent Magnet Field-Type Rotating Machine	Hitachi Ltd.,
US 6,008,559	Motor Using A Rotor Including An Interior Permanent Magnet	Japan

Table A2.2 Functional decomposition table of IPMSM patent survey

Patent no.	Functional decomposition					Effectiveness		
	Magnet shape	Magnet layers	Arrangement	Flux barrier holes	Special Manufacture Process	Performance	Noise	Manufactur-ability
US 4570333	Rectangle	Single	Interior	Yes	No	Good	Good	Easy
US 5510662	Arc	Single	Convex toward axis center	No	No	Excellent	Excellent	Difficulty
US 5684352	Variable types	Single	Variable types	No	Non-permeability regions	Good	Good	Uncertainty
US 5945760	Arc	Double	Convex toward axis center	No	No	Excellent	Excellent	Difficulty
US 5962944	Variable types	Single	Variable types	Yes	No	Good	Good	Uncertainty
US 5990593	Arc	Double	Convex toward axis center	No	No	Good	Good	Difficulty
US 6008559	Variable types	Single	Variable types	Yes	No	Good	Good	Uncertainty
US 6031311	Rectangle	Single	Convex toward axis center	Yes	No	Good	Good	Common
US 6034459	Rectangle	Single	Circular interior	No	No	Good	Good	Easy
US 6072256	Arc	Double	Circular interior & Convex toward axis center	No	No	Good	Good	Difficulty

Table A2.3 Motor specifications of PMSM used for this study

Items	Stator	Rotor
Outside diameter	102 mm	60 mm
Inside diameter	61 mm	18 mm
Stack length	76 mm	80 mm
Material of silicon steel sheet	H-12	
Material of magnets	Ferrite, Br = 0.42 Tesla, iHc = 280KAm	
Configuration	3-phase, 4-poles, 24-slots	
Rated voltage	220 V	
Rated current	2 A	
Maximum current	10 A	
Rated speed	3600 rev/min	

Table A2.4 Comparisons between bench marking products and concept designs

Items	Motor & Magnet mounted type	Air-gap Flux density (Tesla)	Max. Output torque (N-m)	Max. Cogging torque (N-m)
MHI	SPM	0.34	2.15	0.90
Toshiba	IPMSM Arc-shape Single layer	0.35	3.28	0.70
Matsushita	IPMSM Arc-shape Double layer	0.35	3.20	0.78
G. E.	IPMSM Rectangular-shape Flux-barrier holes	0.30	2.60	0.82
Concept design 1	IPMSM Rectangular–shape Arc side face	0.33	3.00	0.5
Concept design 2	IPMSM Rectangular-shape Angle side face	0.35	3.18	0.72
Concept design 3	IPMSM Rectangular-shape Round side face	0.35	2.72	0.46
Concept design 4	IPMSM Rectangular-shape Right angle face	0.35	2.60	1.25
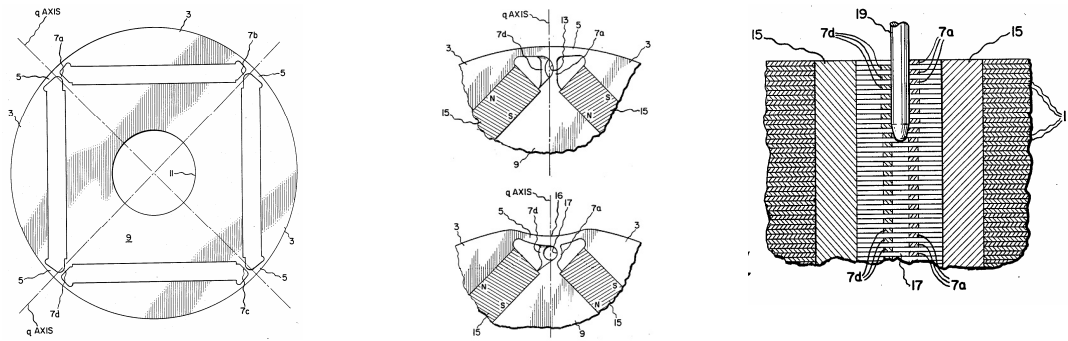
(a) IPMSM patent of G.E. Co.

(Issued by G.E. Co. in US 4,570,333 at Feb. 18, 1986)
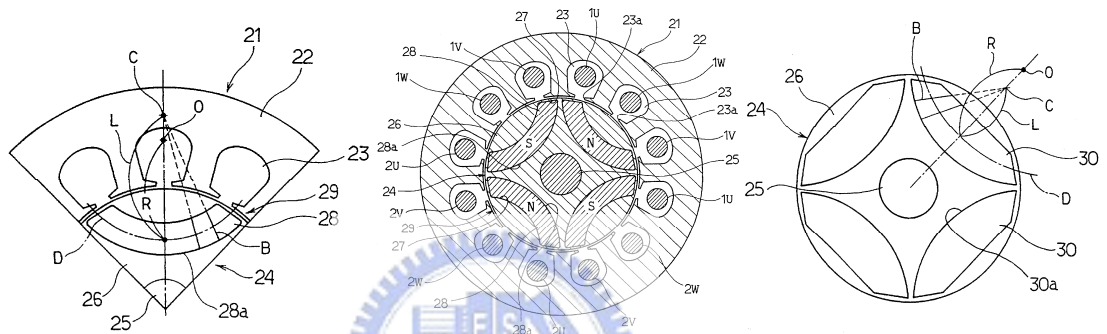
(b) IPMSM patent of Toshiba Co.

(Issued by Toshiba Co. in US 5,510,662 at Apr. 23, 1996)
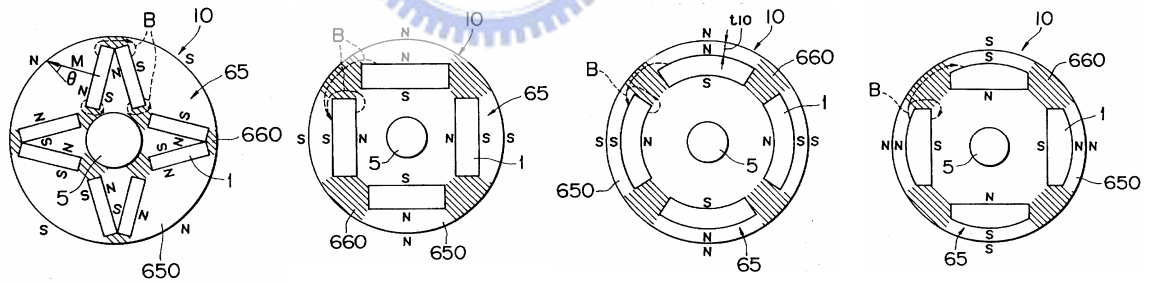
(c) IPMSM patent of Hitachi Metals

(Issued by Hitachi Metals, Ltd. in US 5,684,352 at Nov. 04, 1997)

Fig. A2.1 Prior arts of IPMSM rotor configuration
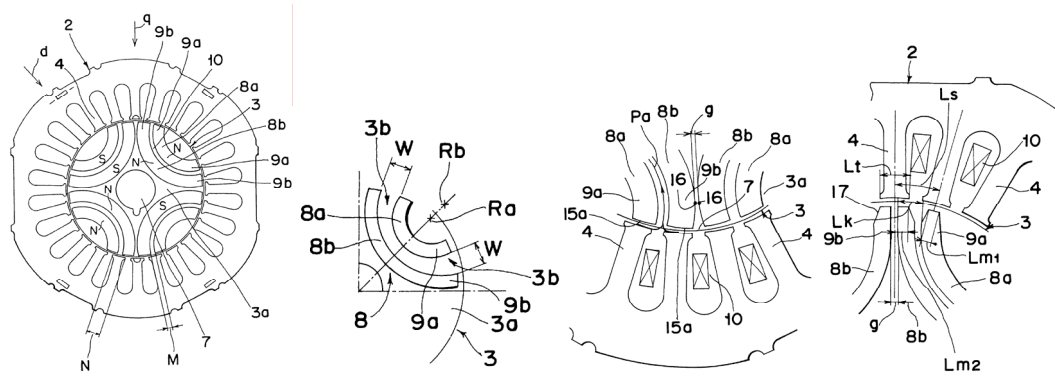
(d) IPMSM patent of Matsushita Co.

(Issued by Matsushita Co. in US 5,945,760 at Aug. 31, 1999)
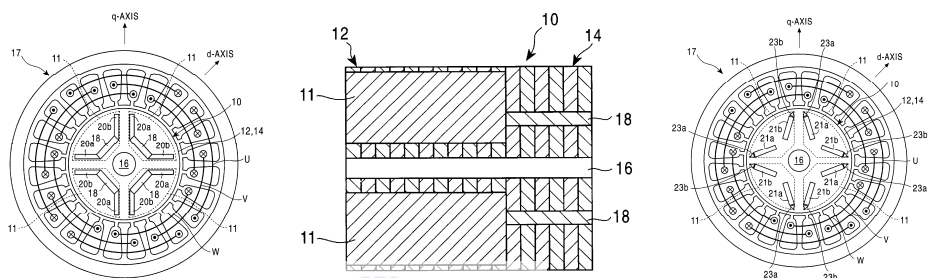
(e) IPMSM patent of Fujitsu General Co.

(Issued by Fujitsu General Ltd. in US 5,962,944 at Oct. 5, 1999)
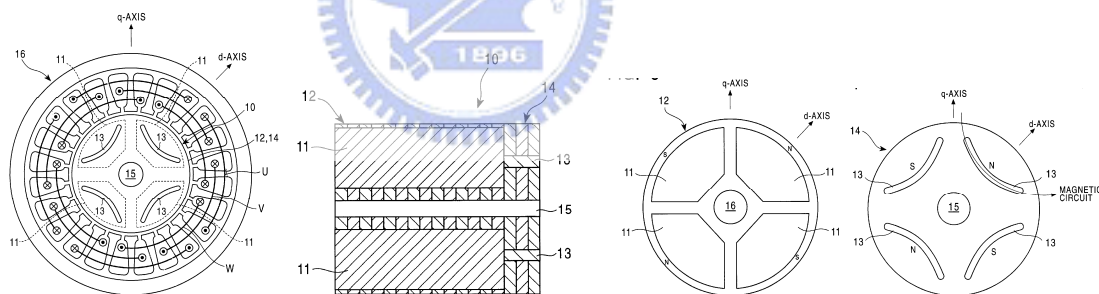
(f) IPMSM patent of Fujitsu General Co.

(Issued by Fujitsu General Ltd. in US 5,990,593 at Nov. 23 1999)
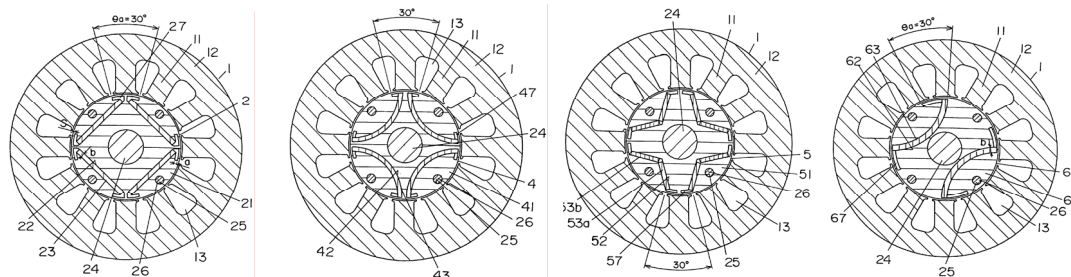
(g) IPMSM patent of Matsushita Co.

(Issued by Matsushita Co. in US 6,008,559 at Dec. 28, 1999)

Fig. A2.1 Prior arts of IPMSM rotor configuration (continued)
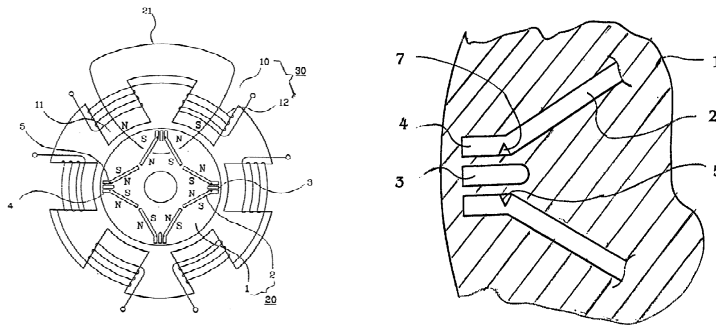
(h) IPMSM patent of Samsung Co.

(Issued by Samsung Co. in US 6,031,311 at Feb. 29, 2000)
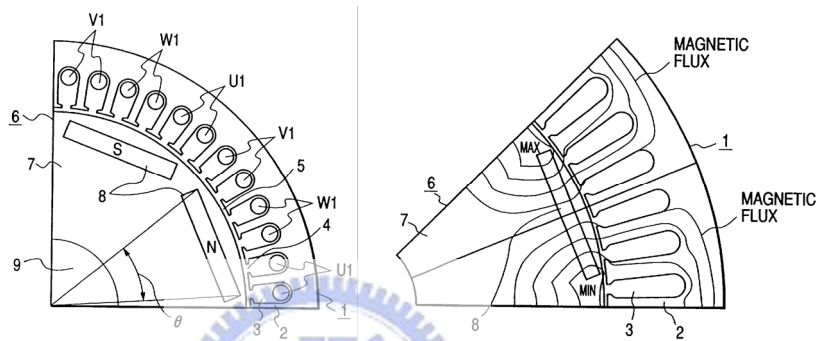
(i) IPMSM patent of Hitachi Co.

(Issued by Hitachi Co. in US 6,034,459 at Mar. 7, 2000)
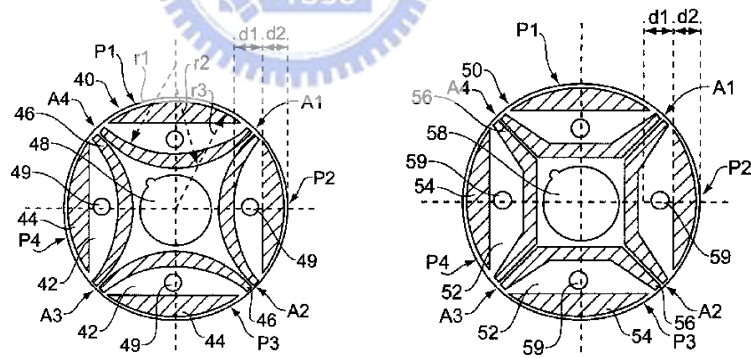
(j) IPMSM patent of Samsung Co.

(Issued by Samsung Co. in US 6,072,256 at Jun. 6, 2000)

Fig. A2.1 Prior arts of IPMSM rotor configuration (continued)
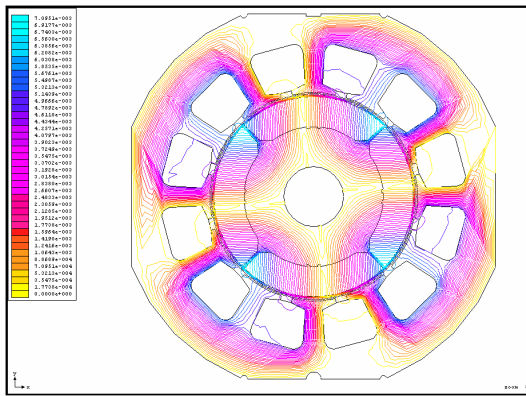
(a) Flux distribution
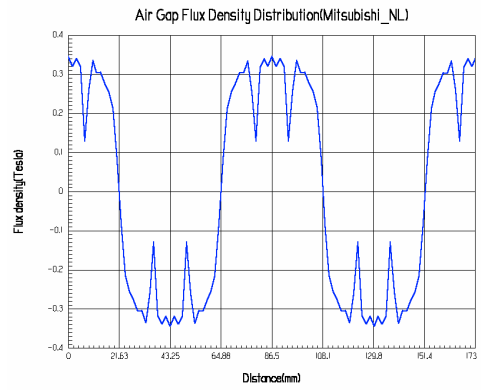
(b) Flux density of air-gap
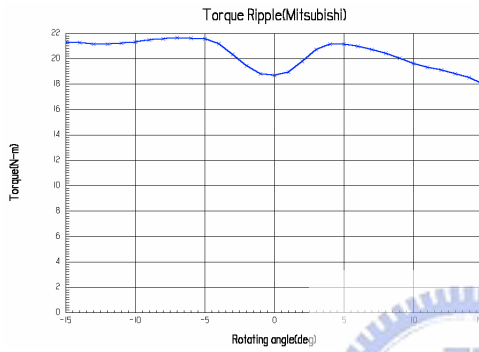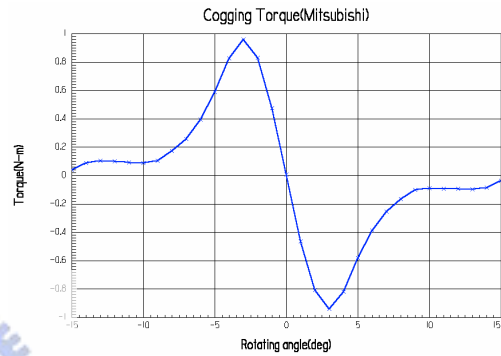
(c) Output torque

(d) Cogging torque

Fig. A2.2 Bench marking analysis of MHI SPM brushless motor product

145
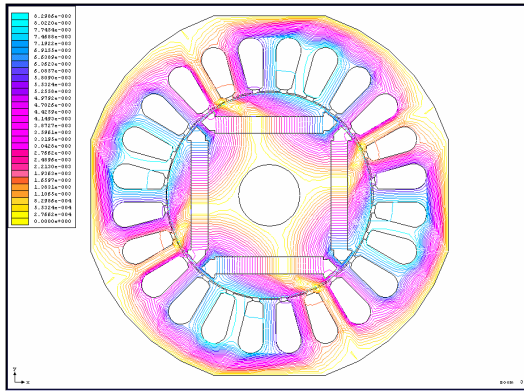
(a) Flux distribution

(b) Flux density of air-gap
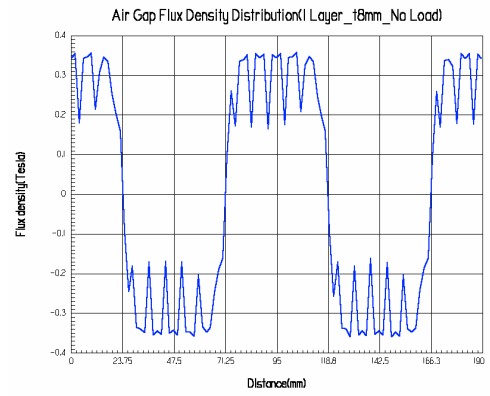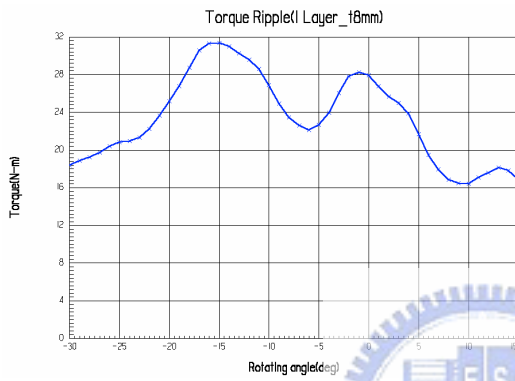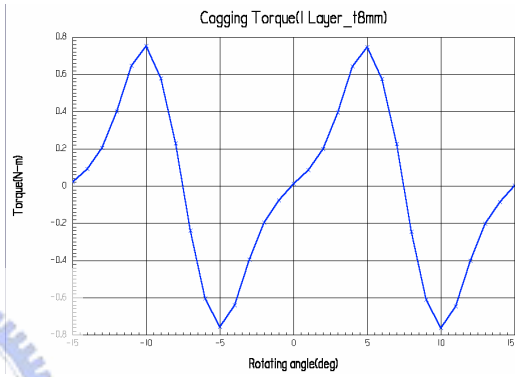

(c) Output torque

(d) Cogging torque

Fig. A2.3 Bench marking analysis of G.E. IPMSM product
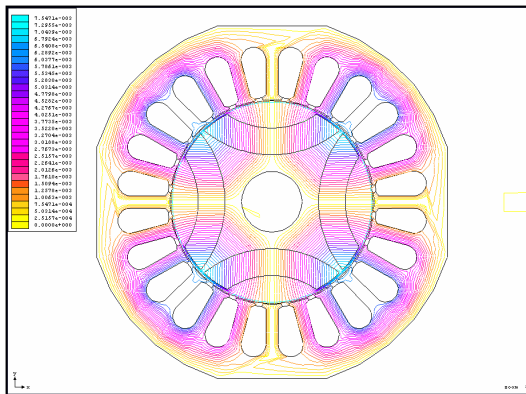
(a) Flux distribution
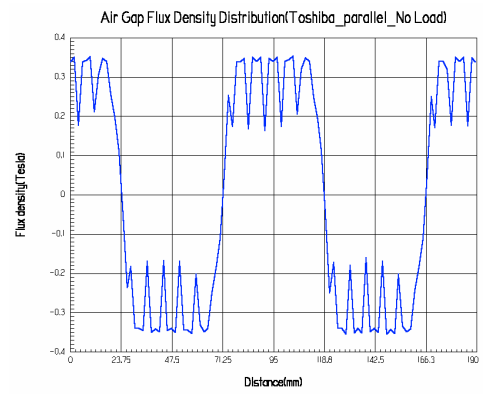
(b) Flux density of air-gap
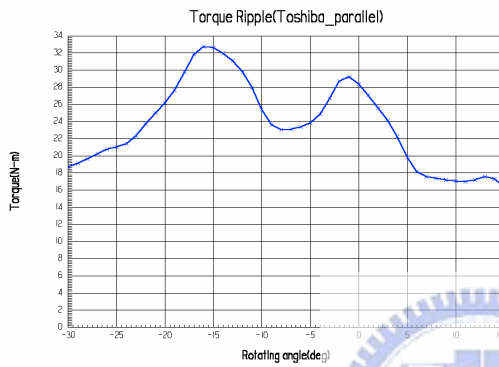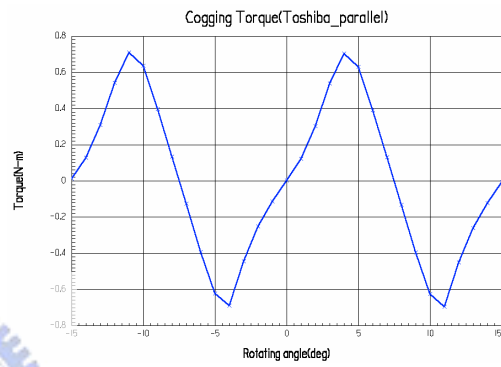
(c) Output torque

(d) Cogging torque

Fig. A2.4 Bench marking analysis of Toshiba IPMSM product

147
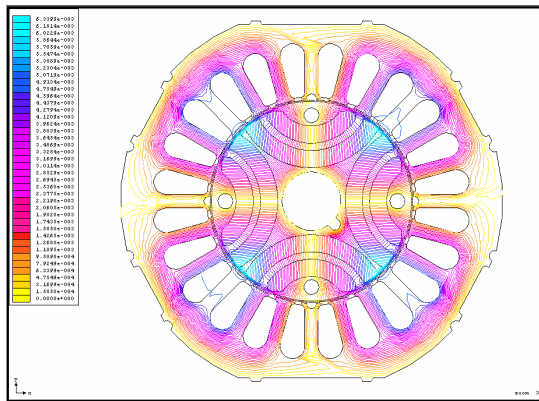
(a) Flux distribution
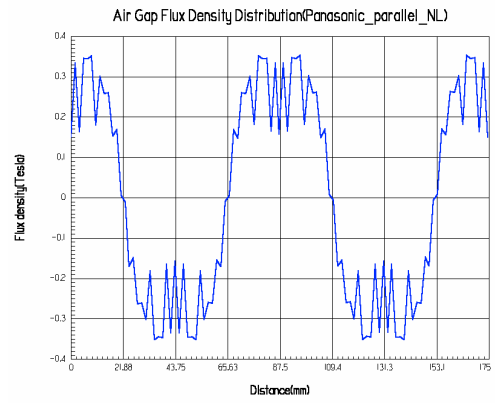
(b) Flux density of air-gap
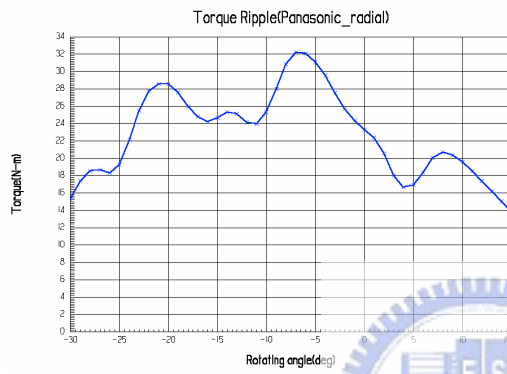
(c) Output torque
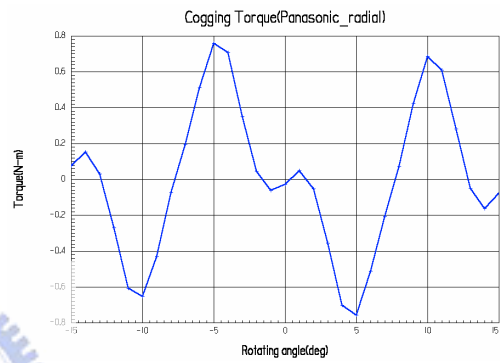
(d) Cogging torque

Fig. A2.5 Bench marking analysis of Matsushita IPMSM product
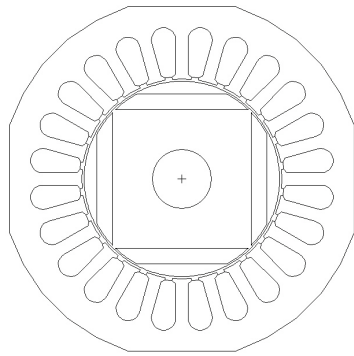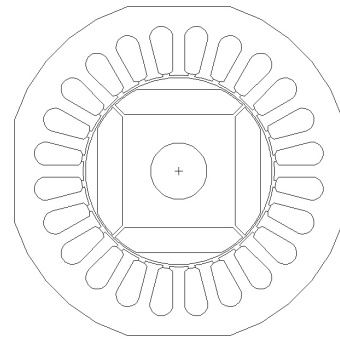
(a) Concept design 1   (b) Concept design 2
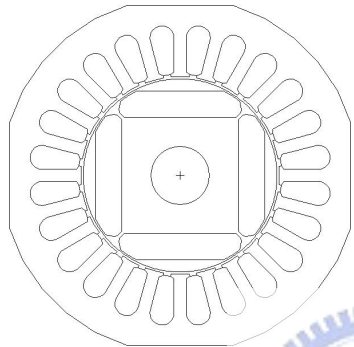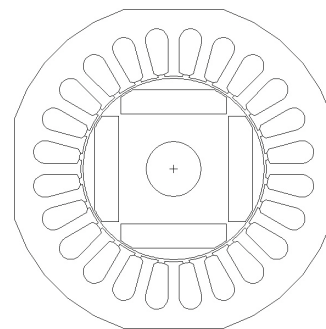
(c) Concept design 3   (d) Concept design 4

Fig. A2.6 Four concept designs of IPMSM of this study innovated
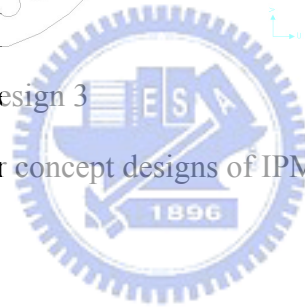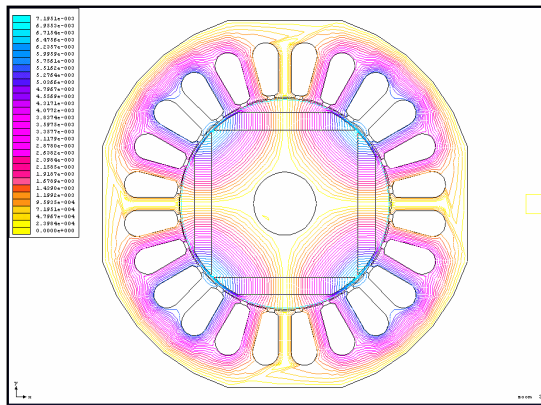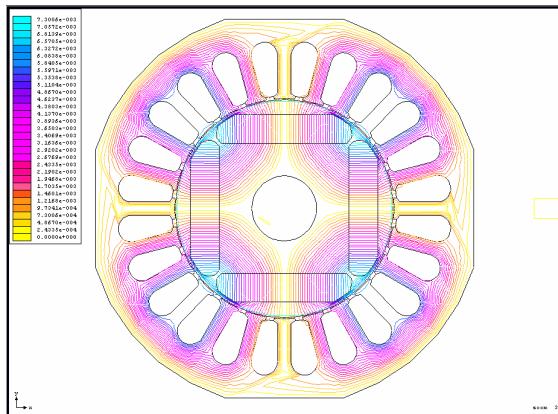
(a) Flux distribution
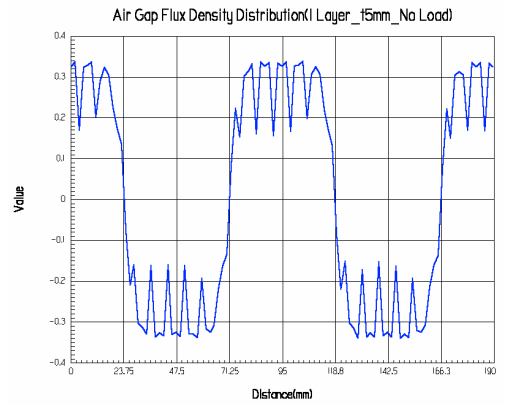
(b) Flux density of air-gap
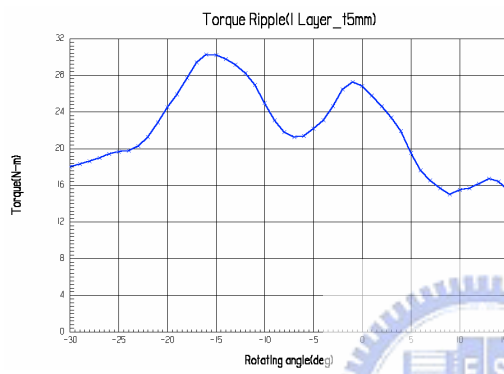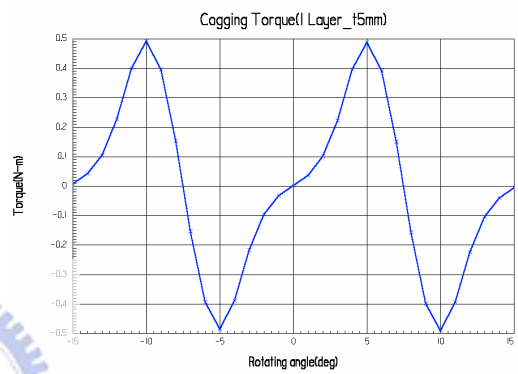
(c) Output torque

(d) Cogging torque

Fig. A2.7 The performance simulation of concept design 1
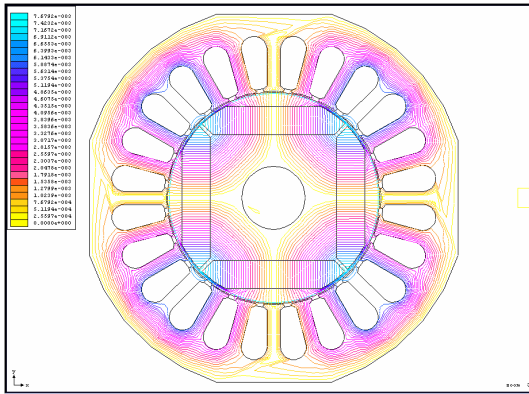
(a) Flux distribution
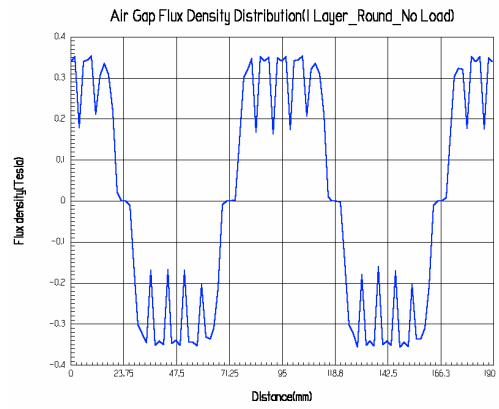
(b) Flux density of air-gap

(c) Output torque
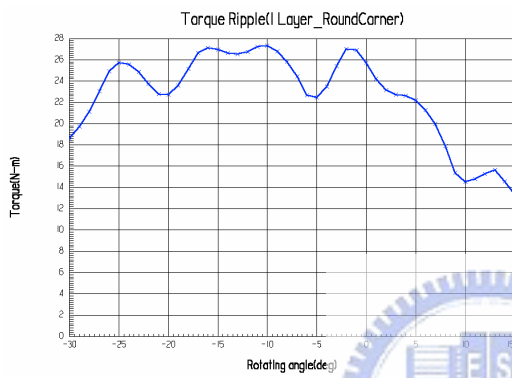
(d) Cogging torque
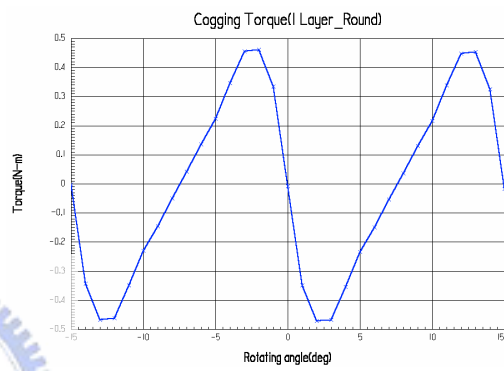
Fig. A2.8 The performance simulation of concept design 2
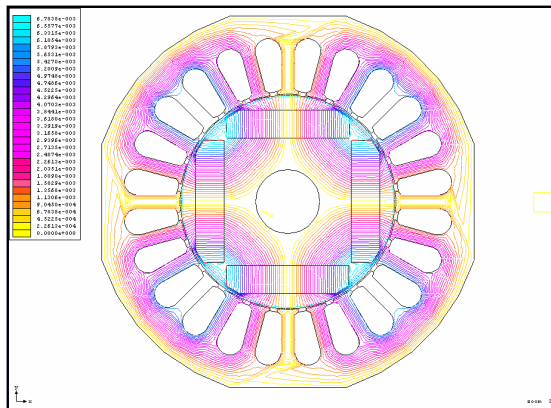
(a) Flux distribution

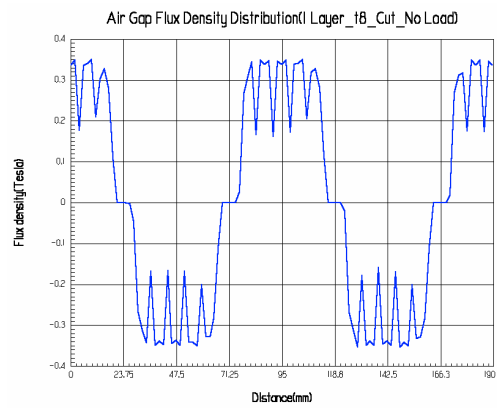
(b) Flux density of air-gap

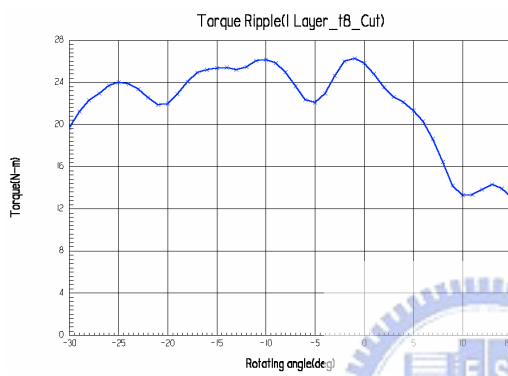
(c) Output torque

(d) Cogging torque

Fig. A2.9 The performance simulation of concept design 3

(a) Flux distribution

(b) Flux density of air-gap

(c) Output torque

(d) Cogging torque

Fig. A2.10 The performance simulation of concept design 4
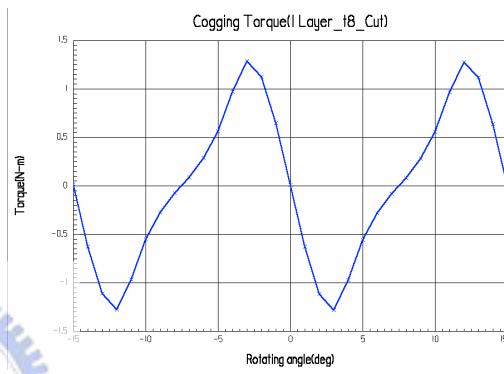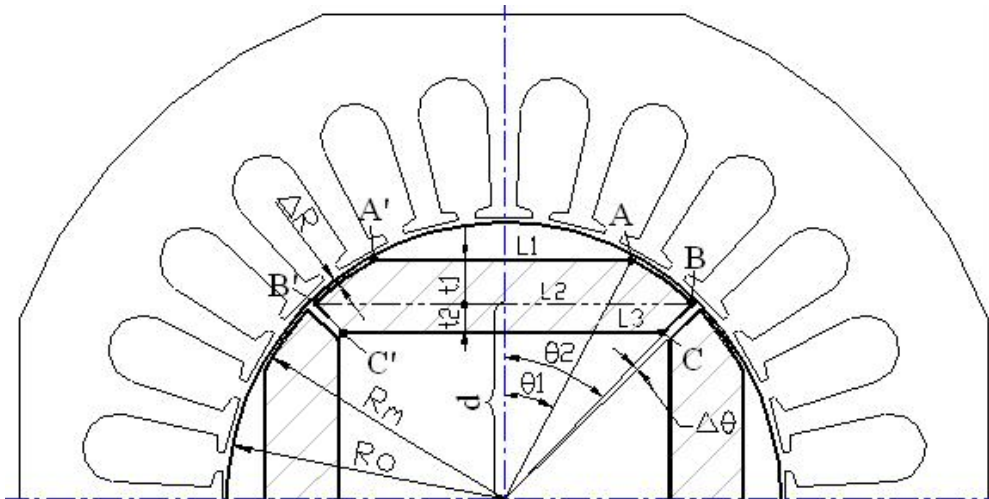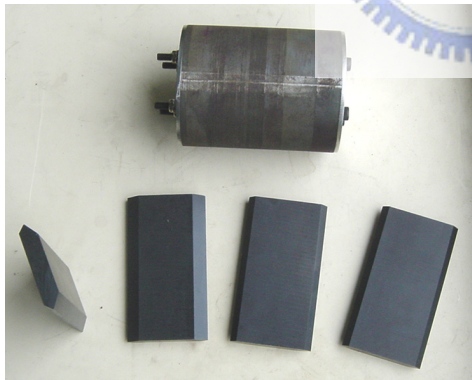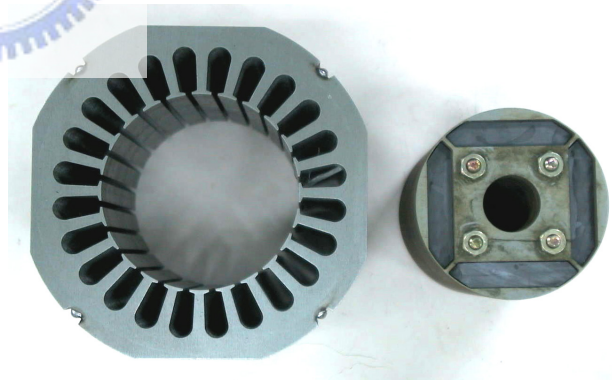
Fig. A2.11 The innovated IPMSM rotor geometry definition

(a) Rotor's magnets

(b) Stator and rotor
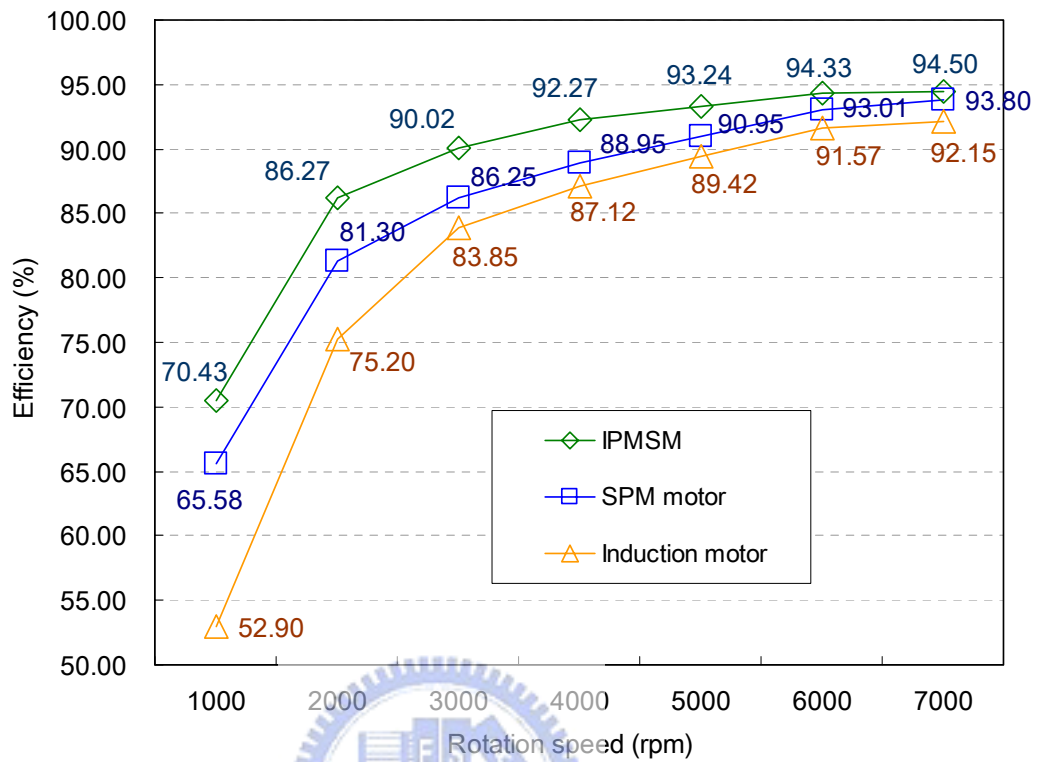
Fig. A2.12 The prototyping of the innovated IPMSM design

Fig. A2.13 The efficiency comparisons between 3Φ AC induction motor, SPM brushless motor of commercial product and the new IPMSM

AUTHOR'S PUBLICATION LIST

I. REFERED PAPERS

1. Chen, H. C., Huang, M. S., Liaw, C. M., <u>Chang, Y. C.</u>, Yu, P. Y., Huang, J. M., "Robust current control for brushless DC motors", Electric Power Applications, IEE Proceedings, Vol. 147, Issue 6, Nov. 2000, pp. 503-512

2. Lin, C. C., <u>Chang, Y. C.</u>, Liang, K. Y., ***Hung, C. H***., "Temperature and thermal deformation analysis on scrolls of scroll compressor", Applied Thermal Engineering Vol. 25, Aug. 2005, pp. 1724-1739.

3. Chen, J. L., Chen, J. W., Chen, H. C., <u>Chang, Y. C</u>., Yang, C. C., Liaw, C. M., "Front-end low-frequency switched-mode rectifier and its control for permanent-magnet synchronous-motor drive", Electric Power Applications, IEE Proceedings, Vol. 152, Issue 4, 8 July 2005, pp. 905-914.

4. ***Tseng, C. H.*** and <u>Chang, Y. C.</u>, "Family design of scroll compressors with optimization", Journal of Applied Thermal Engineering, Vol. 26, Issue 10, July 2006, pp. 1074-1086

5. Chen, H. C., <u>Chang, Y. C.</u>, Huang, J. K., "Development of optimised carrier sequence in MCU-based random-frequency PWM", IET Electric Power Applications, Vol. 1, No. 1, Jan., 2007, pp.43-48.

6. Chen, H. C., <u>Chang, Y. C.</u>, Huang, J. K., "Practical sensorless control for inverter-fed BDCM compressors", IET Electric Power Applications, Vol. 1, No. 1, Jan., 2007, pp.127-132.

II. CONFERENCE PAPERS

1. <u>Chang, Y. C.</u> and ***Tseng, C. H.***, "Family design of scroll compressors – a case study ", Proceedings of the 3rd International Compressor Technique Conference, Wuxi City, China, pp200-207, August, 2001.

2. <u>Chang, Y. C.</u> and ***Tseng, C. H.***, "Performance comparisons between constant speed and variable speed of scroll compressor using R-410A", Proceedings of the 17th International Compressor Engineering Conference at Purdue, USA, C24-2, July, 2002.

3. Lai, C. F., <u>Chang, Y. C.</u> and Yang, B. C., "A case study of theoretical comparisons of 3RT and 35RT scroll compressors", Proceedings of the 17th International Compressor Engineering Conference at Purdue, USA, C24-3, July, 2002.

4. Liaw, C. C., Liaw, C. M. , Chen, H. C., <u>Chang, Y. C.</u>, Huang, C.M., "Robust current control and commutation tuning for an IPMSM drive", Applied Power Electronics Conference and Exposition, 2003. APEC '03. Eighteenth Annual IEEE, Vol 2, 9-13 Feb. 2003, pp. 1045 – 1051.

5. Lin, S. P., Hunag, C. M., <u>Chang, Y. C.</u>, "PC-Based Monitor and Control System for Developing Inverter-Controlled Room Air-Conditioner", Proceedings of the 54th Annual International Appliance Technical Conference, Purdue University, U.S.A., March 10-12, 2003.

6. <u>Chang, Y. C.</u>, *Tseng, C. H.*, Tarng, G. D. and Chang, L. T., "Scroll compressor with solid axial sealing mechanism", Proceedings of the 4th International Conference on Compressor and Refrigeration, Xi'an City, China, pp189-196, October, 2003.

7. <u>Chang, Y. C.</u>, Tsai, C. E., *Tseng, C. H.*, Tarng, G. D. and Chang, L. T., "Computer simulation and experimental validation of scroll compressors", Proceedings of the 18th International Compressor Engineering Conference at Purdue, USA, C016, July, 2004.

8. <u>Chang, Y. C.</u>, Huang, A., Liang, K. Y. and *Tseng, C. H.*, "Design and verification of R-410A scroll compressor used with brushless DC motor controlled", Proceedings of the 2nd Symposium on Air-Conditioning, Refrigeration and Energy Engineering at National Chin-Yi Institute of Technology, Taichung, Taiwan, No. 20, July, 2004.

9. Chen, H. C., <u>Chang, Y. C.</u>, Lin, S. P., Huang, C. M., Chen, Y. C., Liang, K. Y., "Sensorless control for DC inverter-fed compressors", Applied Power Electronics Conference and Exposition, 2004. APEC '04. Nineteenth Annual IEEE, Vol. 2, 2004, pp. 1106 – 1110.

10. Chen, H. C., Liang K. Y., <u>Chang, Y. C.</u>, Yang, C. C., "Speed control for DC compressors", The 25th Symposium on Electrical Power Engineering, Taiwan, Nov. 2004, pp. 951-956.

11. Chen, J. L., Chen, J. W., Liaw, C. M., Chen, H. C., <u>Chang, Y. C.</u>, Yang, C. C., "Front-end low-frequency SMR and its control for PMSM drive", The 25th Symposium on Electrical Power Engineering, Taiwan, Nov. 2004, pp. 1742-1747.

12. Yu, P. Y., Hsiao, T. L., <u>Chang, Y. C.</u>, "Optimum valve design and performance estimation of hermetic reciprocating compressors with computer model", Proceedings of the 5th International Conference on Compressor and Refrigeration, Dalian, China, July 18-21, 2005, pp.71-80.

13. Chang, W. R., Liu, D. Y., Lin, J. Y., <u>Chang, Y. C.</u>, "Implementation for inverter controlled domestic refrigerator/freezer with brushless DC reciprocating compressor", International Conference on Compressors and their Systems 2005, I Mech E, U. K., Sep., 2005, pp. 283-292.

14. <u>Chang, Y. C.</u>, Huang A., Liang, K. Y., ***Tseng, C. H.***, "Development of R-410A scroll compressors used with brushless DC motor control", International Conference on Compressors and their Systems 2005, I Mech E, U. K., Sep., 2005, pp. 413-422.

15. Yu, P. Y., Hsiao, T. L., <u>Chang, Y. C.</u>, ***Tseng, C. H.***, Wang, H. H., "Dimensional analysis and design of scroll wrap of CO_2 scroll compressor", Thermophysical Properties and Transfer Processes of Refrigerants, IIR International Conference, Vicenza, Italy, Sep. 2005, pp.287-294.

16. Hua, C. C., Lin J. D., <u>Chang, Y. C.</u>, Chen, H. C., "An all-digital phase-locked loop with single-cycle lock time for utility interface inverters", The 4th Taiwan Power Electronics Conference & Exhibition, ITRI, Taiwan, Sep. 2005, pp. 238-242.

17. Zeng, J. H., Lai, Y. S., Chen, Y. C., Hsiao, T. L., <u>Chang, Y. C.</u>, "Design and implementation of power supply for driver with pulse amplitude modulation control", The 4th Taiwan Power Electronics Conference & Exhibition, ITRI, Taiwan, Sep. 2005, pp. 424-429.

18. Lo, C. C., Yang, C. C., Huang, A., <u>Chang, Y. C.</u>, "Magnetizing Method for the Post-Assembly Magnetization of a hermetic DC compressor", Proceedings of the 18th International Compressor Engineering Conference at Purdue, U.S.A., C009, July 17-20, 2006.

19. Tang, Y. J., Yang, C. C., <u>Chang, Y. C.</u>, "A study of designing 35RT aluminum alloy scroll compressor", Proceedings of the 18th International Compressor Engineering Conference at Purdue, U.S.A., C031, July 17-20, 2006.

III. PATENTS

1. <u>Chang, Y. C.</u>, Lai, C. F. and ***Tseng, C. H.***, "A motor of rotor with built-in permanent magnet", U.S. Patent 6,987,341, Jan. 17, 2006.

2. <u>張鈺炯</u>, 賴慶峰, ***曾錦煥***, "轉子內置永久磁石之馬達裝置", 中華民國專利, 新型第 200822 號, 2003 年 2 月.

3. <u>張鈺炯</u>, 賴慶峰, ***曾錦煥***, "轉子內置永久磁鐵之馬達裝置", 中國大陸專利, 實

用新型第 ZL01267457.5 號, 2002 年 7 月.

IV. OTHERS

1. 張鈺炯, "壓縮機用內置式磁石無刷馬達之專利介紹", 機械月刊, 第廿七卷第十期, 文 226-238 頁, 2001 年 10 月.

2. 張鈺炯, *曾錦煥*, "由專利分析認識渦卷式壓縮機徑向順從密封機構", 機械月刊, 第廿八卷第十一期, 文 41-54 頁, 2002 年 11 月.

3. 張鈺炯, *曾錦煥*, "CO2 冷媒壓縮機相關技術發展案例", 機械月刊, 第廿九卷第六期, 文 48-68 頁, 2003 年 6 月.

4. 陳鴻祺, 楊錞忠, 賴慶峰, 林紹柏, 梁坤億, 張鈺炯, 黃淑娥, "高效率直流變頻風扇開發技術", 台灣電力公司 93 年節約能源論文發表會, 台灣科技大學, 文 17-32 頁, 2004 年 5 月 19 日.

5. 張鈺炯, "變頻離心式壓縮機的介紹", 冷凍空調&熱交換器, 第 63 期, 文 1-8 頁, 2004 年 11 月.

6. 黃淑娥, 賴慶峰, 梁坤億, 張鈺炯, "渦卷式壓縮機量產商品統計製程分析技術", 機械工業雜誌, 第二六二期, 文 101-123 頁, 2005 年 1 月.

7. 陳鴻祺, 梁坤億, 張鈺炯, "高效率小型空調機用變頻壓縮機之比較與效率分析", 能源季刊, 第三十五卷第二期, 文 78-96 頁, 2005 年 4 月.

8. 張鈺炯, 梁坤億, 蔡慶營, "渦卷式壓縮機電腦模擬分析與測試驗證", 機械月刊, 第三十一卷第九期, 文 34-43 頁, 2005 年 9 月.

9. 蕭澤良, 余培煜, 張鈺炯, "冰箱用直流變頻壓縮機", 機械月刊, 第三十一卷第十期, 文 92-100 頁, 2005 年 10 月.

10. 張鈺炯, 楊錞忠, 洪財旺, "變頻螺旋式壓縮機相關技術簡介", 冷凍與空調, 第三十五期, 文 45-51 頁, 2005 年 10 月.

11. 曾金鴻, 賴炎生, 陳衍璋, 蕭澤良, 張鈺炯, "波幅調變直流無刷變頻器之電源的研製", 電機月刊第一八一期, 文 116-125 頁, 2006 年元月.

12. 張鈺炯, 楊錞忠, "二氧化碳熱泵技術簡介", 冷凍與空調, 第卅十七期, 文 52-60 頁, 2006 年 2 月.

13. 張鈺炯, "變頻螺旋式壓縮機相關專利簡介", 冷凍與空調, 第四十一期, 文 53-67 頁, 2006 年 10 月.

95

博士論文

渦卷式壓縮機族群設計最佳化之研究

交通大學工學院
機械工程研究所

張鈺炯